

NON-TIDAL FLOWS IN THE NORTHWEST PASSAGE

DFO - Library / MPO - Bibliothèque



12014501

by

D.B. Fissel and J.R. Birch
Arctic Sciences Ltd.
Sidney, B.C.

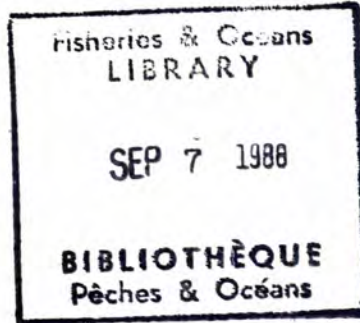
and

H. Melling and R.A. Lake
Institute of Ocean Sciences
Sidney, B.C.

Institute of Ocean Sciences
Department of Fisheries and Oceans
Sidney, B.C.

1988

**CANADIAN TECHNICAL REPORT OF
HYDROGRAPHY AND OCEAN SCIENCES
NO. 98**



GC

1

C37

98

D

eries Pêches
Oceans et Océans

Canada

Canadian Technical Report of Hydrography and Ocean Sciences

These reports contain scientific and technical information of a type that represents a contribution to existing knowledge but which is not normally found in the primary literature. The subject matter is generally related to programs and interests of the Ocean Science and Surveys (OSS) sector of the Department of Fisheries and Oceans.

Technical Reports may be cited as full publications. The correct citation appears above the abstract of each report. Each report will be abstracted in Aquatic Sciences and Fisheries Abstracts. Reports are also listed in the Department's annual index to scientific and technical publications.

Technical Reports are produced regionally but are numbered and indexed nationally. Requests for individual reports will be fulfilled by the issuing establishment listed on the front cover and title page. Out of stock reports will be supplied for a fee by commercial agents.

Regional and headquarters establishments of Ocean Science and Surveys ceased publication of their various report series as of December 1981. A complete listing of these publications and the last number issued under each title are published in the *Canadian Journal of Fisheries and Aquatic Sciences*, Volume 38: Index to Publications 1981. The current series began with Report Number 1 in January 1982.

Rapport technique canadien sur l'hydrographie et les sciences océaniques

Ces rapports contiennent des renseignements scientifiques et techniques qui constituent une contribution aux connaissances actuelles mais que l'on ne trouve pas normalement dans les revues scientifiques. Le sujet est généralement rattaché aux programmes et intérêts du service des Sciences et Levés océaniques (SLO) du ministère des Pêches et des Océans.

Les rapports techniques peuvent être considérés comme des publications à part entière. Le titre exact figure au-dessus du résumé de chaque rapport. Les résumés des rapports seront publiés dans la revue *Résumés des sciences aquatiques et halieutiques* et les titres figureront dans l'index annuel des publications scientifiques et techniques du Ministère.

Les rapports techniques sont produits à l'échelon régional mais sont numérotés et placés dans l'index à l'échelon national. Les demandes de rapports seront satisfaites par l'établissement auteur dont le nom figure sur la couverture et la page de titre. Les rapports épuisés seront fournis contre rétribution par des agents commerciaux.

Les établissements des Sciences et Levés océaniques dans les régions et à l'administration centrale ont cessé de publier leurs diverses séries de rapports depuis décembre 1981. Vous trouverez dans l'index des publications du volume 38 du *Journal canadien des sciences halieutiques et aquatiques*, la liste de ces publications ainsi que le dernier numéro paru dans chaque catégorie. La nouvelle série a commencé avec la publication du Rapport n° 1 en janvier 1982.

Canadian Technical Report of Hydrography
and Ocean Sciences No. 98

1988

Non-Tidal Flows in the Northwest Passage

by

D.B. Fissel and J.R. Birch
Arctic Sciences Ltd.
Sidney, B.C.

and

H. Melling and R.A. Lake
Institute of Ocean Sciences
Sidney, B.C.

Institute of Ocean Sciences
Department of Fisheries and Oceans
Sidney, B.C.

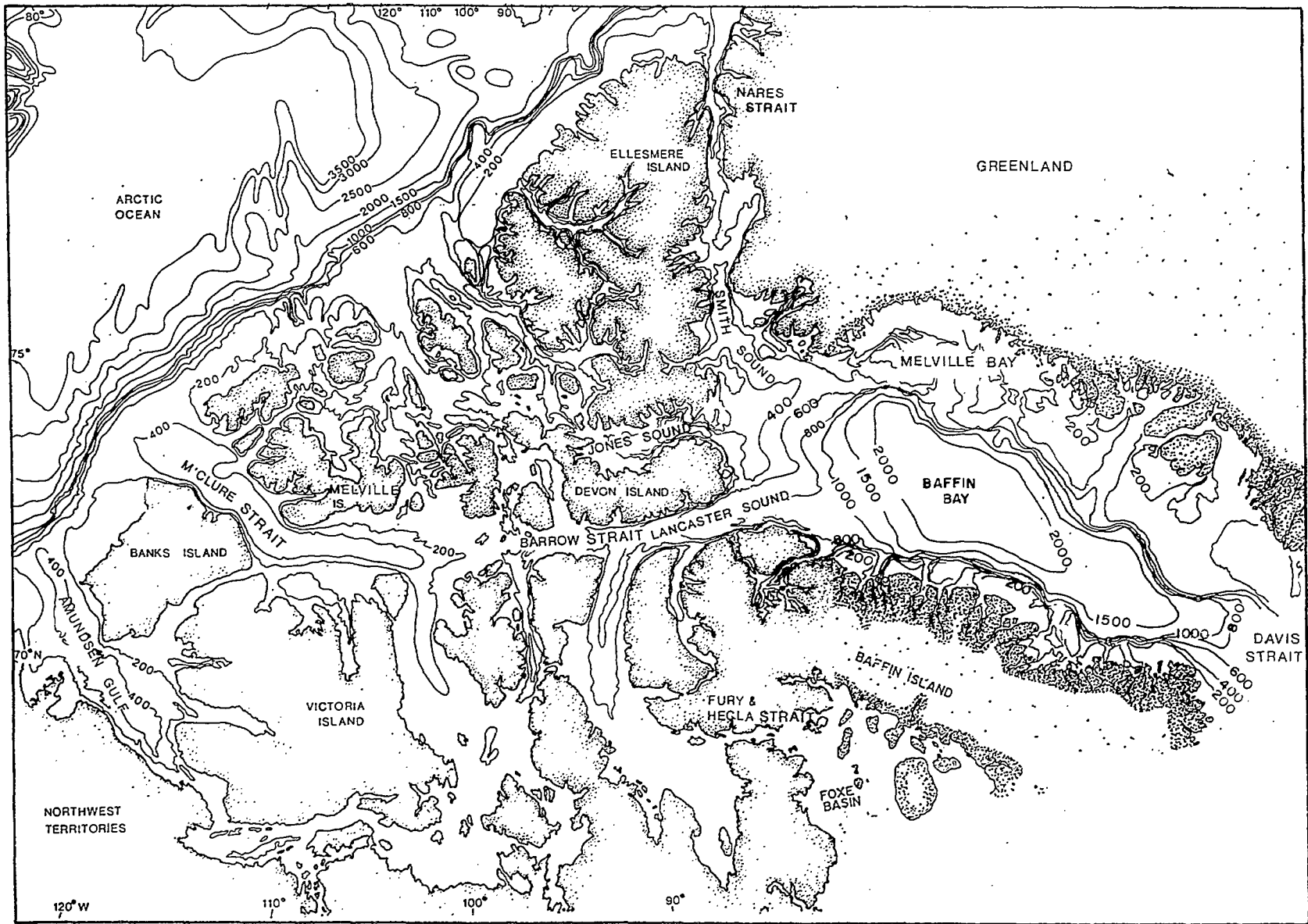
PREFACE

This report is one of eleven pertaining to an investigation of the physical oceanography of the Canadian Arctic Archipelago. Three reports have been published as volumes of the Canadian Data Report of Hydrography and Ocean Sciences No. 39, and document and present CTD measurements acquired during the three years of the project. A further three reports appear as volumes of Report No. 51 in the same series, and document and present current and tide measurements. Two contractor reports document and discuss wide-ranging CTD surveys within the Archipelago and adjacent waters in the winters of 1982 and 1983 (Canadian Technical Report of Hydrography and Ocean Sciences Nos. 15 and 16). The present report deals with non-tidal residual flows and volume transports, and is one of three attempting to synthesize present and past measurements within this vast and complex system of channels into an up-to-date description of its physical oceanography. The two companion reports discuss tides and tidal currents, and water masses and baroclinic structure (Canadian Technical Report of Hydrography and Ocean Sciences Nos. 97 and 79).

Copyright Minister of Supply and Services Canada - 1988

Cat. No. Fs97-18/98 ISSN 0711-6764

Fissel, D.B., J.R. Birch, H. Melling and R.A. Lake, 1988. Non-Tidal Flows in the Northwest Passage. Can. Tech. Rep. Hydrogr. Ocean Sci. No. 98: 143 pp.



Frontispiece: The Canadian Arctic Archipelago, showing the main passages between the Arctic Ocean and Baffin Bay. Bathymetric contours are in metres, based on GEBCO chart 5-17 (1979).

TABLE OF CONTENTS

	Page
LIST OF FIGURES	iii
LIST OF TABLES	ix
ABSTRACT	xii
ACKNOWLEDGEMENTS	ivx
1. INTRODUCTION	1
1.1 Study Background and Objectives	1
1.2 Definition of Residual Currents	2
1.3 Previous Studies of Residual Currents Within the Archipelago	2
2. DATA COLLECTION AND PROCESSING METHODS, 1982-1985 DATA	10
2.1 Data Collection	10
2.2 Data Filtering	14
2.3 Uncertainties in the Speed and Directional Data	15
2.3.1 Weak Residual Flow in the Presence of a Strong Tidal Flow	15
2.3.2 Subthreshold Currents	17
3. RESULTS	19
3.1 Speed and Direction Distribution, and Mean Residual Flow Vectors	19
3.1.1 Springtime, 1982-1985	19
3.1.2 Seasonal Variability	25
3.2 Auto Spectra	27
3.2.1 Springtime, 1982-1985: Regional Comparisons	28
3.2.2 Seasonal Variations	37
3.2.3 Year-long Time Series	39
3.3 Spatial Coherence	40
3.3.1 Springtime, 1982-1985	41
3.3.2 Seasonal Variations	49
3.3.3 Year-long Time Series	50
3.4 Volume Transport	51
3.4.1 Computational Methods and Uncertainty	51
3.4.2 Computed Volume Transports	54
4. SUMMARY AND DISCUSSION	58
4.1 Mean Circulation	58
4.2 Temporal Variability in Residual Currents	63
4.3 Volume Transport	68
5. REFERENCES	71

TABLE OF CONTENTS

	<u>Page</u>
APPENDIX 1: DATA SETS CONTAINING CURRENT MEASUREMENTS WHICH MAY BE USEFUL IN DETERMINING RESIDUAL CIRCULATION PATTERNS IN THE CANADIAN ARCHIPELAGO.	135
APPENDIX 2: SUMMARY STATISTICS OF CURRENT RECORDS USED TO SUPPLEMENT THE DATA OBTAINED BY THE INSTITUTE OF OCEAN SCIENCES DURING 1982-85.	138
APPENDIX 3: SUMMARY OF COMPUTATIONAL TECHNIQUES FOR AUTO- AND CROSS-SPECTRAL ANALYSIS.	143

LIST OF FIGURES

	Page	
Frontispiece:	The Canadian Arctic Archipelago, showing the main passages between the Arctic Ocean and Baffin Bay. Bathymetric contours are in metres, based on GEBCO chart 5-17 (1979).	
Figure 1.3-1:	Trajectories of several ice-beset vessels and of the <u>Polaris</u> ice-floe party (Smith, 1931). Average net speeds are indicated for major segments of each track (from Fissel, Lemon and Birch, 1981).	79
Figure 1.3-2:	Locations of all moored-current-meter data obtained in the Canadian Arctic Archipelago prior to 1982 (from Fissel et al., 1983; Birch et al., 1983, 1987).	80
Figure 1.3-3:	a) Vector-averaged velocities from drogued-drifter measurements in eastern Parry Channel, July-November, 1977. The averaging is applied over rectangles of size 0.2° latitude by 0.8° longitude (from Fissel and Marko, 1978). b) Observed directions of summer ice movements in eastern Parry Channel, 1973-1977. Arrow length is approximately proportional to observed ice speed (from Marko, 1978).	81
Figure 2.1-1:	Institute of Ocean Sciences current measurement sites in 1982, 1983 and 1984.	82
Figure 2.1-2a:	Vane-follower current meters suspended from the sea-ice on hydraulic hose (from Buckingham, Lake and Melling, 1987c).	83
Figure 2.1-2b	Standard configuration current meter on a taut-line mooring (from Buckingham, Lake and Melling, 1987c).	83
Figure 2.1-2c	Bottom-founded mooring with vane-follower current meters (from Buckingham, Lake and Melling, 1987c).	83
Figure 2.2-1:	Response curve of the low-pass filter used to isolate the residual component of the current record. The filter has 72 coefficients, resulting in a data loss of 1.5 days at each end of the record.	84

	Page
Figure 2.2-2:	85
Observed and low-pass-filtered currents at Station 42, May 1984. The observed currents at 100 m depth oscillate between southwesterly (flood tide) and northeasterly (ebb tide), although the residual flow is to the north and east. The progressive vector diagrams are not trajectories but represent the cumulative displacement due to the current observed at Station 42.	
Figure 2.3-1:	86
Estimates of the percent error in measured mean speed, for various tidal signals and compass calibration errors.	
Figure 2.3-2:	87
Percent of recorded speeds below stall speed, summarized according to site identification number and area.	
Figure 2.3-3:	88
Three cases illustrating occurrences of subthreshold currents in M'Clure Strait. A - Rotor stalled for 1-2 hours at both high and low tide; B - Rotor stalled during slack high tide and following ebb; C - Rotor stalled during slack low tide and subsequent flood.	
Figure 3.1-1:	89
Speed and directional distribution, and vector average of near-surface (20 m) residual currents in Prince of Wales Strait, spring 1982. The radial sticks (right-hand side) represent the percentage of values whose directions fall within the given 30° class, while the mean residual speed for each directional class is indicated by the point of intersection of the encircling line and the radial stick. Distribution and vector average of residual speed are provided on the left-hand side. Vector averages less than 2 cm/s have tail-less arrows. Each site is identified by site number/instrument depth.	
Figure 3.1-2:	90
Speed and directional distribution, and vector average of near-surface (20 m) residual currents in M'Clure Strait, spring 1982. Presentation as for Figure 3.1-1.	
Figure 3.1-3:	91
Speed and directional distribution, and vector average of near-surface (20 m) residual currents in central Viscount Melville Sound, spring 1982. Presentation as for Figure 3.1-1.	
Figure 3.1-4:	92
Speed and directional distribution, and vector average of near-surface (20 m) residual currents in eastern Viscount Melville Sound, spring 1983. Presentation as for Figure 3.1-1.	

	<u>Page</u>
Figure 3.1-5: Speed and directional distribution, and vector average of near-surface (20 m) residual currents in M'Clintock Channel, spring 1983. Presentation as for Figure 3.1-1.	93
Figure 3.1-6: Speed and directional distribution, and vector average of near-surface (20 m) residual currents in Byam Martin Channel and Austin Channel, spring 1983. Presentation as for Figure 3.1-1.	94
Figure 3.1-7: Speed and directional distribution, and vector average of residual currents in Penny Strait, spring 1984. Presentation as for Figure 3.1-1.	95
Figure 3.1-8: Speed and directional distribution, and vector average of near-surface (20 m) residual currents in Wellington Channel, spring 1984. Presentation as for Figure 3.1-1.	96
Figure 3.1-9: Speed and directional distribution, and vector average of residual currents in Barrow Strait, spring 1984. Presentation as for Figure 3.1-1.	97
Figure 3.1-10: Computed residual current velocity parameters including vector mean, mean speed and maximum speed (cm/s) for all springtime data sets, 1982-1984.	98
Figure 3.1-11: Seasonal variability in the residual currents at site 71 in Austin Channel. The speed-histogram and direction distribution format is the same as was used for the springtime data. The plot of vector averaged velocities is based on monthly values. If there were not at least 15 days of data then no value was plotted for that month.	99
Figure 3.1-12: Seasonal variability in the residual currents at sites PSE and PSW in Penny Strait. The speed-histogram and direction-distribution format is the same as was used for the springtime data. The plot of vector averaged velocities is based on monthly values. If there were not at least 15 days of data then no value is plotted for that month.	100
Figure 3.1-13: Seasonal variability in the residual currents at site 42 in Barrow Strait. The speed-histogram and direction-distribution format is the same as was used for the springtime data. The plot of vector averaged velocities is based on monthly values. If there were not at least 15 days of data then no value is plotted for that month.	101

	Page
Figure 3.2-1: Residual-flow parameters derived from auto-spectral analyses for all springtime data sets: - root-mean-square (RMS) amplitude of fluctuations (cm/s) - ratio of RMS to vector average - percent of total auto-spectral density having clockwise rotation.	102
Figure 3.2-2: Auto-spectral densities for major and minor components of the residual currents measured in 1982 at sites in (a) Prince of Wales Strait and (b) M'Clure Strait.	103
Figure 3.2-3: Auto-spectral densities for major and minor components of the residual currents measured in 1982 at sites in (a) Central Viscount Melville Sound and (b) M'Clintock Channel.	104
Figure 3.2-4: Auto-spectral densities for major and minor components of the residual currents measured in 1983 at sites in (a) Byam Martin and Austin Channels and (b) Eastern Viscount Melville Sound.	105
Figure 3.2-5: Auto-spectral densities for major and minor components of the residual currents measured in 1984 at sites in: (a) Barrow Strait; (b) Wellington Channel.	106
Figure 3.2-6: Auto-spectral densities for major and minor components of the residual currents measured in 1984 at sites in Penny Strait.	107
Figure 3.2-7: Seasonal auto-spectra computed for year-long data in Austin Channel.	108
Figure 3.2-8: Seasonal auto-spectra computed for year-long data in Barrow Strait.	109
Figure 3.2-9: Seasonal auto-spectra computed for year-long data in Penny Strait.	110
Figure 3.2-10: The seasonal root-mean-square (RMS) amplitudes of residual current fluctuations, along with vector average magnitude.	111
Figure 3.2-11: Auto-spectra computed from the full year-long current-meter data in: (a) Austin Channel (Site 71); (b) Barrow Strait (Site 42).	112

	<u>Page</u>
Figure 3.2-12: Auto-spectra computed from the full year-long current meter data in Penny Strait (Sites PSW and PSE).	113
Figure 3.3-1: Cross-spectra computed for pairs of current-meter records in Prince of Wales Strait.	114
Figure 3.3-2: Cross-spectra computed for pairs of current-meter records in Prince of Wales Strait.	115
Figure 3.3-3: Cross-spectra computed for pairs of current-meter records in M'Clure Strait.	116
Figure 3.3-4: Cross-spectra computed for pairs of current-meter records in Central Viscount Melville Sound.	117
Figure 3.3-5: Cross-spectra computed for pairs of current-meter records in M'Clintock Channel.	118
Figure 3.3-6: Cross-spectra computed for pairs of current-meter records in Eastern Viscount Melville Sound.	119
Figure 3.3-7: Cross-spectra computed for pairs of current-meter records in Byam Martin and Austin Channels.	120
Figure 3.3-8: Cross-spectra computed for pairs of current-meter records in Barrow Strait.	121
Figure 3.3-9: Cross-spectra computed for pairs of current-meter records in Wellington Channel.	122
Figure 3.3-10: Cross-spectra computed for pairs of current-meter records in Wellington Channel.	123
Figure 3.3-11: Cross-spectra computed for each season from vertically-separated current-meter records in: (a) Austin Channel (Site 71); (b) Barrow Strait (Site 42).	124
Figure 3.3-12: Cross-spectra computed for each season from vertically-separated current-meter records in Penny Strait (Sites PSW and PSE).	125
Figure 3.3-13: Seasonal cross-spectra computed for horizontally-separated station pairs in Penny Strait, using Site PSE mid-depth.	126
Figure 3.3-14: Seasonal cross-spectra computed for horizontally-separated station pairs in Penny Strait, using Site PSE lower current meter.	127

	Page
Figure 3.3-15: Cross-spectra computed from full year-long records in: (a) Austin Channel; (b) Barrow Strait.	128
Figure 3.3-16: Cross-spectra computed from full year-long records in Penny Strait.	129
Figure 4-1: Summary plot of near-surface vector averaged residual currents, based on the 1982-1985 data obtained by IOS, and the data identified in Appendix 2. The arrowhead provides the direction of the flow; the speed is given by the length of the tail of each vector, scaled as in the legend. Vectors having an arrowhead but no tail indicate speeds less than 1 cm/s. The dashed vector along the northwest coast of Banks Island indicates a strong flow there, the actual magnitude of which is not available at this time.	130
Figure 4-2: Monthly vector averaged velocities at stations 46 in 1981 and 42 in 1984. Although the data are from different years, the increased flow at station 46 during the summer correlates with a reversal from easterly to westerly flow at station 42. (Note that the Nov. and Dec. values for site 46, 25 m depth, may be too low; see Prinsenbergl and Bennett, 1987.)	131
Figure 4-3: Estimated transport, in hundredth's of Sverdrups ($1 \text{ Sv} = 10^6 \text{ m}^3/\text{s}$), through the channels of the Canadian Archipelago. Sources are the 1982-1985 IOS data and others specified in Appendix 2.	132

LIST OF TABLES

	<u>Page</u>	
Table 1-1:	Summary of baroclinic volume transport computations for Lancaster, Jones and Smith Sounds and for northern Baffin Bay (from Muench, 1971a). Positive signs represent transport into Baffin Bay or southward transport within Baffin Bay. All volume transport rates are in units of $10^6 \text{ m}^3/\text{s}$.	4
Table 1-2:	Summary of volume transport rates based on direct-current measurements made in the Arctic Archipelago, 1970 to 1982. Positive transports are southerly or towards Baffin Bay. Units are $10^6 \text{ m}^3/\text{s}$.	7
Table 1-3:	Lagrangian drift results, using radar and satellite tracking methods.	9
Table 2-1:	Details of current-meter records, as to location, period, depth and summary statistics. Note that the statistics apply to the residual component of the current only and were computed over the entire record. The stability is the ratio of the vector average speed to the mean speed.	11
Table 2-2:	Estimated accuracy and precision of the Aanderaa RCM-4 current-meter data.	15
Table 3.2-1:	The range of periods over the frequency bands used in the spectral analysis of this study for (a) Wellington Channel (springtime), (b) all other areas (springtime) and (c) year-long records.	28
Table 3.2-2:	Residual-flow parameters derived from auto-spectral analyses for all springtime records. The vector means may differ from those of Table 2-1 due to shorter record lengths used in the spectral analyses.	29
Table 3.2.2-1:	Auto-spectral analyses for each season of the year-long current-meter records.	38
Table 3.3-1:	Coherence values between two time series that exceed random noise at 80, 90 and 95 percent probability levels.	40

	<u>Page</u>
Table 3.4-1:	55
<p>The baroclinic, barotropic and total components of volume transport for selected channels in the Canadian Arctic Archipelago, derived from the 1982-1984 data collected by the Institute of Ocean Sciences. The barotropic and volume transports are computed both from the mean residual currents, and alternatively from current measurements obtained within a few days of the temperature-salinity data from which the baroclinic transports were derived (numbers in brackets).</p>	
Table 4-1:	62
<p>A summary of coastal currents in the Canadian Arctic Archipelago, detected using Eulerian current data. Included are the location, mean speed and estimated width for each coastal current.</p>	

ABSTRACT

Fissel, D.B., J.R. Birch, H. Melling and R.A. Lake. 1988. Non-Tidal Flows in the Northwest Passage. Can. Tech. Rep. Hydrogr. Ocean Sci. No. 98: 143 pp.

The residual flow field in the Northwest Passage and adjoining waterways is discussed on the basis of data from 63 current-meter deployments beneath sea ice between 1982 and 1985. Most of these deployments yielded 1-3 months of data, but eight operated for a full year. This basis has been supplemented, where relevant, by other available current records from the Canadian Arctic Archipelago. Data analyses are presented in a convenient "handbook" format, with derived parameters superimposed graphically on maps of appropriate sub-regions of the area. Generally, data are presented separately for each season of the year. Parameters mapped include mean vectors, speed and direction probability densities, band-filtered root-mean-square amplitudes along major and minor principal axes, and cross-spectral coherence and phase. Total volume fluxes in selected channels have been estimated by combining the residual-flow analysis of this study with estimates of baroclinic transport computed from density sections. A regional map of all measured mean currents illustrates the present knowledge of overall circulation in the Canadian Arctic Archipelago. Mean flows vary from 0.2 to 19 cm/s over the area, and the maximum non-tidal current observed was 37 cm/s; the strongest flows were concentrated near the shore. The larger values are found in the shallower central waterways: Byam Martin Channel, Barrow Strait, Penny Strait and Wellington Channel. The smallest currents are found in the broad, deep, ice-bound western channels: western Parry Channel, M'Clintock Channel and the waterways of the Queen Elizabeth Islands; narrow, stronger, coastal currents up to 10 km in width do, however, exist in these areas. Flow fluctuations of significant amplitude occur over periods up to several tens of days in duration, with the largest variance at periods between 10 and 25 days. As with mean values, the fluctuations are generally larger in the central waterways, and larger variances occur in fall and early winter. In the summer, current fluctuations increase noticeably in the near-surface zone (but not at depth), presumably due to more effective wind forcing in the open-water season.

Key Words = Northwest Passage, Canadian Arctic Archipelago, currents, volume fluxes, circulation.

RESUME

Fissel, D.B., J.R. Birch, H. Melling and R.A. Lake. 1988. Non-Tidal Flows in the Northwest Passage. Can. Tech. Rep. Hydrogr. Ocean Sci. No. 98: 143 pp.

Il est question ici du champ de courants résiduels dans le passage du Nord-Ouest et les voies navigables adjacentes, plus précisément des données recueillies grâce au mouillage de 63 courantomètres sous la glace-de mer entre 1982 et 1985. Huit batteries ont été mouillées durant un an, mais la majorité ont permis d'obtenir des données sur un à trois mois. La base de données obtenue a été complétée, le cas échéant, par d'autres données sur les courants dans l'archipel Arctique canadien. L'analyse des données est présentée sous forme d'un "manuel" pratique; les paramètres obtenus sont superposés graphiquement aux données sur les cartes des sous-régions correspondantes. En règle générale, les données sont présentées par saison. Parmi les paramètres cartographiés, notons les suivants: vecteurs moyens, fonctions de densité de la vitesse et de la direction, amplitudes efficaces filtrées le long des axes principaux primaires et secondaires et cohérence et phase interspectrale. On a estimé les flux de volume dans certains détroits en combinant l'analyse des données sur les courants résiduels de la présente étude et des estimations du transport barocline calculé dans des coupes de densité. Une carte régionale de tous les courants moyens mesurés permet de visualiser la circulation globale dans l'archipel Arctique canadien, telle qu'on la connaît aujourd'hui. La vitesse moyenne des courants varie de 0, 2 à 19 cm/s dans la région et la vitesse maximale observée d'un courant non dû à la marée était de 37 cm/s. Les plus grandes valeurs se retrouvent dans les voies navigables centrales moins profondes: détroit de Byam Martin, détroit de Barrow, détroit de Penny et détroit de Wellington. Les courants les plus lents sont ceux des détroits occidentaux, larges, profonds et recouverts de glace: portion ouest du détroit de Parry, détroit de M'Clintock et détroits des îles Reine-Elisabeth; des courants côtiers, puissants et étroits atteignant 10 km de largeur existent cependant à ces endroits. Des fluctuations de courants d'amplitude significative se produisent sur des périodes atteignant plusieurs dizaines de jours; la variance la plus importante se produisant à des périodes d'entre 10 et 25 jours. Comme pour les valeurs moyennes, les fluctuations sont généralement plus importantes dans les voies navigables centrales et les variances les plus importantes s'observent en automne et au début de l'hiver. Durant l'été, les variations de courants augmentent de manière sensible dans la zone superficielle (mais pas en profondeur), probablement parce que l'effet du vent est plus efficace durant la saison des eaux libres.

Mots-Clés: passage du Nord-Ouest, archipel Arctique canadien, courants, flux de volume, circulation.

ACKNOWLEDGEMENTS

The effort expended on the Northwest Passage Oceanography Programme since its inception five years ago is considerable, and the number of people and organizations who have contributed to its success is correspondingly large. Without detailing their specific contributions, our appreciation is extended to the following: Syd Moorhouse, Denny Richards, John MacNeill, Gary Moonie, Bob Sudar, Ron Cooke, Paul Johnson, Al Koppel, Andrew Wharton, Bill Green, Jeff Richards, Lyn Lewis and Ron Perkin, all of the Arctic Group within the Physics Division at the Institute of Ocean Sciences; David Lemon, and Doug Knight of Arctic Sciences Ltd.; Simon Prinsenbergh and Bert Bennett, formerly of the Bayfield Laboratory for Marine Science and Surveys, Burlington, Ontario; George Hobson and the staff of the Polar Continental Shelf Project, Energy Mines and Resources, Canada; Dick MacDougall of the Canadian Hydrographic Service; PanArctic Oils Ltd.; Bradley Air Services Ltd.; Kenn Borek Air Ltd.; Quasar Helicopters Ltd.

In respect of particular contributions to this report the authors thank Bill Buckingham of the Institute of Ocean Sciences for his painstaking and careful work in processing and documenting the current and tide data and to acknowledge the efforts of the following Arctic Sciences personnel: O. Byrne and R. Chave, computer programming; N. Andrew and D. Stover, drafting; and S. Norton and D. Gilbert, word processing. We thank L.S.C. Thomson and L. Giovando for reviewing the manuscript and technical editing.

Funding was provided by the Marine Transportation Research and Development Programme (Transport Canada), and support in kind by the Department of Fisheries and Oceans and by the Polar Continental Shelf Project, Energy, Mines and Resources, Canada.

1. INTRODUCTION

1.1 Study Background and Objectives

In recent years, proposals have been advanced for the year-round transport of natural resources through the Northwest Passage and adjoining waterways. Implementation of such proposals requires a thorough understanding of the regional oceanography and other environmental conditions, both to assess and to minimize the effect of developments on the natural environment, and to optimize the safety and efficiency of the proposed operations.

In order to improve knowledge of the area's oceanography the Ocean Physics Division, Institute of Ocean Sciences (IOS), conducted an extensive observational program in the years 1982 to 1985. The major achievements of the measurement programme consisted of:

- 1) current-meter and water-level data from moored instruments at almost 100 locations;
- 2) water-property distributions obtained using a CTD system operated from aircraft.

This report deals with residual currents of the Northwest Passage. The results obtained from the CTD surveys and the analysis of tidal fluctuations are the subject of other reports (de Lange Boom et al., 1987; Stronach et al., 1987).

The objective of this report is to present a coherent and informative description of the residual currents of the Northwest Passage and adjoining waterways. The findings of the study are derived primarily from an interpretation of the Institute of Ocean Sciences current-meter data of 1982 to 1985, inclusive. Data collected by other investigators have also been examined and presented where appropriate.

1.2 Definition of Residual Currents

The term residual current is generally applied to the non-tidal portion of the current record. The tidal component may be removed by subtracting analyzed tidal harmonics from the observed data. For this study, however, the data were low-pass filtered so that only sub-diurnal frequencies remained.

In the Northwest Passage, the net residual flow is believed to be towards the southeast, forced by water levels in the Arctic Ocean higher than those in Baffin and Hudson bays. Tidal flows are often significant, and in many cases cause flow reversals at tidal frequencies. By removing the tidal currents and other higher-frequency oscillations, the net overall drift or residual circulation is more apparent. (This is illustrated in Figure 2.2-2.)

1.3 Previous Studies of Residual Currents within the Archipelago

Early Studies to the 1960's

The earliest information on residual currents within the Arctic Archipelago was obtained in the 19th century, from the drift of several ice-beset ships depicted in Figure 1.3-1. These drift tracks indicated a flow from the Archipelago into northwestern Baffin Bay, through Lancaster and Smith sounds. A strong southeasterly-flowing current, since named the Baffin Current, occupied the western periphery of Baffin Bay.

From 1860 to 1940, a series of scientific cruises to Baffin Bay was undertaken by American, Swedish and Danish investigators. By the end of this period, the large-scale cyclonic (anti-clockwise) pattern of currents had been described. The West Greenland Current carries warm water, of Atlantic Ocean origin, northward into Melville Bay. Here, it is joined by outflows of cold water originating in the Arctic Ocean and flowing into Baffin Bay from Smith, Jones and Lancaster sounds. The Baffin Current carries waters southeastward along the western shore of Baffin Bay, with a markedly greater current and volume transport than is the case for the West Greenland Current.

Following World War II, oceanographic studies resumed, with increased effort directed at collecting data in the channels of the Canadian Arctic Archipelago. Until the 1970's, most measurements were collected in the short summer season, August to September. During this period, the seasonal deterioration of ice-cover was sufficient, in most years, to permit icebreaking vessels to collect data in the eastern passages of the Archipelago. Only in rare summers could ships penetrate to the western and northern portions of the Archipelago.

Using these early pre-1970 data, volume transports through the channels of the Archipelago were computed, using the dynamic or geostrophic method. This method assumes a simple balance exists between the Coriolis force and the internal pressure gradients determined from differences between nearby profiles of water density. The so-called baroclinic currents, computed from the data of two hydrographic stations involved, are those relative to an assumed "depth of no motion" normally taken to be just above the bottom. By integrating the computed currents over the full channel width, baroclinic volume transports were computed.

Collin (1963) summarized baroclinic volume transport computations for Lancaster, Jones and Smith sounds, obtained from summer transects in the years 1928, 1954 and 1957. Considerable variation occurred in the results; combined transport from all three channels ranged from 0.7 to 1.7×10^6 m^3/s . In all years, Lancaster Sound had the largest computed volume transport, ranging from 0.3 to 1.5×10^6 m^3/s . An extensive review of available baroclinic volume transport calculations was presented by Muench (1971a), as summarized in Table 1-1. Muench found that the total volume transport computed through northern Baffin Bay appeared to be 2.1×10^6 m^3/s , varying from 1.5 to 2.7×10^6 m^3/s . Coachman and Aagaard (1974) agreed that a value of 2.1 Sv ($1 \text{ Sv} = 10^6 m^3/s$) was probably the best estimate of net transport. To satisfy volume continuity, Muench concluded that an average combined transport of approximately 2×10^6 m^3/s is required from Smith, Jones and Lancaster Sounds. However, the sum of the computed transports for these Sounds was smaller, ranging from 0.2 to 1.6×10^6 m^3/s , about a mean probable value of 1.0×10^6 .

Muench attributed the discrepancy to inherent uncertainties in the dynamic method. Sources of uncertainty include: (1) the use of assumed levels of no motion (particularly problematic in the relatively shallow waters of Jones and Smith sounds); (2) neglected terms in the dynamical equation, including local accelerations, curvature effects (centrifugal force) and inertial effects; (3) the absence of complete coverage on the sides of the channel transects, where strong currents have since been directly measured; (4) interpretation of time-dependent change in the water-mass distributions as spatial difference, due to the considerable time (several hours) required for a single ship to occupy the channel transect; (5) the lack of information for the 10 months of the year when sea-ice kept ships from entering the Archipelago.

Table 1-1:

Summary of baroclinic volume transport computations for Lancaster, Jones and Smith Sounds and for northern Baffin Bay (from Muench, 1971a). Positive signs represent transport into Baffin Bay or southward transport within Baffin Bay. All volume transport rates are in units of $10^6 \text{ m}^3/\text{s}$.

Year	Data Source	Reference Level	Lancaster Sound	Jones Sound	Smith Sound	N. Baffin Bay Current	W.Green-land Current
1928	(1)	1000	0.65	0.3	0.4	-	-
1954	(2)	500	1.5	-0.4	-0.4	-	-
1957	(3)	500	1.0	0.25	-	-	-
1961	(5)	Var.	-	-	-	1.7	0.2
1962	(5)	Var.	-	-	-	2.3	0.0
1963	(5)	Var.	-	-	-	3.1	-0.4
1966	(4)	700	0.3	0.4	0	-	-
1966	(4)	700	0.6	0.2	-	-	-
1966	(5)	Var.	-	-	-	2.0	-0.4

(1) Killierich, 1939; (2) Bailey, 1957; (3) Collin, 1963; (4) Palfrey and Day, 1968; (5) Muench, 1971a.

The preferred way to estimate transport is to make an assumption regarding the level of no motion and to adjust the baroclinic flows computed by the geostrophic method, using actual current measurements.

Direct current measurements, using rotor- and vane-type sensors, were first obtained in the Archipelago in the summer of 1963. Ten Richardson current meters were suspended from three surface-flotation moorings in Smith Sound. Due to instrumentation problems, only three of the meters provided acceptable speed and direction readings, limited to a maximum 2.75 days only (Palfrey and Day, 1968). In September 1968, two moorings, with two current meters each, provided 11 days of data in northern Baffin Bay approximately 200 km southeast of Smith Sound (Avis and Coachman, 1971).

Recent Studies: 1970's and 1980's

Beginning in the late 1960's and early 1970's, two developments occurred which led to direct measurements of currents over extended periods in the Archipelago. The first was the availability of dependable, internally-recording current meters, which could be moored from the sea bottom or from sea ice for periods of months or longer. The Aanderaa current meter, first manufactured in 1966, has been used extensively in the Arctic with only minor modifications. The second development involved the refinement of techniques to acquire oceanographic data from sea ice, using specialized instrumentation (Lewis, 1980). With tracked vehicles, and in recent years aircraft, major oceanographic studies became feasible using the sea ice as a stable platform, particularly in the late winter and the spring.

The first current measurements made in the Archipelago using internally-recording instruments deployed from sea ice were obtained in May 1969 in Kane Basin (Muench, 1971b). A Braincon current meter, suspended at 50 m depth, provided 16 days of useful data, and indicated a weak net southerly flow.

From 1969 to 1982 nearly 400 current-meter records have been obtained in the Archipelago (Figure 1.3-2). These records are documented in the Arctic Data Compilation and Appraisal Reports, published in the Canadian

Data Report of Hydrography and Ocean Sciences (No. 5) series (Birch et al., 1983, 1987 and Fissel et al., 1983). More than 100 of these records are of less than 30 days duration. An even larger percentage is from spring, during which daylight and a stable ice platform make collection conditions most favourable. About 60 of the remaining records were collected by Panarctic Oil using Aanderaa current meters. A large percentage of these current data were below the stall speed of the instrument, and often the recorded directions were in error by 180°. As a result, none of these records will be considered here. Thus of the 400-odd records, approximately one-third are most useful for the determination of the residual circulation of the Archipelago. These records are summarized in Appendices 1 and 2. In many cases, these data provide important measurements of water circulation; however, often the data coverage is not adequate for estimates of volume transport.

Table 1-2 highlights the results of transport computations, based on the direct current measurement programs of the 1970's and 1980's. These current data provide a measure of the total current, not just the baroclinic component. For example, the geostrophic method may indicate a surface current of 20 cm/s relative to the assumed level of no motion (generally near bottom). However, the current near-bottom may be 10 cm/s and therefore the total surface current is actually 30 cm/s. Using the geostrophic method, the current through Smith Sound had previously been estimated at $0.4 \times 10^6 \text{ m}^3/\text{s}$ (Killerich, 1939) and $-0.4 \times 10^6 \text{ m}^3/\text{s}$ (Bailey, 1957). Sadler (1976a,b), using direct current measurements, determined a southerly transport of $0.67 \times 10^6 \text{ m}^3/\text{s}$.

The results of Prinsenberg and Bennett (1987) indicate that transport may vary by $\pm 50\%$ on a time scale of 4 to 6 days, similar to the variation associated with that of atmospheric disturbances. Also, a strong seasonal variation was evident in the Barrow Strait data. Walker (1977) noted that monthly and longer-term variability in water levels should be instrumental in altering the flow of water through the Archipelago. Such observations highlight the importance of obtaining long-term direct current measurements in the Archipelago.

Table 1-2: Summary of volume transports based on direct current measurements made in the Arctic Archipelago, 1970's to 1982. Positive transports are southerly or towards Baffin Bay. Units are $10^6 \text{ m}^3/\text{s}$.

Year	Reference	Area	Transport/Comments
1972	Sadler (1976a,b)	Smith Sound	$0.67 \pm 16\%$ for May ($0.67 \pm 28\%$ annual)
1976	Sadler, Serson and Chow (1979)	Fury and Hecla Strait	$0.04 \pm 25\%$ for May. Campbell (1958) computed a flux of 0.05 to 0.10 for late summer, using the dynamic method. Barber (1965) estimated a flux of 0.05 to 0.10, based on 13 hours of Ekman meter readings.
1976- 1977	Greisman and Lake (1978)	Byam and Austin channels, Pullen and Crozier straits	0.16 Byam and Austin; 0.04 Crozier and Pullen straits. These transports are for the spring period; there were indications of stronger flows in the winter.
1981- 1982	Prinsenberg and Bennett (1987)	Barrow Strait	0.5 with variations about the mean of ± 0.25 (April). Seasonal transport peaks in Sept. at 1.2 and falls to a minimum of 0.1 in November.

Measurements of Surface Drift

Ice-beset vessels provided the earliest measurements of surface drift (Figure 1.3-1). In recent years, radar mapping of ice motion and satellite tracking of both ice and drifters have provided most of the data. These Lagrangian data provide information on surface currents over a large area, and are often the first indicators of major currents. A summary of the results using these methods is included in Table 1-3.

The results of Marko (1978) and Fissel and Marko (1978) are presented in Figure 1.3-3. They are included here since the data represent the first evidence of certain important features of the flow in the Archipelago, in particular the preference for easterly flow along the southern side of eastern Parry Channel, and the coastal currents flowing in opposing directions on either side of Wellington Channel, Prince Regent Inlet, Admiralty Inlet, McDougal Sound and Peel Sound.

The overall circulation suggested by these data is a net drift south and east towards Baffin Bay. Currents are usually strongest along the sides of the channels, often being weak and directionally variable in mid-channel. The currents on opposite sides of the channels are often opposite in direction, a combination which is possible in terms of geostrophic dynamics if the width of the channel is large compared to the local internal Rossby radius of deformation (LeBlond, 1980).

Table 1-3: Lagrangian drift results, using radar and satellite tracking methods.

Year	Reference	Area	Comments
1970	Verrall, Ganton and Milne (1974)	Viscount Melville Sound and M'Clure Strait	Ice buoys were tracked by aircraft. During spring and summer, the ice in central M'Clure Strait drifted rapidly to the west, whereas in Viscount Melville Sound the drift was only weak westerly. The wind appeared to be the primary forcing mechanism.
1976	MacNeil, de Lange Boom and Ramsden (1978)	Barrow Strait	Radar was used to track ice motion during late summer and early fall. The ice was forced by both westerly and easterly winds greater than 8 knots. Average ice motion near Griffiths Island was to the east, with an anti-cyclonic flow close to the shore of Griffiths Island.
1973-1977	Marko (1978)	Eastern Parry Channel	Satellite images were used to map ice motion. The strongest easterly flows were observed in the southern portion of Parry Channel. An intrusive flow in Lancaster Sound was found, as was a northerly flow in the eastern half of Wellington Channel. Similar northward-eastern and southward-western flows were observed in McDougall Sound, Prince Regent and Admiralty inlets. Mid-channel ice motions were irregular.
1977	Fissel and Marko (1978)	Eastern Parry Channel	Nine drogued drifters were tracked by satellite. Results were similar to those of Marko (1978) above: northerly flow in eastern Wellington Channel and cyclonic intrusions of Prince Regent Inlet and Peel Sound.
1979	Fissel, Lemon and Birch (1982)	Eastern Parry Channel	Fourteen satellite-tracked drogued drifters indicated a net easterly drift with apparent cyclonic intrusion of Prince Prince Regent and Admiralty inlets.

2. DATA COLLECTION AND PROCESSING METHODS, 1982-1985 DATA

This report presents an analysis of the near-surface residual flow in the Northwest Passage, based on the current-meter data collected as part of a three-year study by the Institute of Ocean Sciences. Data reports are available (Buckingham, Lake and Melling, 1987 c, d, e) which detail the methods used in data collection and processing. Only a brief overview is presented here.

2.1 Data Collection

The large geographic size of the study area (Figure 2.1-1) prohibited detailed synoptic coverage. Therefore a three-year measurement program was planned. The western portion was sampled in 1982, the central portion in 1983 and the eastern portion in 1984 (Figure 2.1-1). Only near-surface currents were measured systematically, generally at 18 to 20 metres depth. Moorings were preferentially located near the coastlines in anticipation of a concentration of measurable flow near the shorelines. The current-meter locations, measurement period, and summary statistics are detailed in Table 2-1. Full details concerning the measurement techniques and initial data processing are provided in the three-volume data report (Buckingham, Lake and Melling, 1987 c, d, e) noted above.

Aanderaa (rotor and vane) current meters were used in all cases. Each instrument was equipped to measure speed, direction, temperature, and conductivity. The Aanderaa current speed measurement is based on the cumulative number of revolutions of the Savonius rotor over the sampling interval. The current direction is determined by the orientation, at the moment of recording, of a vane which is designed to align itself parallel to the flow.

The method used to moor the current meters depended on the ice conditions. Spring deployments from stable ice used a "vane-follower" configuration, in which a small vane monitors the flow direction relative to the pressure case, which was oriented via a torsionally rigid connection to the ice surface (Figure 2.1-2a). For the deployments where the ice was

Table 2-1: Details of current-meter records: location, period, depth, and summary statistics. Note that the statistics apply to the residual component of the current only and were computed over the entire record. The stability is the ratio of the vector-averaged speed to the mean speed.

CM Serial #	Site	Area	<u>Latitude</u>		<u>Longitude</u>		Depth (m)	<u>Period</u>		<u>Vector-Averaged</u>		<u>Res. Speed</u>		Stability (%)
			Deg.	Min.	Deg.	Min.		Start	Stop	Res. Vel. Speed Toward (cm/s) (°True)	Mean Max. (cm/s) (cm/s)			
1982 CM														
3395	01	Pr. Wales Strait	73	15.7	116	16.6	20.5	Mar. 25	June 24	08.3	260	8.5	22.9	97
5475	02	Pr. Wales Strait	73	14.6	116	16.6	20.5	Mar. 25	June 24	04.4	269	4.8	14.7	91
3228	03	Pr. Wales Strait	73	13.5	116	15.8	20.5	Mar. 24	Apr. 19	00.2	191	1.1	3.3	22
0972	04	Pr. Wales Strait	73	12.4	116	13.8	20.5	Mar. 25	Apr. 7*	01.7	242	2.1	4.5	79
5474	05	Pr. Wales Strait	73	11.6	116	15.0	20.5	Mar. 24	June 24	01.4	212	1.8	6.5	75
2470	06	Pr. Wales Strait	73	10.6	116	12.7	20.5	Mar. 24	June 24	00.8	191	1.5	5.8	50
1929	07	Pr. Wales Strait	73	09.2	116	09.7	20.5	Mar. 25	May 23	01.8	273	1.9	5.7	92
2468	08	Pr. Wales Strait	73	08.7	116	08.0	20.5	Mar. 25	May 3	00.6	358	1.1	3.7	55
3388	09	Pr. Wales Strait	73	05.0	116	34.7	20.5	Mar. 25	June 13	01.1	208	1.5	5.3	76
1935	10	Pr. Wales Strait	73	12.1	115	58.1	20.5	Mar. 25	June 24	00.5	311	1.6	5.2	30
2693	PW1	Pr. Wales Strait	72	47.1	117	49.7	10.0	Mar. 30	Apr. 29	02.9	205	3.4	7.3	85
5390	17	M'Clure Strait	74	26.9	113	51.0	18.5	Apr. 7	June 21	00.9	119	3.5	9.5	27
5473	16	M'Clure Strait	74	24.9	114	00.0	18.5	Apr. 6	June 21	01.5	318	2.7	10.4	54
2466	15	M'Clure Strait	74	17.7	114	30.0	18.5	Apr. 7	June 21	00.6	72	1.7	4.2	36
5472	14	M'Clure Strait	74	10.0	115	02.0	18.5	Apr. 7	June 21	00.7	296	1.9	5.8	37
5471	13	M'Clure Strait	73	59.9	115	27.7	18.5	Apr. 6	June 21	00.7	71	1.6	3.8	46
5456	12	M'Clure Strait	73	56.2	115	51.6	18.5	Apr. 6	June 21	00.9	81	2.1	4.2	45
1936	11	M'Clure Strait	73	55.7	116	08.9	18.5	Mar. 30	May 5	00.6	115	1.7	4.8	36
1939	19	Peel Point	73	29.7	113	19.3	18.5	Apr. 9	June 23	02.8	266	3.5	7.6	79
5391	18	Peel Point	73	19.8	113	58.0	18.5	Apr. 9	June 23	00.8	128	1.9	4.6	42
5389	26	Viscount Melville Sd	74	51.2	107	14.0	18.5	Apr. 18	June 20	00.8	150	2.3	7.1	33
5361	25	Viscount Melville Sd	74	48.0	107	11.0	18.5	Apr. 18	June 20	00.4	14	2.7	6.1	14
1932	24	Viscount Melville Sd	74	41.1	107	06.3	18.5	Apr. 18	June 19	01.4	270	2.4	6.4	59
1930	22	Viscount Melville Sd	74	00.8	106	35.8	18.5	Apr. 18	June 19	00.6	259	1.7	5.4	33
3387	21	Viscount Melville Sd	73	53.6	106	30.0	18.5	Apr. 18	May 30	01.6	167	2.8	6.3	59
1931	20	Viscount Melville Sd	73	48.7	106	25.9	18.5	Apr. 18	June 20	01.1	357	1.8	4.3	62

Table 2-1 (Cont'd):

CM Serial #	Site	Area	Latitude		Longitude		Depth (m)	Period		Vector-Averaged				Stability (%)
			Deg.	Min.	Deg.	Min.		Start	Stop	Res. Vel. Speed (cm/s)	Toward (°True)	Res. Speed Mean (cm/s)	Max. (cm/s)	
1983 CM														
3223	62	Byam Martin Channel	75	55.6	105	22.6	18.5	Apr. 2	May 23	06.5	158	6.5	10.9	99
3278	63	Byam Martin Channel	75	58.1	105	10.6	18.5	Apr. 2	May 18	05.2	175	5.4	10.1	96
3387	65	Byam Martin Channel	76	02.9	104	38.8	18.5	Apr. 2	Apr. 19*	05.9	149	6.1	9.1	97
3388	66	Byam Martin Channel	76	04.6	104	27.9	18.5	Apr. 2	May 23	05.1	124	5.5	11.1	93
3395	71	Austin Channel	75	23.2	102	29.3	18.5	Apr. 1	May 23	03.0	87	4.0	8.3	76
2466	71	Austin Channel	75	23.3	102	38.6	73.0	Apr. 1'83	Mar. 31'84 ³	02.6	48	3.9	11.5	68
2470	71	Austin Channel	75	23.3	102	38.6	123.0	Apr. 1'83	Mar. 31'84 ³	03.0	42	3.5	11.4	85
1939	57	Byam Martin Island	74	51.6	104	12.8	18.5	Apr. 3	May 4*	01.7	113	1.9	3.2	86
1936	58	Byam Martin Island	74	59.1	104	13.4	18.5	Apr. 3	May 6 ¹ *	02.0	230	2.7	7.4	75
2467	72	Bathurst Island	74	57.1	100	26.9	18.5	Apr. 6	May 22	03.9	284	4.3	8.6	91
1932	74	Bathurst Island	74	51.0	100	49.7	18.5	Apr. 6	May 22	02.4	175	2.7	6.7	90
5361	81	Pr. of Wales Island	73	52.9	100	59.7	18.5	Apr. 6	June 11	03.1	62	3.2	6.1	97
1931	79	Pr. of Wales Island	74	00.2	101	39.8	18.5	Apr. 6	May 2*	00.4	203	1.8	4.0	25
1930	82	M'Clintock Channel	72	56.3	104	52.0	18.5	Apr. 7	June 10	01.2	165	2.3	5.9	53
5456	83	M'Clintock Channel	72	54.8	104	29.0	18.5	Apr. 7	June 10	01.2	351	1.7	7.0	70
5474	86	M'Clintock Channel	72	51.9	103	08.6	18.5	Apr. 7	June 10	01.8	181	2.1	5.0	87
0972	87	M'Clintock Channel	72	50.5	102	54.1	18.5	Apr. 7	May 8*	01.2	26	1.5	2.9	83

Table 2-1 (Cont'd):

CM Serial #	Site	Area	<u>Latitude</u>		<u>Longitude</u>		Depth (m)	<u>Period</u>		Vector-Averaged				Stability (%)
			Deg.	Min.	Deg.	Min.		Start	Stop	<u>Res. Vel.</u>		<u>Res. Speed</u>		
										Speed	Toward	Mean	Max.	
										(cm/s)	(°True)	(cm/s)	(cm/s)	
1984 CM														
1936	46	Barrow Strait	74	12.5	93	46.8	18.5	Apr. 25	June 8	18.9	73	19.0	26.7	99
1386	42	Barrow Strait	74	34.2	94	01.2	18.5	Apr. 27	June 8	04.7	54	4.8	9.0	97
3388	42	Barrow Strait	74	34.2	94	01.2	51.0	Apr.27'84	Apr. 12'85	02.6	146	5.6	20.5	46
1935	42	Barrow Strait	74	34.2	94	01.2	100.0	Apr.27'84	Mar. 24'85	02.9	115	4.5	20.5	64
0217	WC13	Wellington Ch. (S)	74	47.7	93	17.8	18.5	May 1	June 9	02.4	207	3.1	7.9	78
0218	WC12	Wellington Ch. (S)	74	47.7	92	48.1	18.5	May 1	June 9	03.7	324	4.3	8.7	86
1939	WC11	Wellington Ch. (S)	74	47.8	92	27.8	18.5	Apr. 19	June 1	00.8	331	2.4	7.3	35
1932	WC10	Wellington Ch. (S)	74	47.5	92	21.6	18.5	Apr. 19	May 19	01.1	223	2.1	5.6	52
3223	WC 8	Wellington Ch. (S)	74	47.7	92	09.2	18.5	Apr. 19	June 9	01.8	193	2.6	5.8	68
3228	WC 7	Wellington Ch. (N)	75	15.2	93	22.8	18.5	Apr. 19	June 9	07.8	159	8.1	16.2	97
2686	WC 6	Wellington Ch. (N)	75	14.4	92	59.6	18.5	Apr. 20	June 9	02.7	145	3.3	6.9	82
2687	WC 5	Wellington Ch. (N)	75	14.4	92	44.4	18.5	Apr. 8	June 7	05.2	148	5.6	11.5	93
1931	WC 4	Wellington Ch. (N)	75	14.1	92	40.0	18.5	Apr. 8	June 7	02.7	334	3.7	9.0	75
1930	WC 3	Wellington Ch. (N)	75	14.1	92	35.4	18.5	Apr. 8	June 7	12.3	338	12.4	23.2	99
0972	WC 2	Wellington Ch. (N)	75	14.1	92	33.8	18.5	Apr. 7	Apr. 23*	12.5	338	12.5	21.6	99
0801	WC 1	Wellington Ch. (N)	75	13.3	92	31.7	18.5	Apr. 7	June 7	05.2	318	5.8	15.0	89
5391	PSW	Penny Strait (W)	76	36.2	97	25.2	49.0	Apr.23'84	Apr.12'85	11.2	184	12.2	26.7	92
5471	PSW	Penny Strait (W)	76	36.2	97	25.2	138.0	Apr.23'84	Apr.18'85	03.0	274	5.4	23.0	55
5361	PSE	Penny Strait (E)	76	38.7	96	54.6	43.0	Apr.16'84	Apr.16'85	13.8	220	14.7	36.6	94
5456	PSE	Penny Strait (E)	76	38.7	96	54.6	131.0	Apr. 23	Sep. 10 ²	8.1	219	8.7	16.8	93

*Relatively short record

¹Bad data, April 13-16²Record ends Sep. 10, 1984³Records actually end Apr. 30, 1984. The Apr. 1984 portion was not analyzed for this project.

not expected to remain stable, two methods were employed. The first, used in regions of relatively strong geomagnetic field, relied on a traditional bottom-anchored taut-line mooring, and directional reference was based on the instrument's internal magnetic compass (Figure 2.1-2b). In the second method, used in the central and eastern regions where the geomagnetic field is too weak for the current-meter compass to be reliable, the instruments were anchored to bottom using a torsionally-rigid pipe (Figure 2.1-2c). The orientation of the instrument was determined after deployment using a gyrocompass attached to the mooring until this time and brought immediately to the surface for reading.

An error was discovered in the processing of seven current-meter data sets: at sites 57, 58, 65 and 83 for 1983 data and at sites WC12, WC13 and PSW (138 m depth) in 1984. All current directions were in error by constant amounts throughout the full record; corrections were applied to all results herein.

2.2 Data Filtering

Currents in the Archipelago vary over wide ranges of amplitude and period. Higher frequency motion, greater than 2 cycles per day (cpd), largely reflects turbulence and forcing by local winds. At frequencies near 1 and 2 cpd, the motion is mainly due to tidal forcing and inertial oscillations. For this study, the residual current was assumed to be the component of the flow at frequencies less than 1 cpd, or equivalently at periods greater than 1 day.

In order to remove the variability at frequencies greater than 1 cpd, a low-pass digital filter was applied to the hourly data. The filter is symmetric and has 72 coefficients; therefore 36 data points (or 1.5 days) are lost at each end of the record after filtering. The filter response curve is illustrated in Figure 2.2-1, and the typical effect on hourly data is presented in Figure 2.2-2. At Station 42 in Barrow Strait, the hourly observed currents reversed direction daily, due to the tidal flow. However, after filtering, one can see that the residual flow is toward the north and east, with only one reversal in direction, on May 20.

2.3 Uncertainties in the Speed and Directional Data

The estimated accuracy and precision of the current meter data are presented in Table 2-2. The values for speed are based on the manufacturer's specifications, whereas those for direction are largely governed by the mooring configuration and the accuracy of the system for directional referencing of the instrument. Refer to Buckingham, Lake and Melling (1987 c, d, e) for further information.

Table 2-2

Estimated accuracy and precision of the
Aanderaa RCM-4 Current Meter Data
(from Buckingham, Lake and Melling [1987 c, d, e])

Instrument	Parameter	Accuracy	Precision	Resolution
RCM4	Speed (cm/s)	±2%	±7%	.05 cm/s
RCM4 (hose)	Direction (°T)	±11°	±7°	0.4°
RCM4 (pipe)	Direction (°T)	±30°	±16°	0.4°
RCM4 (freely suspended)	Direction (°T)	±11°	±7°	0.4°
RCM 4	Temperature (°C)	±.005	±.005	±.005
RCM4	Conductivity Ratio	±.0025	±.0008	0.00016

Measurements of residual currents are subject to some uncertainties in addition to these basic measurement errors in the speed and direction data.

2.3.1 Weak Residual Flow in the Presence of a Strong Tidal Flow

At measurement sites where comparatively large tidal currents occur in combination with weak residual flows, uncertainties in the compass calibrations of a meter can cause significant errors in the computed residual flows. Under these circumstances, the error in the measured

direction of the tidal currents can result in an erroneous contribution to the computed mean flow.

To estimate the magnitude of this effect, a mathematical model was applied. In this model, the currents at a particular point in space consist of a mean flow U_m and a tidal flow U_T at single frequency σ , having a major axis amplitude A and minor axis B . The tidal ellipse is oriented at an angle θ_T with respect to the direction of the mean flow, i.e.

$$U_T = e^{i\theta_T} [A \cos(2\pi\sigma t) + iB \sin(2\pi\sigma t)].$$

The measured currents are subject to a direction error modelled as:

$$\Delta = C \cdot \cos(\theta - \theta_C) + D$$

where θ_C is the direction at which the error is a maximum (i.e. $\Delta = C + D$). The currents as measured, U' , then are:

$$U' = e^{i\Delta}(U_m + U_T)$$

The error in the mean flow is then computed as the difference between the mean measured flow U' averaged over two tidal cycles, and the true mean flow.

The model described above was applied at the M2 tidal frequency ($\sigma = 0.080511 \text{ h}^{-1}$), for a mean speed in alignment with the maximum tidal flow ($\theta_T = 0$). The model was run for four cases ranging from maximum (Case II) to typical (Case III) directional errors (Figure 2.3-1). The uncertainty in the computed mean flows can be substantial for weak mean flows combined with strong tidal flows. For example, a 1.0 cm/s mean flow in the presence of a 10 cm/s tidal flow would be subject to uncertainties of 7 to 47%, for the typical and maximum direction errors.

2.3.2 Subthreshold Currents

The Aanderaa current meter senses current speed using a rotor; the current speed is proportional to the rate of rotor revolution. Direction is determined by the orientation of a large vane. Subthreshold currents occur when the current speed is less than that required to make the rotor complete the necessary number of revolutions (usually 4) to produce a speed count. This occurs at speeds less than about 2.2 cm/s ("stall" speeds). In the translation of the data tapes, records with no speed counts were arbitrarily assigned a speed value of 2.2 cm/s, although the actual speed may have been anywhere between 0.0 and 2.2 cm/s. This procedure may result in erroneously high speeds. As an example, consider a unidirectional steady flow of 0.5 cm/s. No rotor counts would occur, and the translation of the Aanderaa current meter tape would assign a speed of 2.2 cm/s to these data, indicating speeds four times too high.

In areas of weak currents in the Arctic, the flow is generally not unidirectional. Moreover, the Aanderaa vane has a much lower threshold than the 2.2 cm/s threshold of the rotor. Consequently the direction of the flow is recorded even at speeds less than 2.2 cm/s. Thus, the overestimated speeds generally occur over varying directions, with the result that the overall effect on the vector average velocity is much reduced.

The 1982-1985 data were examined for frequent occurrences of stall speeds. In most regions the rotor was stalled less than 10% of the time (Figure 2.3-2). The highest percentage of stall speeds occurred in 1982 in M'Clure Strait and Viscount Melville Sound. The raw, 15-minute data from two of these records were examined to determine what effect there may have been on the computed mean velocities.

In the M'Clure Strait and Viscount Melville Sound region, the mean vector-averaged currents were very small, generally less than 1.0 cm/s. The currents are dominated by the tidal flow which is mainly semi-diurnal, flooding towards the west and ebbing to the east. Figure 2.3-3a shows a portion of the 15-minute speed and direction data from CM16 in M'Clure Strait. This period occurred during a time of strongest tidal flows

(spring tides). The semi-diurnal tide resulted in four periods of peak flow per day, two floods and two ebbs. The record shows that during both the slack high-water and slack low-water periods the rotor was stalled for 1 to 2 hours, but the direction vane continued to respond to the oscillatory flow. As a result of the rotor being stalled, the current during slack-water periods was assigned a probably higher-than-actual speed of 2.2 cm/s. However, any error thus introduced would tend to be minimized by the averaging process resulting from the correctly-recorded direction reversals.

In other instances, again in M'Clure Strait the rotor responded to only the flood or the ebb flow, but not both (Figure 2.3-3b,c). In such cases the assigned stall speed of 2.2 cm/s results in an overestimate of either the flood or ebb flow. However, the errors would again tend to be balanced out since one can find cases where both the flood and ebb cycles are similarly affected.

Although it is difficult to quantify, in general the effect of subthreshold currents on the mean flows appears to have been minimal. Occurrences of rotor stalls were most common in the 1982 M'Clure Strait-Viscount Melville Sound data; here the vector averaged flows were generally less than 1 cm/s. The dominant flow there was tidal and during periods of neap tides the rotors often stalled, indicating a very weak residual flow. The adverse effect of the assignment of a speed of 2.2 cm/s to stalled counts is believed to be minimal due to the oscillatory nature of the flow, resulting in a general averaging out of the error. Since the residual flows are so small the net error is not believed to be significant.

3. RESULTS

3.1 Speed and Direction Distribution, and Mean Residual Flow Vectors

The vector-averaged velocity, and the distributions by speed and by direction of the residual currents, are presented graphically in this section. The results are largely from near-surface measurements, typically 20 m depth, from moored current meters. The data are grouped into springtime (Section 3.1.1) and seasonal (Section 3.1.2). Only the 1982-1985 data collected by IOS are presented here. Unless specified otherwise, discussion always refers to the residual portion of the current.

3.1.1 Springtime, 1982-1985

The low-pass-filtered residual currents were analyzed to determine the distribution of speed and of direction, and the vector-average mean. The results are summarized in Figures 3.1-1 through 3.1-9. Results are also included for the springtime (April 1-July 1) portion of the year-long records. There are three figures per year, with each figure covering a specific area. Map scales vary from 1:0.5 million to 1:2.0 million. Current-meter sites are identified by station number/depth. Included with each figure are the appropriate portions of Table 2-1, summarizing the current statistics from the instruments in that area.

The right-hand side (r.h.s.) of each figure depicts the directional distribution of the residual currents at each site. The lengths of the radial sticks represent the percentage of directions within each 30° class; the mean speed for each directional class is represented by the distance from the centre to the intersection of the perimeter line and the radial stick. The left-hand side (l.h.s.) of each figure illustrates the distribution of residual speeds, as well as the vector-averaged mean flow vectors. Mean flow vectors of magnitude less than 2 cm/s are represented by an arrowhead without a tail. The actual values of the vector mean, the mean speed and the maximum speed for the residual flows may be obtained from Table 2-1.

Prince of Wales Strait

During the spring of 1982, the net residual flow through Prince of Wales Strait was toward the southwest (Figure 3.1-1). The flow was concentrated on the northwest side, where the speed reached a maximum value of 23 cm/s, and averaged 8.5 cm/s (Site 01). At Site 01 the flow was very steady and the vector-averaged magnitude was 8.3 cm/s. The main flow appeared to be centred near Site 01 and spanned a 4-6 km width.

Towards the centre of the Strait, the residual flow was weaker and more directionally variable than near the northwest shore. Mean speeds were typically 2 cm/s, and peak speeds 5 cm/s. The net circulation remained southwesterly. On the southeastern shore, a weak counter-current was evident at Site 08, with a mean speed of only 1 cm/s. The direction distribution confirms the tendency for southwesterly flow through this section. A weak southwesterly residual flow also occurred downstream at Site PW1.

M'Clure Strait

During the spring of 1982, the residual circulation in M'Clure Strait and near Peel Point was weak and variable in direction. Vector-averaged velocities were generally less than 1 cm/s (Figure 3.1-2) and maximum residual speeds were less than 10 cm/s. The records from the meters nearest shore (Sites 11, 12, 16, 17, 18 and 19) indicated at least some bathymetric control, since the flow directions generally paralleled the depth contours. Mean current speeds were greatest at Sites 16 and 17, on the northern side of M'Clure Strait, and at Site 19 near Peel Point. The vector-averaged velocities at Sites 16 and 17 remained small, however, with no evidence of a well-defined coastal current. The largest vector-averaged velocity was 2.8 cm/s, recorded at Site 19 near Peel Point. This net westerly flow, averaging 3.5 cm/s, may have provided at least some of the waters flowing southwestward into Prince of Wales Strait in 1982.

Central Viscount Melville Sound

Data were collected at six sites across Viscount Melville Sound during the spring of 1982. The vector-averaged residual flows were weak, typically 0.5 to 1.5 cm/s (Figure 3.1-3). Mean speeds were 2 to 3 cm/s. At Sites 22, 24 and 26, there was a preference for along-bathymetric flow, as evident from the current roses. Off Stefansson Island (Sites 20 and 21) however, the flows tended to cross bathymetry and the vector-averaged currents were in opposition. No strong coastal currents are evident along either shore.

Eastern Viscount Melville Sound

During the spring of 1983, current data were gathered at six sites in the area adjoining Barrow Strait in the west (Figure 3.1-4). The residual flows here were slightly stronger than in central Viscount Melville Sound; vector averaged velocities were 2 to 4 cm/s and the currents were quite stable (except at Site 79). The residual flows were generally parallel to the bathymetry, and evidence for coastal currents along the coasts of Bathurst and Prince of Wales Islands can be seen in the directional distribution at Sites 72 and 81, respectively. The largest velocities were at Site 72, toward the northwest; these opposed the net outflow from Austin Channel. The next strongest flow was at Site 81, where the currents were easterly towards Barrow Strait. Away from the coastline, at Sites 57 and 79, the residual flows were weaker and more directionally variable.

M'Clintock Channel

The residual flow along the shores of M'Clintock Channel in the spring of 1983 was weak, with vector-averaged speeds of 1.2 to 1.8 cm/s (Figure 3.1-5). The flow was generally north-south, aligned with the bathymetry. However, between each station the net flow vector reversed direction, suggesting a complicated, although weak, flow structure.

Byam Martin Channel and Austin Channel

The residual flow through Byam Martin Channel during the spring of 1983 was southerly (Figure 3.1-6) with mean speeds of 5.5 to 6.5 cm/s, and maximum values of 10 to 11 cm/s. The currents varied little in direction, as is evident from the high stability values (Table 2-1). Reversals towards the north were observed only at Site 66, near the eastern shore, and these were relatively short-lived events which occurred at intervals of about 12 days.

At Site 71, on the eastern side of Austin Channel, the residual flow was weaker, averaging 3.0 cm/s, and variable in direction. However, the results suggest a continued south-southeasterly flow in this area.

Penny Strait

The uppermost instruments in Penny Strait were near 45 m depth, deeper than the 18.5 m depth of the other near-surface meters. The near-surface residual flow in Penny Strait during the spring of 1984 was southerly with mean speeds of 12 to 15 cm/s, and maximum values of 30 to 40 cm/s (Figure 3.1-7). Directional variability was low, resulting in vector-averaged velocities only slightly less in magnitude than the mean speeds. The southwesterly flow at Station PSE reflects the local bathymetry.

Near-bottom residual flows were weaker, about half as strong as those near the surface. At both stations the directional variability was similar at both depths.

Wellington Channel

Midway up Wellington Channel at its narrowest section (WC1-WC7), the residual flow was southerly in the western and central portions, and northerly along the eastern shore (Figure 3.1-8), during the spring of 1984. The northerly flow was confined within about 6 km of shore. In the core of this current (Station WC3), large mean and maximum residual speeds of 12.4 and 23.2 cm/s occurred (Table 2-1) with a vector-averaged velocity

of 12.3 cm/s. The southerly flow appears to have been centred near Station WC7, although the station spacing is too large to assess whether the core of the main southerly current was sampled. At WC7, the mean and maximum residual speeds were 8.1 and 16.2 cm/s, with a vector-averaged velocity of 7.8 cm/s.

Further to the south, near the junction of Wellington Channel and Barrow Strait (Stations WC8-WC13), the measured residual flows were much weaker, and there was no evidence of the two counter-flowing currents observed at the more northern section. The strongest flows occurred at WC12 and were northerly. One can speculate that the station spacing, particularly between WC12 and WC13, was insufficient to define adequately the residual circulation.

Barrow Strait

Current-meter data were obtained on the northern and southern sides of Barrow Strait during the spring of 1984. Both sites recorded a residual easterly flow; however, the strongest and most stable flow by far was at Station 46 on the southern side (Figure 3.1-9). At Station 46 the mean and maximum residual flows were 19.0 and 26.7 cm/s, with a vector-averaged velocity of 18.9 cm/s. At the northern site, the vector-averaged velocity was only 4.7 cm/s.

Summary

The magnitudes of the vector-mean and of the maximum residual flow in springtime vary considerably within the Northwest Passage (Figure 3.1-10). From the 73 individual current records, the amplitude of the vector mean ranged from near-zero (0.2 cm/s) to 18.9 cm/s, while the maximum residual current varied from near 3 cm/s to 36.6 cm/s. Geographic variations on the velocity statistics for residual currents in springtime are summarized below.

The residual currents were larger in the easterly and northerly channels: Barrow Strait, Penny Strait, Wellington Channel and Byam Martin Channel. The smallest magnitudes were measured in M'Clintock Channel and the western portions of Parry Channel.

Within individual channels, large differences were evident in the magnitude of residual flows, most notably in Prince of Wales Strait, eastern Viscount Melville Sound and Wellington Channel.

In each of these channels, narrow, enhanced residual currents were present along the coastline. These flows were parallel to the coastline and local bathymetry, and with the coast to laying the right of the current direction.

The characteristics of the coastal currents are summarized for each channel in which they were clearly observed:

Prince of Wales Strait: A strong southwesterly current occurred within 4-6 km of the Banks Island coast. At the two stations situated in the core of the current, the residual flow was nearly unidirectional, with measured vector-mean magnitudes of 8.3 and 4.4 cm/s (maximum values of 22.9 and 14.7 cm/s).

Eastern Viscount Melville Sound: A northeasterly flowing coastal current (3.1 cm/s) was measured at Site 81, approximately 9 km offshore of Prince of Wales Island on the southern side of the sound. This current was confined to a width of less than 30 km; the currents at adjoining Site 79 were much weaker (0.4 cm/s) and more directionally variable. On the opposite side of the sound, a westerly flowing coastal current (3.9 cm/s) was observed 9 km from the shore of Bathurst Island at Site 72.

Wellington Channel: Two oppositely directed coastal currents were present in the northern transect of current-meter moorings. On the eastern side of the channel, the northerly-flowing coastal current had a width of approximately 7 km. The strongest net flow, 12.5 cm/s, occurred 3 km from the coast. A southerly coastal current was present on the opposite side of the channel.

Coastal currents were not evident in all areas. For example, in Byam Martin Channel, strong southerly flow was present across the full width of this comparatively narrow waterway. The very small mean flows in the southern and western regions did not provide evidence of coastal current régimes.

In other areas, the array of current meter moorings was not adequate to delineate coastal currents (eg. Barrow Strait and Penny Strait). A different situation occurred across southern Wellington Channel, where an array of seven current-meter moorings was insufficient to detect opposing currents, such as were measured simultaneously 60 km to the north. This may be an indication of more complex current patterns on the more southerly section due to the proximity of the junction of Wellington Channel and Lancaster Sound.

3.1.2 Seasonal Variability

In Section 3.1-1, the residual-current measurements for the springtimes (April through June) of 1982 through 1984 were summarized. Some current meters were moored throughout the winter, and nearly year-long records were thereby obtained (Table 2-1). These include two records at Site 71 in Austin Channel, two at Station 42 in northern Barrow Strait, and three at two sites in Penny Strait. In all cases, the year-long records were obtained from greater depths than were the springtime records. Springtime instruments were moored near 20 m depth, whereas the year-long meters were at least 25 m deeper. The choice of seasons applied here is: April 1-June 30, spring; July 1-September 30, summer; October 1-December 31, fall; January 1-March 31, winter. The rationale for this particular choice is the desire to relate the currents to the extent of ice cover. July, August and September are generally the months of lightest ice concentration. Freeze-up is most rapid after September and breakup first occurs during June in Lancaster Sound and Amundsen Gulf.

Austin Channel

The year-long data records from Site 71 in Austin Channel indicate that the flows at mid-depth and near the bottom were of strength equal to or greater than those near the surface. In nine of the twelve months, the vector-averaged speed at 123 m depth was greater than that at 73 m depth. There was also a tendency for the residual flow vectors to rotate counterclockwise with increasing depth (Figure 3.1-11). This may reflect a

response, to the bottom topography, increasing with proximity to the seafloor.

The direction of the residual flow vectors did not vary substantially with month. The flow remained northeasterly. There did appear to be a seasonal variation in speed at both 73 and 123 m depths. The strongest residual currents occurred during fall (123 m) and winter (73 m). The weakest flows were recorded during the summer months.

Penny Strait

A strong vertical shear was evident in the measured current structure in Penny Strait (Figure 3.1-12). The residual flow in the 43 to 49 m depth range was nearly twice as strong as that near the bottom. The shear was most pronounced at Site PSW. Near the bottom at PSW the flow was significantly slower than near the surface, and reversals to the north occurred frequently.

The largest near-surface, vector averaged flows occurred during the summer months. A strong seasonal variability was observed only at Site PSW, where the October and November currents were noticeably reduced in magnitude and stability.

The peak flow speed of 36.6 cm/s during the fall at Site PSE/43, was the largest recorded during the 1982-1985 period.

Barrow Strait

Little vertical shear is apparent from an examination of the monthly vector averaged velocities at 50 and 100 m depths at Site 42 in northern Barrow Strait (Figure 3.1-13).

A seasonal variation occurs, since the flow during late summer and early fall was westerly and southerly, whereas during the remaining months it was primarily easterly. Peak speeds were largest during the summer/fall period. In 1981, data collected, by the Canada Centre for Inland Waters

(OCIW), in southern Barrow Strait (Site 46) indicated a significant strengthening of flow towards the east during the summer months (Prinsenberg and Bennett, 1987). The reversal to westward flow at Site 42 during summer in 1984 may perhaps be related to a postulated simultaneous increase in easterly flow along the southern side of the Strait, such as occurred in 1981.

3.2 Auto-Spectra

Spectral (or Fourier) analysis techniques were applied to the low-pass filtered current data to elucidate the frequency composition of residual current fluctuations. Each record was initially divided into N segments or blocks of equal duration. The raw spectral estimates, computed individually from each block, were averaged to improve the statistical reliability of the spectral estimates. The results from the auto-spectral analysis consist of the computed variances for a discrete set of frequency (or period) ranges (bands). The range of frequencies (or periods) for each band is summarized in Table 3.2-1. For each frequency band, we compute the following parameters:

- root-mean square amplitude of current fluctuations along the major and minor axes of variation;
- root-mean square amplitude of current fluctuations resolved into clockwise (cw) and counterclockwise (ccw) rotating current vectors. This representation is independent of the coordinate system used.

The analytical methods are described in Appendix 3.

3.2.1 Springtime, 1982-1985: Regional Comparisons

Current fluctuations in a spectral representation are summarized in Figure 3.2-1 and in Table 3.2-2. Spectral variances have a notably different regional distribution than do the magnitudes of residual currents. At sites with the largest residual currents (vector mean >5 cm/s), the amplitudes of the flow fluctuations are the largest recorded in

Table 3.2-1

The range of periods over the frequency bands used in the spectral analysis of this study for (a) Wellington Channel (springtime), (b) all other areas (springtime) and (c) year-long data sets.

Band Label	Centre Frequency	Frequency Bandwidth	Periods in Each Band			No. of Statistical Degrees of Freedom
			Lowest	Middle	Highest	
(a) Wellington Channel - N Blocks of 11.25 days duration						
I	0.089	0.089	22.50	11.25	7.50	2xN
II	0.178	0.089	7.50	5.63	4.50	2xN
III	0.311	0.178	4.50	3.22	2.50	4xN
IV	0.489	0.178	2.50	2.05	1.73	4xN
V	0.711	0.267	1.73	1.41	1.18	6xN
(b) all other areas - N Blocks of 12.5 days duration						
I	0.080	0.080	25.00	12.50	8.33	2xN
II	0.160	0.080	8.33	6.25	5.00	2xN
III	0.280	0.160	5.00	3.57	2.78	4xN
IV	0.440	0.160	2.78	2.27	1.92	4xN
V	0.640	0.240	1.92	1.56	1.32	6xN
(c) year-long data sets - N blocks of 62.5 days duration						
A	0.016	0.016	125.00	62.50	41.70	2xN
B	0.032	0.016	41.70	31.30	25.00	2xN
IA	0.056	0.032	25.00	17.90	13.90	4xN
IB	0.096	0.048	13.90	10.40	8.33	6xN
II	0.160	0.080	8.33	6.25	5.00	10xN
III	0.280	0.160	5.00	3.57	2.78	20xN
IV	0.440	0.160	2.78	2.27	1.92	20xN
V	0.640	0.240	1.92	1.56	1.32	30xN

the study area. However, the fluctuation amplitude amounts to only 30 to 50% of the magnitude of the mean flow. The low relative amplitude of the fluctuations reflects the directional steadiness of current at these locations.

Where the residual-flow magnitude is low, the relative amplitude of the fluctuations shows considerable variation. In M'Clintock Channel, very low levels of fluctuation accompany the very low mean flow. However in M'Clure Strait and western Viscount Melville Sound, the amplitude of fluctuations is large relative to the residual flow. The fluctuations in the residual flow are particularly enhanced at Sites 16 and 17 on the

Table 3.2-2: Residual-flow parameters derived from auto-spectral analyses for all springtime records. The vector means may differ from those of Table 2-1 due to shorter record lengths used in the spectral analyses.

STN	START	#SAM	#NBLK	POW.	MAJ SP.	MIN SP.	CCW SP.	CW SP.	BAND I SP.	% CCW	% CW	CC/C RATIO	%	MAX BAND	ALL RMS	LOW RMS
<----(CM/S)**2-DAY----->																
1984 AUTO-SPECTRA																
46	4/28/12	300	3	112.1	93.8	18.3	41.6	70.5	32.0	37%	63%	1.69	28.6%		4.2	2.3
42	4/28/12	300	3	40.7	31.7	9.0	26.3	14.4	19.5	65%	35%	1.83	48.0%		2.6	1.8
WC1	4/10/6	270	5	204.2	178.8	25.4	125.1	79.1	120.7	61%	39%	1.58	59.1%		6.0	4.6
WC2	4/10/6	270	1	472.0	461.6	10.4	240.1	232.0	349.2	51%	49%	1.03	74.0%		9.2	7.9
WC3	4/10/6	270	5	199.0	185.3	13.7	113.1	85.8	153.4	57%	43%	1.32	77.1%		5.9	5.2
WC4	4/10/6	270	5	91.2	61.6	29.6	35.7	55.5	65.5	39%	61%	1.55	71.8%		4.0	3.4
WC5	4/10/6	270	5	68.7	46.7	22.0	39.3	29.4	36.5	57%	43%	1.34	53.2%		3.5	2.5
WC6	4/21/12	270	4	50.9	31.4	19.4	13.7	37.2	23.0	27%	73%	2.72	45.1%	*	3.0	2.0
WC7	4/21/12	270	4	89.2	77.9	11.3	42.2	47.0	41.1	47%	53%	1.11	46.1%		4.0	2.7
WC8	4/21/12	270	3	31.4	28.7	2.7	12.4	19.0	8.2	40%	60%	1.52	26.0%		2.4	1.2
WC10	4/21/12	270	2	47.9	38.9	9.0	20.3	27.7	17.4	42%	58%	1.37	36.2%		2.9	1.8
WC11	4/21/12	270	3	78.0	55.5	22.5	28.4	49.6	20.6	36%	64%	1.75	26.4%		3.7	1.9
WC12	5/2/18	270	3	102.1	60.9	41.2	26.2	75.9	62.8	26%	74%	2.90	61.5%	*	4.3	3.3
WC13	5/2/18	270	3	46.8	31.1	15.7	13.4	33.3	19.6	29%	71%	2.48	41.9%		2.9	1.9
PSWu	4/28/12	300	6	182.9	127.7	55.2	117.7	65.1	109.5	64%	36%	1.81	59.9%		5.4	4.2
PSWI	4/28/12	300	6	109.2	68.0	41.2	53.7	55.5	50.6	49%	51%	1.03	46.4%		4.2	2.8
PSEu	4/28/12	300	6	149.4	96.0	53.4	59.8	89.6	80.4	40%	60%	1.50	53.8%		4.9	3.6
PSEI	4/28/12	300	6	185.7	82.7	103.1	66.8	118.9	101.0	36%	64%	1.78	54.4%	*	5.5	4.0
1983 AUTO-SPECTRA																
57	4/8/10	300	2	19.7	15.8	3.9	8.1	11.6	12.2	41%	59%	1.44	61.8%		1.8	1.4
58	4/8/10	300	2	68.4	53.8	14.6	38.9	29.5	37.7	57%	43%	1.32	55.1%		3.3	2.5
72	4/8/10	300	3	99.3	89.1	10.2	41.6	57.8	68.3	42%	58%	1.39	68.7%		4.0	3.3
74	4/8/10	300	3	41.9	24.9	16.9	28.1	13.8	16.8	67%	33%	2.04	40.2%	*	2.6	1.6
79	N/A															
81	4/8/10	300	3	33.2	19.9	13.4	12.2	21.0	9.6	37%	63%	1.73	29.0%	*	2.3	1.2
71	4/8/11	300	3	120.8	85.8	35.0	73.8	46.9	63.8	61%	39%	1.57	52.8%		4.4	3.2
62	4/8/11	300	3	50.2	41.8	8.4	21.0	29.3	33.6	42%	58%	1.40	66.8%		2.8	2.3
63	4/8/11	300	3	69.2	42.9	26.3	30.5	38.8	15.9	44%	56%	1.27	22.9%		3.3	1.6
65	N/A															
66	4/8/11	300	3	103.0	84.7	18.4	60.1	42.9	57.7	58%	42%	1.40	56.0%		4.1	3.0
82	4/9/11	300	4	29.8	19.6	10.2	12.6	17.1	17.0	42%	58%	1.36	57.2%		2.2	1.7
83	4/9/11	300	4	10.6	6.4	4.2	4.5	6.1	5.8	43%	57%	1.35	54.8%		1.3	1.0
86	4/9/11	300	4	17.8	9.3	8.6	7.8	10.0	7.3	44%	56%	1.27	41.0%	*	1.7	1.1

northern side of M'Clure Strait, where they reach values near 3 cm/s. The fluctuation amplitudes also are notably greater than the mean flow at Sites 6, 8 and 10 in Prince of Wales Strait, and at Sites 10 and 11 on the eastern side of southern Wellington Channel.

The spectral results, using rotary coordinates, reveal generally low levels of rotary polarization. Such a result is hardly surprising in view of the tendency, at most sites, for the residual currents to be oriented along a single axis, usually parallel to the coastline or to local bathymetry. Two sites exhibiting large clockwise preference in the residual current fluctuations were Sites 6 and 12, both located in the western half of Wellington Channel, where clockwise rotations represented 72 and 74% of the total variance. Counterclockwise fluctuations were dominant at Sites 18, 19, 21 and 22 in the southern half of Western Viscount Melville Sound, (ranging from 69 to 76% of total variance) and at Site 74, further to the east in this Sound (67% of total variance).

The current fluctuations are dominated by longer-period variations. Of the 55 spectra of springtime currents, 42 had peak values in frequency band I (periods of 8.3 to 25 days). Spectral levels in the two highest frequency bands IV and V (periods of 1.3 to 2.8 days) were very low. Note that fluctuations of the residual flow also occur with periods greater than 25 days, as seen of the spectral analyses of the year-long current records (Section 3.2-3). However, the record length of the springtime data limits the statistically-reliable spectra to a long-period limit of 25 days.

A more detailed presentation of the auto-spectral results, displayed for each area in Figures 3.2-2 to 3.2-6, follows.

Prince of Wales Strait (Figure 3.2-2A)

In the spectra of the major component, most of the current variations occurred within the three lowest bands (periods of 2.8 to 25 days) at all measurement locations. The dominance of the lowest bands was most notable at Sites 1 and 2 off Banks Island, within the strongest portion of the residual flow. At Site 1, a broad spectral peak occurred in the second and

third bands, over periods of 2.8 to 8.3 days, although at Site 2 the spectral level did not differ appreciably over the three bands. In the spectra of the minor component, the levels were much smaller and showed no consistent frequency variation among the measurement locations. At some locations (Sites 5, 10 and PW1) the spectra were dominated by the lowest frequencies, while at others (Sites 2 and 8) they tended to peak in the higher frequency bands.

M'Clure Strait (Figure 3.2-2B)

Spectral levels were generally low through the central and southern portions of M'Clure Strait. At Stations 11, 12, 13, 14 and 15, the amplitudes of the individual bands never exceeded 1 cm/s. Moreover, the major and minor axes differed little in amplitude, indicating a directionally-variable residual flow. At the two measurement sites in northern M'Clure Strait, Stations 16 and 17, the residual flow variations were better aligned with the local bathymetry; this is indicated by the large amplitude of the major axis, relative to that of the minor axis (approximately 1.5 cm/s). Moreover, the spectra show that the flow variability was concentrated in the lowest resolvable bands, with the peak in the 8.3- to 25-day band.

At the two measurement sites (18 and 19) off Peel Point in southwest Viscount Melville Sound, the residual flows were aligned along a northwest-southeast major axis, with an amplitude twice as large as the minor component amplitudes. Low-frequency variations were dominant at both sites.

Central Viscount Melville Sound (Figure 3.2-3A)

The spectral amplitudes are indicative of weak and directionally-disorganized flow variability at most locations. Only at the most northerly Sites 24, 25 and 26, situated within 15 km of Melville Island, were the flow variations in rough alignment with local bathymetry. At these sites, the lowest frequency band had the largest amplitude. Interestingly the flow variations at Site 24, situated furthest offshore from Melville Island, were the least energetic.

On the southern side of Viscount Melville Sound, the spectra were of lower amplitude than those at the more northerly locations. At the stations furthest from shore, Sites 21 and 22, no strong direction preference was evident in the flow variations. The spectral amplitudes were larger at Site 21, exceeding 1 cm/s in the two lowest frequency bands: a net residual flow to the south was computed for this location. At Site 20, located nearest Stefansson Island, spectral amplitudes were less than those at Site 21. The flow variability was mostly directed along a northeast-southwest orientation, roughly perpendicular to that of the local bathymetry.

M'Clintock Channel (Figure 3.2-3B)

Spectral levels were uniformly low (<1 cm/s) throughout the transect of stations across M'Clintock Channel. At all sites, the spectra for the major components were largest at the lowest resolvable frequency for the major components, and directed approximately north-south. The along-channel spectral levels were somewhat larger at Sites 82 and 87, nearest the coasts on opposite sides of the channel. At both these sites the ratios of the major-axis to minor-axis amplitude were greater than at the other two Sites, 83 and 86, located further from shore.

Byam Martin and Austin Channels (Figure 3.2-4A)

Comparatively high spectral levels were computed for Sites in Byam Martin Channel, where a strong southeasterly residual current was present throughout the cross-section. The largest spectral levels occurred in the lowest frequency band at the two sites located nearest a coastline. At the mid-channel location, spectral levels were uniform with frequency, and the cross-channel spectral levels were considerably larger than those measured at the sites on either side of the channel.

At the single multilevel measurement location in Austin Channel (Site 71, at depths of 19, 73 and 123 m), spectra exhibited large peaks in the lowest band with a fluctuation amplitude about one-half of the magnitude of

the easterly flowing net residual current (3.0 cm/s) at this site. Interestingly, at the near-surface level, the major component of the principal axis was directed north-south, at right angles to the mean residual flow direction. At greater depth, the mean and principal axis directions were more closely aligned, although the mean flow remained to the right (clockwise) of the major axis.

Eastern Viscount Melville Sound (Figure 3.2-4B)

At the measurement sites located directly south of Byam Martin Island (Sites 57 and 58), and southwest of Bathurst Island (Sites 72 and 74), spectral levels increased with proximity to the coastline, and the current fluctuations became more directionally biased. While all spectra followed the usual pattern of increasing amplitudes with decreasing frequency, a secondary spectral peak was present in the third frequency band (periods of 2.8 to 5.0 days) at Sites 57, 72 and 81.

Low spectral levels were computed from the residual flows off Prince of Wales Island (Site 81), on the southern side of Viscount Melville Sound. At this location, fluctuations in the residual flow were nearly omnidirectional. A preference for clockwise over anti-clockwise oscillations was suggested by the rotary spectra.

Barrow Strait (Figure 3.2-5A)

Spectral amplitudes had intermediate values at the two measurement sites in Barrow Strait. At the northern Site 42, spectral amplitudes were just over 1 cm/s in the first and third frequency bands. In the lowest band, fluctuations were almost entirely directed along the 070-250° direction, in rough alignment with local bathymetry. However, the directional bias was less pronounced for fluctuations in the third band (periods of 2.8 - 5.0 days).

On the southern side of Barrow Strait, within the strong (20 cm/s) eastward residual flow, spectral levels were uniform and comparatively high in the three lowest bands (periods of 2.8 to 25 days), and oriented along

the direction of the mean flow. In the cross-channel direction, the spectral amplitudes were very low at the low frequencies, but increased at higher frequency. In these same frequency bands (periods of 1.9 to 8.3 days), the rotary spectra revealed that clockwise oscillations were larger in amplitude than were the anti-clockwise oscillations.

Wellington Channel (Figure 3.2-5B)

The fluctuations of the flow in Wellington Channel had intermediate-to-large amplitudes. The largest amplitudes were measured at Sites WC1 and WC3, located on the northern transect of stations, approximately 1 and 3 km from the coast of Devon Island. At both sites, spectral levels increased with decreasing frequency, reaching values of 3 to 3.5 cm/s for the along-channel direction in the lowest band. Spectral levels were much lower for the cross-channel flow component, never exceeding 1 cm/s.

At Sites WC4 and WC5, also located on the east side of Wellington Channel but further offshore (5 and 7.5 km from the coast), the spectral levels decreased with distance from shore. The maximum amplitude, for the major component at the lowest frequency, was around 2 cm/s. At Site WC5, a secondary peak occurred in the third frequency band.

On the western side of the Channel, spectral levels were lower. In the lowest frequency band, that having the largest amplitude, the value for the major component was only 1.8 cm/s at WC6, decreasing to 1.3 cm/s within the stronger (3.9 cm/s) southward-flowing current at WC7.

At Station WC13, also situated in the southerly flowing current further to the south, the maximum spectral amplitude was also small. Virtually all fluctuations at the lowest frequencies occurred along the major axis but at higher frequencies the amplitude of cross-channel flows was considerably greater, particularly in the second band (5.0 to 8.3 days period).

Among the remaining stations on the southern transect in Wellington Channel, spectral levels were largest at Site WC12 which was situated in a northwesterly mean flow of 3.7 cm/s. Here, the maximum amplitude of 2.0 cm/s occurred in the lowest band.

Site WC11 was one of the few sites in Wellington Channel which showed a spectral peak in a band other than the lowest. Here, the peak occurred in the second band (periods of 5 to 8.3 days) with an amplitude of 1.7 cm/s. This band also exhibited a clockwise rotational tendency, with an amplitude of 1.5 cm/s, approximately 65 percent larger than the anti-clockwise amplitude.

At Sites WC8 and WC10, the easternmost sites on this transect, spectral levels were the lowest observed in Wellington Channel. The peak amplitudes occurred in the lowest band, with values slightly larger than the weak mean flow measured at these sites (1.8 and 1.1 cm/s, respectively). With increasing proximity to the coastline, the flow variations become more parallel to the coastline, as indicated by the sharp decrease in minor-axis levels.

Penny Strait (Figure 3.2-6)

The spectral amplitudes computed from the four current records were moderate to large in comparison with those characterizing most other areas. The spectral amplitudes of the major component in the lowest band ranged from 1.5 cm/s at depth to 2.5 cm/s (PSW) in the uppermost records.

The largest spectral levels occurred in the lowest frequency band, although a secondary peak in the third frequency band was evident at all sites. The low-frequency amplitudes differed little with depth at Site PSE, but at Site PSW, a large vertical shear was evident within the lowest frequency band (factor of 1.7).

3.2.2 Seasonal Variations

The seasonal variation in the residual current fluctuations was examined through the computation of seasonal spectra, using the year-long current records obtained in Austin Channel (2 data records), Barrow Strait (2 data sets) and Penny Strait (3 data sets). The spectral amplitudes are displayed in Figures 3.2-7, 3.2-8 and 3.2-9, with a summary listing given in Table 3.2.2-1.

In previous sections, regional variation in both the mean flow and the spectral amplitudes of the springtime residual currents have been noted. In Penny Strait, the vector-mean flows are very large, accompanied by smaller but still comparatively large flow fluctuations. At the site in northern Barrow Strait, the amplitudes of both the vector-mean and the flow fluctuations are much smaller, being in the intermediate range for the entire study area. As in Penny Strait, the amplitude of the fluctuations is only half the magnitude of the vector-mean. By contrast, in Austin Channel, the amplitudes of the vector-mean and of fluctuations, although small.

Given the differences between the areas where year-long current records were obtained, a surprisingly consistent pattern of seasonal variations emerged (Figure 3.2-10):

- (1) Current fluctuations were smallest in the spring and reached peak values in fall or winter. The minimum occurred in spring for all areas and depths.
- (2) The remarkable similarity in the seasonal variation of residual current fluctuations (minimum in spring; maximum in fall or winter) was in marked contrast to the absence of a consistent pattern in the magnitude of the vector mean currents, where maximum values occurred in all seasons.
- (3) Fluctuations in the summer differed according to location and depth: in Austin Channel, they were small and comparable to those of spring, while those in Barrow Strait reached their largest levels at mid-depth

Table 3.2.2-1: Auto-spectral analyses for each season of the year-long current-meter records.

STN	DEP.	START	#SAM	#BLK	POW.	MAJ	MIN	CCW	CW	BAND	I	%	%	%	CC/C	MAX	ALL	LOW	RMS/	VECT	VECT	
		m																				
			←(CM/S)**2-DAY→													CM/S		CM/S				
1983	AUTO-SPECTRA																					
71	73	4/08/11	300	6	120.7	75.4	45.3	66.6	54.1	60.0	49.7%	55%	45%	0.81		3.1	2.2		1.1	2.9	3.4	
71	73	7/01/0	300	7	95.6	56.7	38.9	43.3	52.4	32.1	33.6%	45%	55%	1.21		2.8	1.6		1.7	1.6	3.3	
71	73	10/01/0	300	7	94.0	66.2	27.8	44.0	50.1	48.7	51.8%	47%	53%	1.14		2.7	2.0		0.9	3.1	2.8	
71	73	1/01/1	300	7	123.2	129.0	34.1	73.7	89.5	90.1	55.2%	45%	55%	1.21		3.6	2.7		1.1	3.3	4.1	
71	123	4/08/11	300	6	62.9	42.1	20.8	28.3	34.6	26.3	41.8%	45%	55%	1.22		2.2	1.4		0.7	3.2	2.4	
71	123	7/01/0	300	7	60.0	47.5	12.5	28.6	31.4	25.1	41.9%	48%	52%	1.10		2.2	1.4		1.2	1.8	2.6	
71	123	10/01/0	300	7	97.4	79.4	18.1	50.6	46.8	32.4	33.3%	52%	48%	0.92		2.8	1.6		0.9	3.2	3.2	
71	123	1/01/1	300	7	73.7	57.9	15.9	32.6	41.2	38.5	52.3%	44%	56%	1.26		2.4	1.8		1.0	2.5	2.5	
1984 SEASONAL AUTO-SPECTRA																						
42	51	4/28/12	300	6	92.7	48.6	44.1	57.5	35.2	42.9	46.3%	62%	38%	1.63		2.7	1.9		0.6	4.4	2.9	
42	51	7/01/0	300	7	339.3	252.5	86.9	144.6	194.8	230.7	68.0%	43%	57%	0.74		5.2	4.3		1.4	3.7	6.6	
42	51	10/01/0	300	7	303.2	208.2	95.0	169.9	133.3	129.4	42.7%	56%	44%	1.28		4.9	3.2		1.5	3.2	5.9	
42	51	1/01/0	300	6	196.6	163.6	33.0	102.7	93.9	85.8	43.6%	52%	48%	0.91		4.0	2.6		1.1	3.5	4.3	
42	100	4/28/12	300	6	55.4	39.9	15.5	39.5	15.9	25.9	46.8%	71%	29%	0.40		2.1	1.4		0.6	3.7	2.0	
42	100	7/01/0	300	7	145.5	111.2	34.3	54.4	91.1	94.5	64.9%	37%	63%	1.67		3.4	2.7		1.4	2.4	4.0	
42	100	10/01/0	300	7	216.7	177.7	38.9	110.9	105.7	76.9	35.5%	51%	49%	0.95		4.2	2.5		1.5	2.7	5.1	
42	100	1/01/0	300	6	154.7	132.5	22.1	72.4	82.3	77.8	50.3%	47%	53%	1.14		3.5	2.5		0.9	3.7	4.2	
PSW	49	4/28/12	300	6	239.0	158.3	80.7	143.8	95.2	109.6	45.8%	60%	40%	0.66		4.4	3.0		0.3	12.6	4.4	
PSW	49	7/01/0	300	7	334.7	216.0	118.7	138.5	196.2	182.9	54.6%	41%	59%	1.42		5.2	3.8		0.4	14.7	5.3	
PSW	49	10/01/0	300	7	343.8	288.6	55.5	144.3	199.5	199.7	58.1%	42%	58%	1.38		5.2	4.0		0.7	7.3	7.4	
PSW	49	01/01/0	300	7	373.4	299.9	73.6	146.4	227.0	234.9	62.9%	39%	61%	1.55		5.5	4.3		0.5	10.9	7.0	
PSW	138	4/28/12	300	6	149.1	94.1	55.0	71.0	78.1	50.7	34.0%	48%	52%	0.91		3.5	2.0		0.8	4.1	3.5	
PSW	138	7/01/0	300	7	149.5	102.9	46.6	67.4	82.1	42.1	28.2%	45%	55%	1.22		3.5	1.8		0.7	5.2	3.7	
PSW	138	10/01/0	300	7	213.9	166.9	47.0	99.8	114.0	91.2	42.6%	47%	53%	1.14		4.1	2.7		3.2	1.3	6.4	
PSW	138	01/01/0	300	7	245.3	204.6	40.8	87.4	157.9	134.5	54.8%	36%	64%	1.81		4.4	3.3		1.6	2.8	6.5	
PSE	43	4/28/12	300	6	204.0	132.7	71.3	78.5	125.4	80.6	39.5%	39%	61%	1.60		4.0	2.5		0.3	13.4	4.2	
PSE	43	7/01/0	300	7	391.2	314.5	76.6	187.8	203.3	241.5	61.7%	48%	52%	0.92		5.6	4.4		0.4	15.8	6.2	
PSE	43	10/01/0	300	7	562.2	450.3	111.9	281.3	280.9	367.5	65.4%	50%	50%	1.00		6.7	5.4		0.5	14.2	8.2	
PSE	43	01/01/0	300	7	342.1	232.1	110.1	155.1	187.0	191.9	56.1%	45%	55%	1.21		5.2	3.9		0.4	12.7	7.8	
PSE	131	4/28/12	300	6	253.1	109.4	143.7	98.6	154.5	101.1	39.9%	39%	61%	0.64	*	4.5	2.8		0.5	8.2	4.2	
PSE	131	7/01/0	300	7	268.9	128.6	140.2	129.4	139.5	88.4	32.9%	48%	52%	0.93		4.6	2.7		0.7	6.4	4.9	

No. of data points-----
 No. of analysis blocks-----
 Total power-----
 Power (major component)-----
 Power (minor component)-----
 Power (counter-clockwise component)-----
 Power (clockwise component)-----
 Power in lowest band-----
 % of power in lowest band-----
 % of power in CCW component-----
 % of power in CW component-----
 Ratio of CCW-to-CW power-----
 Band with largest power-----
 Root-mean-square speed (overall)-----
 Root-mean-square speed (lowest band)-----
 Ratio of RMS-to-mean speed-----
 Mean velocity-----
 Standard deviation of velocity-----

in summer. Summertime fluctuations had intermediate values in Penny Strait. In both Barrow and Penny Straits, the magnitude of current fluctuations was considerably larger at mid-depth than near the bottom, indicating that the vertical shear in current is largest in the summer.

- (4) In all records, the largest current fluctuations occurred in the lowest band (8.3 to 25 day periods). In some records, the amplitude of shorter-period fluctuations became more prominent in fall, although it never exceeded that in the lowest band. This autumnal increase in shorter-period current variations was particularly evident at both measurement depths in Barrow Strait, as well as at the near-bottom level in Austin Channel.

3.2.3 Year-Long Time Series

Current fluctuations of longer period were studied using the year-long current records. The four-fold increase in duration of the year-long time series permits examination of periodicities as long as 125 days with some confidence.

For the three records from Penny Strait (Figure 3.2-12), an area of strong residual flows, the largest fluctuations occurred at the lowest resolvable frequencies (band A: periods of 42 to 125 days). Here, the amplitudes were up to twice as large as fluctuations with periods of 8.3 to 25 days, the lowest resolvable band in the seasonal spectra.

Large-amplitude fluctuations at very long periods also occurred at Site 42 in northern Barrow Strait (Figure 3.2-11), although the amplitudes were smaller than those computed for Penny Strait, particularly at the deeper measurement depth.

In Austin Channel (Figure 3.2-11), fluctuations at the very long periods were markedly smaller. Here, the current fluctuations were most energetic at intermediate periods, those of 8.3 to 13.9 days.

3.3 Spatial Coherence

To examine the spatial scales of residual flows in the Northwest Passage, cross-spectral analysis techniques were applied to pairs of current records. The results are presented as coherence and phase values. The coherence value at each frequency, ranging from 0 to 1, represents the fraction of the amplitude of one signal that matches a similar oscillation in the other signal. The phase difference between the two signals at each frequency represents the angle, ranging from 0 to 360 degrees by which the second signal leads the first. 360° represents a lead equal to the period of the signal being investigated.

When presenting coherence values, some criterion must be used to decide whether the coherence is statistically significant. Here we take the significance level to be that value of coherence (Table 3.3-1) below which a truly random coherence will fall with a chosen probability (Groves and Hamman, 1968).

Table 3.3-1

Coherence values between two time series that exceed random noise at 80, 90 and 95 percent probability levels.

No. of Blocks	Percentage Significance Levels		
	80	90	95
3	0.74	0.83	0.88
4	0.64	0.73	0.79
5	0.58	0.66	0.73
6	0.52	0.61	0.67

3.3.1 Springtime, 1982-1985

For the springtime measurements, the bulk of the cross-spectral analyses dealt with horizontally separated pairs of current records. The examination of vertically separated pairs is presented for all seasons in the following section (3.3.2) of this report. The horizontally separated pairs used in the analyses were selected as follows:

- (1) All adjoining pairs of current-meter records;
- (2) On each cross-channel transect of current-meter moorings, a current record at one side was chosen (on the basis of largest flow speeds). Cross-spectra were computed between this record and all other records on the transect;
- (3) Where significant coherence was determined from the current records selected, additional pairs of other nearby current records were selected for cross-spectral analysis.

The cross-spectral results are presented for individual areas, followed by a summary of the results throughout the full study area.

Prince of Wales Strait (Figures 3.3-1, 3.3-2)

Current fluctuations exhibited larger coherence in Prince of Wales Strait than in any other region. Fluctuations within the southwesterly coastal current off Banks Island had the highest coherence. Within the coastal current itself (at Sites 1 and 2), over 90 percent of the current fluctuations tracked one another with time lags of 4 hours or less.

The similarity in the current fluctuations extended beyond the core of the southwesterly coastal current, to locations throughout the Strait. High coherence with the fluctuations in the current core was observed at Sites 5 and 9. The phase differences between measurement sites were generally small, with the largest differences occurring in the lowest frequency band. The most pronounced phase differences were found for Site

9, indicating fluctuations there which were 16 to 24 hours ahead of current fluctuations on the transect of sites across the Strait (Sites 1, 2 and 5). This pattern of current phases decreasing towards the northeast, in the lowest frequency band, was also observed at Site 10 located to the northwest, where current fluctuations lagged behind those at transect Sites 5, 6 and 7 by 20 to 60 hours.

Coherence was lower, but still statistically significant, for locations on opposite sides of the Strait. The reduction in coherence was most apparent in the very lowest frequency band, where the computed values were consistently below the significance level. Large and statistically significant coherence did occur in the higher frequency bands, particularly in band III (periods of 2.8 to 5 days), which was generally the most energetic of all bands in Prince of Wales Strait. In this band and the two highest frequency bands (III, IV and V), the fluctuations exhibited a progressive time lag with increasing distance from the strong-current core. The largest phase difference, found between Sites 1 and 7 on opposite sides of the Strait, indicated that weaker currents on the southern side of the Strait lagged behind the current core by 8 to 20 hours.

M'Clure Strait (Figure 3.3-3)

Coherence in M'Clure Strait was uniformly low. For example at Sites 16 and 17, on the northern side of the Strait, where the largest fluctuations occurred, the coherence was low in all frequency bands. The only pair of current records having significant coherence in the dominant lowest band was that for Sites 12 and 17, located on opposite sides of the Strait. For these widely-separated sites (85 km) the coherence was 0.75, with a large phase difference of 161 degrees, indicating changes almost out of phase on opposite sides of the Strait.

Near Peel Point, at the mouth of Prince of Wales Strait (Sites 18 and 19), the fluctuations in the minor component were highly coherent in the most energetic, low frequency band. At both of these sites, the flow

exhibited a pronounced tendency for counter-clockwise oscillation. Statistically significant coherence (0.70 to 0.74) was found in the counter-clockwise rotary spectrum between these two sites.

Central Viscount Melville Sound (Figure 3.3-4)

As in M'Clure Strait, coherence here was generally low, particularly in the lowest frequency band, which had the largest amplitude fluctuations. On the northern side of the Sound, current fluctuations were coherent at significant levels for intermediate and higher frequency bands (periods of 1.3 to 5 days). The fluctuations were out of phase for both adjoining station pairs: Sites 24 and 25, and Sites 25 and 26, separated by 8 and 20 km, respectively.

At the three measurement sites on the southern side of the Sound, some significant values of coherence were also computed for the middle and higher frequency bands (Site 22 with 20), but not for the lowest frequency band, which had the largest amplitude fluctuations. No significant coherence was found for measurement pairs located on opposite sides of the Sound.

M'Clintock Channel (Figure 3.3-5)

As might be expected given the very small amplitude of the residual current and its fluctuations in M'Clintock Channel the coherence was uniformly low. In the most energetic, low frequency band, the computed coherence fell below the 90 percent significance level in all six pairs of current records.

Eastern Viscount Melville Sound (Figure 3.3-6)

Current fluctuations at both of two measurement Sites (72 and 74) situated off the southwest corner of Bathurst Island exhibited very high coherence in the lowest band for both the major and minor current components. This is remarkable, since the principal axes are poorly aligned. The largest coherence of 0.94 applies to fluctuations between

the two minor components, setting northeasterly at the near-coastal Site 72 and easterly at Site 74 located further from shore. The coherence (0.80) for the major-axis component was nearly significant at the 90-percent level. The phase difference indicates that the current fluctuations at the offshore site lead those nearer the coast by 90 degrees or 1.5 to 6 days. These results could be indicative of a narrow coastal current which meanders, flowing nearer the coast at times, perhaps into Austin Channel, or moving further offshore and turning southward.

High coherence was found in the highest band between Sites 72, 74, and 71 located nearly 80 km to the northwest in Austin Channel (at the 73 m or mid-depth level only). Although the amplitude of fluctuations is small in comparison to that in the lowest band (Figure 3.2-4), a small peak was evident in the auto-spectra for all three records.

Low coherence was found for residual currents measured on opposite sides of Viscount Melville Sound (Sites 72/74 with Site 81), particularly in the lowest band.

Byam Martin Channel (Figure 3.3-7)

Currents in Byam Martin Channel exhibited low coherence. For Sites 62 and 63, separated by only 6 km, the coherence was uniformly low, with the only statistically significant value occurring in the highest band, for which fluctuations were very small at Site 62. In a statistical sense, the residual currents at Site 63 appeared to be better correlated with those at Site 66, located approximately 21 km away on the opposite side of the Channel. Coherence was well above the 95% significance level in band III (periods of 2.8 to 5 days), where a small peak occurs in the auto-spectra for both sites.

Low coherence was found between the three Byam Martin Channel Sites 62, 63, 66 and Site 71 which was located over 90 km to the southeast in Austin Channel.

Barrow Strait (Figure 3.3-8)

The current fluctuations measured on opposite sides of Barrow Strait appear to be coherent at the mid-range frequencies, but not at the lowest frequencies. Over periods of 2.9 to 5 days, the near-surface fluctuations at Site 46 were coherent at the 90-95 significance levels with the along-shore fluctuations for all three measurement depths at Site 42. The fluctuations on the southern side of the Strait lead those at the northern site, by approximately 7 to 10 hours. The statistically significant coherence extends into the next lowest frequency band (II: 5 to 8.3 days) for the upper and lower measurement depths at Site 42. The middle band has large amplitudes throughout Barrow Strait (Figure 3.2-5), particularly at Site 46 on the southern side of the Strait.

Highly coherent fluctuations were observed at the vertically-separated measurement levels of the northern measurement site in Barrow Strait. As for the computed coherences between horizontally-separated sites, the residual current fluctuations were most coherent in the middle frequency bands, and dropped off sharply at the lowest frequencies. Unlike the situation for horizontal pairs, the current fluctuations in the cross-strait component are highly coherent for the vertically-separated pairs. The phase differences are small.

Wellington Channel (Figures 3.3-9 and 3.3-10)

Due to the comparatively large number of measurement locations in Wellington Channel, the cross-spectral results are displayed in two sets: Figure 3.3-9 displays the results for station pairs on the same cross-channel transect, while Figure 3.3-10 provides the results between stations from the northern and southern transects.

In the strong northward-flowing current found off Devon Island on the northern transect (Sites WC1, WC3 and WC4), current fluctuations are highly coherent with small phase differences. The coherence is largest in the second and third bands (periods of 2.5 to 7.5 days). In the western and

central portions of the northern transect, the coherence of current fluctuations is much lower, and generally below the 90-percent significance level. One noteworthy feature is the high coherence between the cross-channel flow fluctuations at mid-Channel pairs WC4-WC5, and WC5-WC6. As with the station pairs further to the east, the highest coherence occurs in the middle bands, but only for cross-channel fluctuations at these locations. The high correlation in the cross-channel component may be indicative of mid-Channel lateral exchanges between the oppositely-flowing currents on either side of the Channel.

Stronger coupling in middle-frequency bands is also suggested in the cross-spectral results computed between the site immediately off Devon Island (WC1) and each of the other sites on the northern transect. The coherence for bands II and III was in the vicinity of the 90 percent significance level for all along-channel current components. The phase differences appear to increase with horizontal separation between sites. For Sites WC1 and WC7, separated by 16 km and on opposite sides of the Channel, the current fluctuations were nearly out of phase. This apparent coupling between residual fluctuations does not occur in the lowest frequency band, which contains the largest fluctuations, particularly off Devon Island.

On the southern transect in Wellington Channel, coherent current fluctuations were evident for the three easternmost sites: WC8, WC10 and WC11. Unlike the eastern sites on the northern transect, the residual currents observed at these locations were not particularly large in amplitude nor did they set consistently in a particular direction. The coherence was largest in the middle bands, and decreased to levels below statistical significance in the lowest band, which had the largest current fluctuations. Coherence was much lower for station pairs involving Sites WC12 and WC13 on the western half of the Channel; this may reflect the considerably larger station separation (9 km) than that present further to the east.

The coupling between currents at the southern and northern transects, separated by 32 km, can be inferred from selected cross-spectral results displayed in Figure 3.3-10. In this figure, the cross-spectra are presented only for those station pairs having two or more statistically significant coherence levels at or exceeding 90 percent. Station pairs for which cross-spectra were computed, but not displayed, are indicated by the circled symbol 'N' in Figure 3.3-10.

Residual currents measured in the core of the strong, north-flowing current at the northern Site WC3 are coherent with those at Sites WC11 and WC12, for fluctuations having periods of 2.5 to 7.5 days. At these two southerly sites, the flows are also directed north but at much reduced speed. The current at the northern Site WC1, situated just off the Devon Island coastline, also exhibited fluctuations coherent with those measured on the southern transect at central and easterly locations (Sites WC8, WC10, WC11 and WC12), particularly for the mid-range frequency bands. The computed phase differences were generally large, usually between 90 to 180 degrees, for currents at the northern and southern sites. The phase differences are consistent, with currents on the southern transect leading those on the northern transect by 1.5 to 3 days when the reversed orientation of coordinate systems is taken into account.

The largest overall coherence computed between north and south station pairs occurred between Sites WC5 and WC11. For this pair, current fluctuations in the energetic, lowest band attained a very high coherence level of 0.98. The phase difference of -70 degrees corresponds to currents at the southern site leading those to the north by approximately 1.5 to 4.5 days. Of the 13 station pairs between the northern and the southern transects, only this pair had statistically significant coherence in the lowest frequency band.

Low coherence was found for measurement sites on the western side of Wellington Channel (WC6, WC7 and WC13), where the flows set to the south. The low coherence may be indicative of greater spatial variability, although the less dense sampling network could also have been a factor.

Summary

The coherence of horizontally separated currents was generally low, falling below statistical significance in the great majority of cases examined. These findings indicate that the spatial scale of most residual flows during spring are smaller than the typical station separation of 5 to 25 km. The areas having the lowest coherence were M'Clure Strait, Viscount Melville Sound, M'Clintock Channel and Byam Martin Channel. The first three of these areas had the smallest residual flows within the study area.

Well-defined coastal currents appear to be associated with high coherence in the lowest resolvable frequencies, over periods of 8 to 25 days. Instances of strong coastal currents with this spectral characteristic were found on the western side of Prince of Wales Strait and on the eastern side of Wellington Channel. A less clearly defined coastal current, having high coherence at low frequency, was noted off the southwest corner of Bathurst Island in Viscount Melville Sound. The spatial scale of the low frequency coupling in the current fluctuation is generally small, ranging from 2 km (Wellington Channel) to 8 km (Prince of Wales Strait). The small spatial scale suggests that the fluctuations in the coastal currents are baroclinic, since the internal Rossby radius is of the same order of magnitude as the spatial scale inferred from the spectral analysis of the current data.

Coherence was generally higher in the middle-frequency band (periods of 2.5 to 5 days) than in the more energetic low-frequency band. The comparatively large coherence at mid-frequencies was most evident in areas having moderate-to-large current fluctuations. As well as more occurrences of statistically significant coherence values, the fluctuations at mid-range frequencies exhibited large coherences over larger station separations, of up to 20 to 30 km or more. The larger spatial scales exhibited in the mid-range frequencies suggest that a driving mechanism different from that responsible for the low frequency fluctuations may be operating. The larger spatial scales inferred for the middle range

frequencies exceed the internal Rossby radius; barotropic processes may be more important for these fluctuations.

3.3.2 Seasonal Variations

Vertically Separated Current Measurements

The cross-spectral results, computed for each season between residual currents at mid-depth and near-bottom levels (Figures 3.3-11 and 3.3-12), reveal a consistent seasonal pattern in all regions.

- (1) Vertically separated currents have the highest coherence in winter and the lowest during spring or summer.
- (2) In the summer months, the coherence of vertically separated currents exhibited the largest differences among regions. In Barrow Strait, the vertical coherence was very high at this time, particularly in the lowest frequency band; large amplitude fluctuations of low frequency are present at this site in summer (section 3.2.2). In Penny Strait during summer, vertical coherence was the lowest of any season.
- (3) The phase differences computed were generally small, particularly when associated with high coherence. For the lowest band, having the greatest contribution to fluctuations of residual currents, the phase differences ranged from +15 to -45 degrees, corresponding to mid-depth fluctuations leading those near-bottom by as much as 1.5 days. During winter, when coherence was largest, the lead time of mid-depth currents was reduced to -2 to 9 hours.
- (4) For the cross-channel current component, the coherence was usually smaller than that computed for the along-channel component, and exhibited a much less consistent pattern of seasonal variation. Some notable differences included a few instances where the cross-spectral coherence exceeded the along-channel values: at the Barrow Strait and the Penny Strait East locations in spring; and at the Penny Strait West location in summer. In the winter the coherence between

cross-channel components decreased sharply, particularly at the Penny Strait West site.

- 5) During fall, coherence was noted for some of the higher-frequency bands, especially III and IV. At this time the auto-spectral results (section 3.2.2) indicated an increase in activity in this range of periods (2 to 8 days) for the sites in Barrow Strait and in Austin Channel. Apparently this greater activity is also reflected in the larger coherence. In summer, the coherence at these higher bands is much reduced, to levels at or near the seasonal minimum.

Horizontally Separated Current Measurements - Penny Strait

The residual currents measured at both sites in Penny Strait had very low coherence in the vertical during the spring and summer months, but much higher values in fall and winter (current measurements were only available at the western site in fall and winter). The coherence computed for currents at either of the two sites (Figures 3.3-13 and 3.3-14), reveal a similar seasonal pattern. During spring and summer, the coherence between the two sites is uniformly low (<0.7) for the along-channel component in all frequency bands.

Coherence increases to statistically significant levels in fall and increases to much higher levels (0.8 to 0.9 for band I) in winter. The coherence results between the uppermost currents measured at the eastern site (PSE) and either measurement depth at the western site (PSW) are very similar. During winter, the phase differences indicate that the currents at the eastern site lead those to the west by approximately 12 to 15 hours.

3.3.3 Year-Long Time Series

The coherence between residual current fluctuations of longer period was examined by computing the cross-spectra between pairs of year-long current measurements from Austin Channel, Barrow Strait (Figure 3.3-15) and Penny Strait (Figure 3.3-16). The apparent coupling at very low frequencies differs according to region.

In Penny Strait, where the magnitude of current fluctuations at the very long periods was high relative to that at the periods resolved in seasonal time-series measurements (< 25 days), a high coherence of 0.97 was computed for the two measurement depths at Site PSW. The phase difference was very small, indicating that the fluctuations followed one another with a delay of less than 12 hours. For currents measured on opposite sides of Penny Strait, the coherence over very long periods, although lower (0.64 to 0.78), indicated that the fluctuations in current at these periods were related to one another.

Large coherence for very long periods also occurred in Barrow Strait for the mid-depth and near-bottom currents measured at Site 42. In the lowest band, the computed coherence was 0.88 with a phase difference of -10 degrees, indicating that the mid-depth currents led those near the bottom by approximately 1.5 days.

3.4 Volume Transport

3.4.1 Computational Methods and Uncertainty

From the large number of temperature and salinity profiles which were obtained concurrently with flow data during the Northwest Passage Oceanography Programme, the total volume transports through various instrumented channel cross-sections of the archipelago can be computed. The total volume transport through a channel is the sum of the baroclinic (depth-varying) and barotropic (or depth-invariant) components. The temperature and salinity data (Buckingham, Lake and Melling, 1987 a, b, c, d, e) have been used in a companion study to estimate the baroclinic portion of the volume transport (de Lange Boom, Melling and Lake, 1987). In these computations, the reference "level of no motion" was taken as the sea surface.

We estimated the barotropic component from the residual currents determined from the flow data. At each current-measurement site, the barotropic transport component was computed as the residual current minus the computed baroclinic flow at the measurement depth, relative to the sea surface. In order to be computationally consistent with the baroclinic transport estimates (de Lange Boom, Melling and Lake, 1987), the barotropic transport was calculated by means of a linear interpolation over the area segments defined by successive pairs of temperature-salinity (TS) stations. For the portions of the channel between the coasts and the nearest TS stations, the barotropic component derived from the nearest current-meter site was assumed to apply to the cross-sectional area. The total barotropic transport through the channel cross-section was then computed as the sum of the transport for each area segment.

The total volume transport through each cross-section was determined as the sum of the baroclinic transport computed by de Lange Boom, Melling and Lake (1987), and the barotropic transport estimated in this study.

Whenever possible, the barotropic and the total volume transports were determined from residual currents which were computed for times within 3 to 4 days of the temperature-salinity profile measurements. For those channels for which the time difference between the current record and the TS observations was larger than 3 to 4 days, the mean residual currents determined over the full duration of the current record were used in place of the near-concurrent flow values.

Uncertainties in the volume transports were estimated. The following sources of uncertainty were explicitly considered:

- (1) Horizontal Positioning Errors - The uncertainty in the location of the measurement sites, estimated as 0.5 to 1.0 km, causes uncertainty in the estimate of the area of each segment in the channel cross-section. For this study, this uncertainty was computed as:

$$(1.414 * 0.75) / DX$$

where DX is the separation between adjacent measurement sites in km.

- (2) Other Measurement Errors - For the range of currents measured in this study, the uncertainty in current measurement was taken as ± 1 cm/s.
- (3) Residual-Current Estimation Errors - In some parts of the study area, two additional errors were encountered as described in Section 2.3. If either of these two errors was important, the estimate of volume transport uncertainty was increased accordingly. The additional current measurement error was determined as a typical value of the estimates described in section 2.3.
- (4) Mean Residual Current - Volume transports computed from residual currents, which are estimated as the mean measured value, are subject to an additional statistical uncertainty. This was computed using the standard deviation of the flow fluctuations and an estimate of the available degrees of freedom in the current record:

$$3 * \text{STD.DEV} / \text{SQRT}(T/F)$$

where STD.DEV is the computed standard deviation, T is the record length in days, and F is the estimated integral time scale, assumed to be 1.5 days.

A troubling source of uncertainty in volume transport estimates was the poor spatial resolution in measurement, as indicated by the low levels of coherence for horizontally-separated current pairs (Section 3.3). In channel sections showing low coherence in current fluctuations and exhibiting differences in mean current of magnitude comparable to the fluctuations, volume transport was not computed; the uncertainties in the result were expected to be greater than the result itself.

3.4.2 Computed Volume Transports

In 1982, a very dense array of current meters placed across a section of Prince of Wales Strait provided one of the best estimates of volume transport obtained to date in the Archipelago. The spatial coherence between adjoining station pairs was generally high, particularly in the strong southwesterly coastal current on the northwestern side of the Strait. The three estimates of volume transport computed for Prince of Wales Strait (see Table 3.4-1) ranged from 4 to 6×10^4 m³/s, directed to the southwest. The volume transport was largest on the northwest side of the channel, due to the coastal current there, and was directed southwestward across the full width of the channel in the upper 50 m. At greater depths, strong vertical shears occurred (de Lange Boom, Melling and Lake, 1987), and flow reversed to northeasterly at some mid- and eastern measurement sites.

The volume transport computed for M'Clure Strait was subject to large uncertainty. Because of the weak residual currents in this area, uncertainties in the direct current measurements arise from the high proportion of measurements (about 40 percent) in which the speeds are below the threshold level of the speed sensor. This problem, in combination with the large separation between current meters across the comparatively large width of M'Clure Strait, led to a large uncertainty in the estimate of barotropic transport. However, unless some narrow, intense circulation feature was not detected, it appears that the total volume transport is very small through this channel.

Volume transport computations were not possible for the remaining 1982 measurements, obtained in eastern Viscount Melville Sound, as the current data were too widely separated in this area.

The 1983 volume transport computations were limited to cross-sections through Byam Martin and M'Clintock Channels (Table 3.4-1). As in 1982, the current measurements collected in central Viscount Melville Sound were too widely separated to permit estimation of the barotropic transports over the width of the Sound.

Table 3.4-1

The baroclinic, barotropic and total components of volume transport for selected channels in the Canadian Arctic Archipelago, derived from the 1982-1984 data collected by the Institute of Ocean Sciences. The barotropic volume transports are computed both from the mean residual currents, and alternatively from current measurements obtained within a few days of the temperature-salinity data from which the baroclinic transports were derived (numbers in brackets). Positive transports indicate flow toward the north and east.

Channel	Date	Transport ($10^4 \text{ m}^3/\text{s}$)						
		Baroclinic Value \pm Error		Date	Barotropic Value \pm Error		Total Value \pm Error	
(a) 1982 Results								
Prince of Wales St.	30/03	-1 \pm	7		-3 \pm	1	-4 \pm	7
				1/04	(-4 \pm)	(1)	(-5 \pm)	(7)
	24/06	-4 \pm	7		-3 \pm	1	-6 \pm	7
M'Clure Str.	31/03	5 \pm	23		0 \pm	18	5 \pm	29
(b) 1983 Results								
Byam Martin Channel	29/03	26 \pm	4		-37 \pm	5	-12 \pm	6
				4/04	(-38 \pm)	(5)	(-11 \pm)	(6)
M'Clintock Channel	26/03	-6 \pm	8		0 \pm	11	-6 \pm	12
(c) 1984 Results								
Barrow Str.	8/04	-29 \pm	4		75 \pm	25	45 \pm	25
Wellington Channel	12/04	-23 \pm	2		-1 \pm	4	-24 \pm	5
Penny Str.	15/04	28 \pm	4		-62 \pm	25	-34 \pm	25

In M'Clintock Channel, the coherence in current was very low between adjoining stations. Moreover, the current meter for Site 88 in the middle of the Channel was not recovered, resulting in a large separation of 36 km between mid-channel measurement locations. Nevertheless, the very low residual currents measured in the remainder of the Channel, and the absence of any strong baroclinic flows in the middle of the Channel, provide some indication that the very weak volume transport computed for this channel is reasonably representative of the actual conditions.

The volume transport computed for Byam Martin Channel was considerably larger, being directed southward at 11 to 12 x 10⁴ m³/s. The uncertainties in the barotropic transport arise from the lack of spatial coherence between adjacent current-meter sites, and from the absence of a mid-channel current meter record.

Volume transports were computed for three channels using the 1984 data. For two of these channels, Barrow Strait and Penny Strait, only two current records were available. Nevertheless, the volume transport was estimated since the very strong currents observed indicated substantial values for this feature. In Barrow Strait, the TS stations situated across the eastern end of the Strait were selected as the basis for the baroclinic transport. The current-meters at Sites 42 and 46 located on opposite sides of the Strait, were situated 25 and 10 km to the west of the CID transect line, respectively. Because the mean residual current was larger at the southern site than at the northern, the estimated current values for the mid-channel locations were very important in determining the barotropic transport result. We assumed that the moderate flows on the north side of the Strait applied to the mid-channel locations as well, using as guidance springtime current measurements obtained at four sites in 1981 (Prinsenberg and Bennett, 1987). The result was a total volume transport of 45 x 10⁴ m³/s for the spring of 1984. Given the very limited number of current records available for 1984, the resulting uncertainty in the barotropic transport could be as large as 25 x 10⁴ m³/s.

In Penny Strait, the same problem arises, as only two current records are available. Here, the mean residual currents were more nearly equal as measured at the 40 to 50 m depth level. Residual currents for mid-channel locations were computed as interpolations between the two sites of direct measurement. The current measurements were obtained at sites deeper than those at which CTD measurements were made, being located about 12 km to the southeast. This factor introduced additional uncertainty, due to the very complex bathymetry of the area. Given all these factors, the total volume transport of $34 \times 10^4 \text{ m}^3/\text{s}$ has an uncertainty of $\pm 25 \times 10^4 \text{ m}^3/\text{s}$, largely arising from the assumptions required to compute the barotropic transport.

The volume transport computation for Wellington Channel was derived for the northernmost of the two instrumented sections of the channel, since the circulation pattern was better resolved there (Section 3.1). On the eastern side of the channel, the higher-than-average spatial coherence allowed comparatively precise computation of barotropic and total-volume transport. Due to the larger station separation, and lower coherence on the channel's western half, the transport computation had larger uncertainty there. The net volume transport of $24 \times 10^4 \text{ m}^3/\text{s}$, was directed southward indicating that about two-thirds of the southward transport through Penny Strait passes through Wellington Channel. Another feature of interest was the strong vertical shear in currents occurring on the eastern half of the channel. The strong, narrow coastal current is confined to the upper 50 m of the water column, while the flow at depth reverses to southerly (de Lange Boom, Melling and Lake, 1987).

Further discussion of volume transports throughout the Archipelago is presented in Section 4.3, based on these transports and the results of earlier studies.

4. SUMMARY AND DISCUSSION

The extensive 1982-1985 current measurement program in the Northwest Passage has provided the most comprehensive data set collected to date within the Canadian Arctic Archipelago. In the present study, these data have been processed and analysed to provide a quantitative description of the residual circulation patterns within the area. Other data available from earlier studies, identified in Appendix 2, have also been examined, particularly for those geographical regions not instrumented in 1982-1985. However, the use of these supplementary data sets has been limited to determining the vector-mean current at each measurement site.

4.1 Mean Circulation

The mean near-surface residual circulation through the Archipelago is illustrated in Figure 4-1. At each of the approximately 100 measurement sites, the mean current was determined over an averaging period of 30 days or more of consecutive measurement. Since all measurements were obtained in the spring or summer, uncertainties due to seasonal variability are reduced. However, the collection of data sets used in Figure 4-1 spans a period of 10 years. Because the magnitude of interannual variability in residual currents is largely unknown (section 4.2), some uncertainty arises in deriving circulation patterns from such non-synoptic data.

The general flow through the Archipelago is directed to the south and east, representing the transport of Arctic Ocean surface waters into Baffin Bay. A southward-and-eastward flow through the Archipelago is consistent with that indicated in the earliest descriptive studies of the Archipelago (Bailey, 1957; Collin and Dunbar, 1964; Barber and Huyer, 1971; Coachman and Aagaard, 1974), which inferred circulation indirectly from water-property distributions.

From the direct measurements of residual currents, as assembled and displayed in Figure 4-1, the circulation patterns within the Archipelago are seen to be complex and varied. Large differences in residual currents were evident within some individual channels. The variable and intricate

pattern of the mean residual circulation is far more complex than anticipated on the basis of earlier, region-wide oceanographic studies, which relied on indirect measurement techniques and widely-separated measurement sites.

The residual flow field in the different channels is summarized below, for each region in the Archipelago:

Queen Elizabeth Islands: In the broad and comparatively deep channels occupying the most northerly portion of the Archipelago, the mean residual flow is generally weak (5 cm/s or less) and is variable in direction. The circulation patterns remain poorly resolved, due to the small number of direct measurement sites and the spatial complexity of the measured flows. A net southeasterly flow can be inferred for this area, to provide continuity with the strong southeasterly flows in Byam Martin Channel and Penny Strait, which connect the channels of the Queen Elizabeth Islands with the remainder of the Archipelago.

Northern Connecting Passages: Two sets of channels connect the broad passages of the Queen Elizabeth Islands with Parry Channel to the south. In both cases, the most northerly channel, Byam Martin Channel in the west and Penny Strait in the east, is quite narrow. Further to the south, the connecting passages have a more complex geometry, splitting into a series of channels which connect to the northern side of Parry Channel. As might be expected in these constricted waterways, large residual currents occur in Byam Martin Channel and Penny Strait. In both channels, the mean flow is to the southeast and is very steady near the surface, with virtually no current reversals being observed. The largest vector-averaged residual flows were measured in Penny Strait (13 cm/s); average flows of 5 to 7 cm/s were measured in Byam Martin Channel.

Southerly residual currents are found in the adjoining passages to the south: Byam and Austin Channels in the west; and Crozier and Pullen Straits and Wellington Channel in the east. Here, the residual currents are of lesser magnitude than those in the northern passages, and exhibit more directional variability. In Wellington Channel, a strong northward

coastal current, directed opposite to the southerly flow, is present on the east side of the Channel. There is no evidence of opposing currents in the other instrumented channels.

Strong southerly flows also occur in the constricted waterway of Nares Strait, which forms part of another passageway linking the Arctic Ocean to Baffin Bay. Cardigan Strait and Hell Gate, two passages within the Archipelago which connect the Queen Elizabeth Islands with Jones Sound, are also expected to have strong southerly residual flows. While no direct current measurements are available for these channels, indirect supporting evidence for strong currents is the occurrence of polynyas each winter and spring in these areas (Smith and Rigby, 1981). Inferences from summertime water-property distributions (Barber and Huyer, 1977) are also consistent with southerly transports through Cardigan Strait and Hell Gate.

Western Parry Channel: The broad and deep channels of the western end of the Northwest Passage, M'Clure Strait and Viscount Melville Sound, have very weak and directionally variable residual flows. The residual currents here are so small that the velocities are prone to measurement uncertainties of up to 40 percent.

Eastern Parry Channel: Much larger residual flows are found farther to the east in Parry Channel, particularly in Barrow Strait, its shallowest and narrowest portion. In Barrow Strait, the residual currents set to the east, with the strongest flows concentrated on the southern side. During the summer months, the flows on the northern side of the Strait reverse to the west, while easterly flows on the south side are observed to attain their strongest values of the year (Prinsenbergh and Bennett, 1987). Further to the east, in the deeper waters of Lancaster Sound, the residual currents are dominated by a branch of the Baffin Current, which intrudes approximately 35 to 75 km into Lancaster Sound before exiting as a strong easterly flow on the south side of the Sound (Fissel, Lemon and Birch, 1982). The easterly flow from Barrow Strait also contributes to the very strong currents observed on the south side of Lancaster Sound at its junction with Baffin Bay. However, the residual currents through the western and central portions of Lancaster Sound are not clearly resolved;

surface-drifter and water-property data (Fissel and Marko, 1978; Fissel, Lemon and Birch, 1982) suggest considerable time-dependent variability in the residual flows in this area.

Southern Channels: Generally weak residual flows occur in the broad expanses of M'Clintock Channel and Prince Regent Inlet, located to the south of Parry Channel. The residual flows in M'Clintock Channel are among the weakest measured throughout the Archipelago, and have no well-defined directional preference. Based on the very few direct measurements available for Prince Regent Inlet, the residual currents appear to be weak, although drifters have delineated a strong intrusive flow into the mouth of Prince Regent Inlet in the summer (Fissel and Marko, 1978). There is evidence for a similar pattern at the northern entrance to Peel Sound, where a northerly flow on the east side of the Sound may represent the return portion of an intrusion of the easterly flow through Barrow Strait. No direct current measurements are available at this time for most areas of the southern channels.

Southern Connecting Passages: Residual-current measurements are available, in the west, only for Prince of Wales Strait connecting the Archipelago with the Arctic Ocean by way of Amundsen Gulf, and in the east for Fury and Hecla Strait, a narrow channel connecting the Gulf of Boothia with the northern reaches of Foxe Basin - Hudson Bay. In both cases the net residual flows are directed out of the Archipelago into the adjoining waterway to the south. The upstream source for the southwesterly flow through Prince of Wales Strait is not clear, as direct measurements in western Parry Channel did not reveal any flows directed into Prince of Wales Strait. However, de Lange Boom et al. (1987) traced the water source to the area north of Banks Island, through a similarity in water properties. A net flow into Amundsen Gulf from the Archipelago also is believed to occur through Dolphin and Union Strait, on the basis of some measurements of short duration current (Kashino, 1979) and of water-property distributions (Fissel, Knight and Birch, 1984).

Coastal Current: One of the most notable features of residual flows within the Archipelago is the common occurrence of coastal currents, often flowing in opposing directions on opposite sides of a channel. In most

cases, the coastal currents are considerably larger than the mean near-surface residual currents occurring at mid-channel locations. Invariably the coastal currents are directed alongshore, with the nearest coastline to the right of the flow direction, consistent with buoyancy-driven geostrophic flow. Through direct current measurement (see Table 4-1), coastal currents were detected in six channels.

Table 4-1

A summary of coastal currents in the Canadian Arctic Archipelago detected using Eulerian current data. Included are the location, mean speed and estimated width for each coastal current.

Channel	Side	Mean Flow Speed (cm/s)	Est. Width (km)
Prince of Wales Strait	NW	8	8 (a)
E. Viscount Melville (off SW Bathurst Is.)	N	3	8 - 30 (b)
	S (off Prince of Wales Is.)	4	8 - 35 (b)
Peel Sound	E	10	<12 - 25 (b)
Barrow Strait	S (spring)	16	8 - 28 (b)
	S (summer)	26	>6 (c)
	N (summer only?)	12	>8 (b)
Wellington Channel	E (middle transect)	13	2 - 5 (a)
E. Lancaster Sound	N	55	<10 (d)
	S	50	<11 - 33 (d)

Notes on estimation of coastal current width:

- (a) computed from cross-spectral analysis (section 3.3 this report)
- (b) estimated from the reduction or reversal in mean currents with distance across a transect of current measurement sites
- (c) from Prinsenberg and Bennett (1987)
- (d) determined from an analysis of a combined set of current-meter, surface-drifter and CTD data (Fissel, Lemon and Birch, 1981)

As mentioned previously, summer surface-drifter data and satellite-tracked ice-floe trajectories (Fissel and Marko, 1978; Marko, 1978) suggest that the pattern of oppositely-directed coastal currents also occurs at the entrances to Prince Regent Inlet, Admiralty Inlet, Wellington Channel and Peel Sound (Figure 1.3-3).

LeBlond (1980) showed that oppositely-directed coastal currents within the Archipelago are explicable as a pair of oppositely-directed coastal geostrophic flows. This condition of opposing flows is possible when the channel width is large relative to the local internal Rossby radius of deformation. Opposing coastal currents occur when currents flow across the mouths of wide channels (eg. the Baffin Current flowing past the mouth of Lancaster Sound), producing a re-entrant circulation. The coastal current flows into the adjoining channel, eventually turns across the channel and then flows out of the channel along the opposite shore.

Interestingly, there was no evidence of a coastal current in other channels having a width comparable to that of channels listed in Table 4-1. In channels, such as M'Clintock Channel, M'Clure Strait and W. Viscount Melville Sound, the residual currents are weak, and station spacing large; perhaps such features are therefore beyond detection. However, in other areas, most notably Byam Martin Channel, Byam and Austin Channels, comparatively large residual flows are present. The absence of coastal currents in these areas may indicate that the channel is narrow relative to the internal Rossby radius and that opposing flow may be forced to occur at depth. Alternatively, other physical mechanisms, such as barotropic or baroclinic instability or the effects of sharp curvature around corners (LeBlond, 1980) or of complex bathymetry, may result in more complex flow patterns.

4.2 Temporal Variability in Residual Currents

Within-Season Variability

In the 1982 - 1985 programme the amplitude of fluctuations in the residual flow differed considerably from site to site. The largest

fluctuations were generally associated with the strongest mean currents (> 5 cm/s). However, at these locations, the fluctuations amounted to only 30 to 50 percent of the the magnitude of the mean flow, thus generating a directional steadiness, and only rare reversals of the residual current. Fluctuations associated with weak residual flows were often larger than the mean flow itself, although there were large variations among measurement sites. Areas having current fluctuations of larger amplitude than the vector mean flows, are the northern side of M'Clure Strait, the eastern side of Prince of Wales Strait and the eastern side of the southern transect through Wellington Channel.

Rotating fluctuations in the residual currents are small in comparison with the amplitude of fluctuations aligned with the channel. The geometrical constraints on residual flows within the channels of the Archipelago appear to reduce or eliminate any tendency for residual flows to be rotary.

At most measurement locations, the largest residual current fluctuations occur at periods of 8 to 25 days, the longest periods resolvable from the seasonal data sets. The fluctuations extend to even longer periods; an analysis of year-long data sets showed that fluctuation amplitudes were even larger over periods ranging from 40 to 120 days. Comparatively large fluctuations extended to periods as short as 3 days, particularly in the strong coastal current in Prince of Wales Strait, in southern Barrow Strait, and at some locations in Wellington Channel. At periods less than 3 days, the amplitude of the fluctuations was very low at all measurement sites.

The coherence levels for horizontally separated current records were generally low in most areas, indicating that the spatial scale of most current fluctuations is smaller than the typical station separation of 5 to 25 km. Areas having the lowest coherence levels were M'Clure Strait, Viscount Melville Sound, M'Clintock Channel and Byam Martin Channel. The first three areas had very small residual currents.

The longer-period fluctuations in currents appear to have the shortest spatial scales, as indicated by coherent current fluctuations at horizontally-separated sites. Horizontal spatial scales, determined from the cross-spectral analysis for longer periods, ranged from only 2 km for the northward coastal current in Wellington Channel to 8 km for the southeasterly coastal current in Prince of Wales Strait. These results lend support to the suggestion that the coastal currents are baroclinic geostrophic flows, whose length scale will be approximated by the internal Rossby radius of deformation (a few to several km within the study area). However, at shorter periods (3 to 5 days) current fluctuations exhibit larger spatial scales, at least for those areas with moderate or larger fluctuations. The spatial scale for these intermediate periods is 20 to 30 km, generally exceeding the internal Rossby radius of deformation. These larger scales suggest that barotropic mechanisms may be more important in driving the shorter-period fluctuations.

Seasonal Variability

The seasonal variations in the mean residual currents differ among the dozen or so sites at which year-long current measurements have been obtained in the Archipelago. For the seven of these sites involved in the 1982-1985 Institute of Ocean Sciences study, the summer residual currents represented the seasonal maximum at the site in Penny Strait, but were the smallest seasonal value measured in Austin Channel. In northern Barrow Strait, summer residual currents had intermediate levels between those of the spring maximum and fall to winter minimum. The seasonal variation in current fluctuations was more consistent among measurement sites, with the smallest fluctuations occurring in spring at all locations. The largest fluctuations were recorded in fall or winter, with the single exception of the northern Barrow Strait site, where the largest fluctuations occurred in summer.

Other studies involving year-long current measurements can assist in understanding the seasonal cycle. A year-long record of near-bottom current in Crozier Strait from 1977 to 1978 (Greisman and Lake, 1978) exhibited the largest mean speeds in the fall, with the weakest currents between February and August.

An eight-month record of currents at the southern Barrow Strait site obtained from April to December 1981 (Prinsenberg and Bennett, 1987) revealed that the strong easterly coastal current at this site was largest in the summer, increasing sharply from the values measured in spring and fall. The seasonal pattern determined for site 42 in northern Barrow Strait appears to be correlated with the strengthening of the easterly coastal current on the opposite side of the Strait. The currents on the northern site were reversing to westerly in August and September, the same time (but in a different year) as the maximum occurred in eastward flow on the south side of the Strait (Figure 4-2). This circulation pattern may arise from a strengthening of the westward circulation into northern Barrow Strait from Wellington Channel, or from northern Lancaster Sound, during the summer. The westward flow in northern Barrow Strait may be a re-entrant flow, eventually turning south clockwise and crossing the Strait to contribute to a stronger flow on the south side.

Further to the east, year-long current measurements were obtained at several sites in Baffin Bay near the entrance to Lancaster Sound (Lemon and Fissel, 1982). Here, the strong Baffin Current exhibited the largest flows in the summer months, with reduced flows and fluctuations through the fall and minimum values in spring.

It appears that the seasonal variation in residual currents differs between the western and eastern portions of the Archipelago. From the results of this study and previous work, the residual currents at eastern sites are largest in the summer. A summertime maximum in residual currents was observed in Penny Strait (this study), southern Barrow Strait (Prinsenberg and Bennett, 1987) and Lancaster Sound (Lemon and Fissel, 1982). However, at more westerly locations in Austin Channel (this study) and Crozier Strait (Greisman and Lake, 1978), the largest residual currents occurred in fall and winter.

Prinsenberg and Bennett (1987) suggested that the seasonal variation in the residual current measured in southern Barrow Strait were related to corresponding variations in large-scale sea level gradient. They showed that the seasonal cycle in sea-level difference between the Beaufort Sea

and Barrow Strait was similar to the cycle in residual current in Barrow Strait. However, if a sea-level gradient on this scale is responsible for the seasonal pattern in residual current, the seasonal pattern should be similar throughout the Archipelago. One possible explanation for the observed regional differences in seasonal cycle is that large-scale sea-level gradients differ with direction in the Archipelago. An examination of monthly mean sea-level data from Alert and Resolute between 1963 and 1974 (Walker, 1978) indicates that the north-south sea-level gradient has minimum value in summer and peak level in fall and winter. This north-south gradient, is similar in magnitude, but reversed in sense from the west-east gradient noted by Prinsenberg and Bennett (1987).

The variation in sea-ice clearing during summer may also be related to the seasonal pattern in residual current. Extensive clearing of sea-ice occurs in most years in the eastern Archipelago, but the clearing of ice cover is more limited and variable in the west. The presence of sea ice through the summer reduces wind forcing on the ocean. In addition, the contribution of ice melt water to the development of a less dense upper layer is reduced at western locations in the Archipelago.

Interannual Variability

Few areas have been studied sufficiently to allow estimates of year-to-year variability.

Current data were obtained during April through June 1978 at sites in Wellington Channel, along a line nearly identical to the northern one of 1984. The net transport in 1984 was southerly, with the strongest flow (7.8 cm/s vector-average) along the western side. However, a strong, narrow counter-current with vector-average speeds of up to 13 cm/s was present along the eastern shore. The 1978 current data are consistent with the 1984 data. Flow in the central and western portions of the channel was southerly at 2 to 7 cm/s (vector-averaged), with a counter-flow of 1.7 cm/s at the easternmost site. The station spacing in 1978 was probably too large to permit adequate sampling of the counter-flow. This flow

pattern in Wellington Channel seems to be a fairly permanent feature of the circulation: a counter-current was evident here in 1977 drifter data (Fissel and Marko, 1978) and in 1973-1977 ice-drift data (Marko, 1978).

The largest set of direct measurements of currents in the Archipelago were made in Barrow Strait by OGIW and IOS between 1981 and 1985. Although not continuous, and not always at the same site, these provide the best indications of seasonal and year-to-year variability in the residual circulation in the Archipelago.

The strong easterly flow along the southern side of Barrow Strait appears to be a permanent feature of the circulation. It was apparent in each of the springtime data sets collected from 1981 to 1983, as well as in the summer of 1981, as discussed previously, and in the summer of 1977 (Fissel and Marko, 1978).

4.3 Volume Transport

Volume transports were computed for seven channels using the 1982-1985 Institute of Ocean Sciences data. In previous studies, springtime volume transport computations are available for: Byam and Austin Channels, and Grozier and Pullen Straits, in 1975 (Greisman and Lake, 1978); Barrow Strait in 1982 (Prinsenberg and Bennett, 1987); Fury and Hecla Strait in 1975 (Sadler et al., 1979); and Nares Strait in 1972 (Sadler, 1976a). All available springtime volume transports derived from direct current measurement along with temperature and salinity distributions, are displayed in Figure 4.3-1.

The volume transport results reflect the net flow from the Arctic Ocean into Baffin Bay through the Archipelago. The largest transport measured, $67 \times 10^4 \text{ m}^3/\text{s}$, occurred through Nares Strait, leading directly into Northern Baffin Bay. The outflow from the Archipelago through Lancaster Sound appears to be about the same value ($68 \times 10^4 \text{ m}^3/\text{s}$) based on combined values from Barrow Strait ($44 \times 10^4 \text{ m}^3/\text{s}$) and Wellington Channel ($24 \times 10^4 \text{ m}^3/\text{s}$). A relatively small eastward transport, $4 \times 10^4 \text{ m}^3/\text{s}$, leaves the Archipelago through Fury and Hecla

Strait. The transport through Jones Sound has not been directly measured, but early indirect (baroclinic only) measurements indicate that the discharge from this Sound is about half that from Lancaster Sound in the summer (section 1.3). Assuming these results are applicable to the direct springtime measurements, the total volume discharge into Baffin Bay is approximately $170 \times 10^4 \text{ m}^3/\text{s}$, which within uncertainties is in agreement with the $210 \times 10^4 \text{ m}^3/\text{s}$ total transport southward in summer from Baffin Bay to Davis Strait (Coachman and Aagaard, 1974; Muench, 1971).

Within the Archipelago, about one-half ($34 \times 10^4 \text{ m}^3/\text{s}$) of the outward flow through Barrow Strait and Wellington Channel appears to come through Penny Strait. About 12 to $16 \times 10^4 \text{ m}^3/\text{s}$ flows into Parry Channel from Byam Martin Channel, leaving an apparent imbalance of 18 to $22 \times 10^4 \text{ m}^3/\text{s}$. In view of the large uncertainties in the volume transport estimates, the imbalance may simply arise due to a combination of errors from individual transport computations, and the absence of any transport estimates for Peel Sound, one of the adjoining channels to the south of Barrow Strait.

Alternatively, the imbalance may indicate an underestimate of the eastward transport entering the Archipelago from M'Clure Strait. The computed value of $5 \times 10^4 \text{ m}^3/\text{s}$ had a large uncertainty of $30 \times 10^4 \text{ m}^3/\text{s}$; this arose, in large part, both from the sparse sampling over this very wide and deep channel and from the small current speeds measured over most of the Strait. There is indirect evidence for an inflow of Arctic Ocean water at depths near 120 m over the southern two-thirds of M'Clure Strait (de Lange Boon, 1988; Melling et al., 1984). Some of the flow into M'Clure Strait likely exits through Prince of Wales Strait, while any additional, undetected, amount may contribute to the eastward transport through Barrow Strait.

Seasonal variability in volume transport within the Archipelago remains largely unknown. Prinsenberg and Bennett (1987) computed volume transport through Barrow Strait; it ranged from a low of $20 \times 10^4 \text{ m}^3/\text{s}$ in January to a high of $100 \times 10^4 \text{ m}^3/\text{s}$ in August. The annual mean of

$50 \times 10^4 \text{ m}^3/\text{s}$ is approximately the same as the springtime value. However, the transport computed for seasons other than spring were derived from direct-current measurements obtained at just one site in Barrow Strait (Site 46 in the strong eastward flowing current on the south side of the Strait), using the springtime relationship between total transport and current measurements at Site 46 (Prinsenber and Bennett, 1987). This analytical approach appears to make no allowance for changes in the large-scale flow patterns within the Strait, such as the development of a westward counterflow on the northern side of the Strait observed in the summer of 1984 (Figure 4-2). The westerly inflow would reduce the net transport unless the inflowing water was fully recirculated into the easterly flow on the southern side of the Strait. However, even if this were the case, the algorithm of Prinsenber and Bennett (1987) derived from the springtime situation (eastward flow throughout the channel), may tend to overestimate the net transport in summer, when two opposing flows are present.

Interannual variability of the volume transports within the Archipelago can only be examined in a very preliminary fashion, given the paucity of transport results available at the same location in more than one year. The best repeated estimate derived from direct current measurement is for Barrow Strait. The volume transport measured in April 1982 (Prinsenber and Bennett, 1987) and in April 1984 from this study show good agreement (50×10^4 and $44 \times 10^4 \text{ m}^3/\text{s}$, respectively). A second comparison of volume transport for Byam Martin Channel also reveals good agreement. In this study a net southward transport of $12 \pm 4 \times 10^4 \text{ m}^3/\text{s}$ was obtained from April 1982 data. Greisman and Lake (1978) computed a total southerly transport of $16 \times 10^4 \text{ m}^3/\text{s}$ for the connecting passages of Byam and Austin Channels. Based on these two comparisons, volume transports may not exhibit large year-to-year variations. However, many additional comparisons, in combination with a better understanding of the underlying dynamics of large-scale flows through the Archipelago, are required to reach a definitive conclusion on interannual variability of transports.

5. REFERENCES

- Avis, R.A. and L.K. Coachman, 1971. Current measurements in Smith Sound-northern Baffin Bay, September 1968. Baffin Bay-North Water Project Scientific Report No. 2, Arctic Institute of North America, Washington, D.C.: 26 pp.
- Bailey, W.B., 1957. Oceanographic features of the Canadian Archipelago. J. Fish. Res. Board Can. 14(5): 731-769.
- Barber, F., 1965. Current observations in Fury and Hecla Strait. J. Fish. Res. Bd. Can. 22(1): 225-229.
- Barber, F.G. and A. Huyer, 1971. On the water of the Canadian Arctic Archipelago - an atlas presentation of 1961 and 1962 data. Unpublished manuscript. MRS Rep. 21. Canada Dept. Energy, Mines and Resources, Marine Sciences Branch, Ottawa: 76 pp.
- Bath, M., 1974. Spectral analysis in geophysics. Elsevier, Amsterdam. 325 pp.
- Birch, J.R., D.B. Fissel, D.D. Lemon, and R.A. Lake, 1987. Arctic Data Compilation and Appraisal. Vol. 14. Northwest Passage: Physical Oceanography - Temperature, Salinity, Currents, Water Levels and Waves. Revised and updated to include 1820 through 1986. Can. Data Rep. Hydrogr. Ocean Sci. No. 5, (Vol. 14): 300 pp.
- Birch, J.R., D.B. Fissel, D.D. Lemon, A.B. Cornford, R.H. Herlinveaux, R.A. Lake, B.D. and Smiley, 1983. Arctic Data Compilation and Appraisal. Baffin Bay: Physical Oceanography - Temperature, Salinity, Currents and Water Levels. Can. Data Rep. Hydrogr. Ocean Sci. 5, (Vol. 5): 372 pp.
- Buckingham, W.R., R.A. Lake and H. Melling, 1985. Temperature and Salinity Measurements in the Northwest Passage in March and April, 1982. Can. Data Rep. Hydrogr. Ocean Sci. No. 39: 371 pp.
- Buckingham, W.R., R.A. Lake and H. Melling, 1987a. Temperature and Salinity Measurements in the Northwest Passage, Volume 2, March 1983. Can. Data Rep. Hydrogr. Ocean Sci. No. 39: 152 pp.
- Buckingham, W.R., R.A. Lake and H. Melling, 1987b. Temperature and Salinity Measurements in the Northwest Passage, Volume 3, March - April, 1984. Can. Data Rep. Hydrogr. Ocean Sci. No. 39: 604 pp.
- Buckingham, W.R., R.A. Lake and H. Melling, 1987c. Current and Sea-Level Measurements in the Northwest Passage, Volume 1, March 1982 - April 1983. Can. Data Rep. Hydrogr. Ocean Sci. No. 51: 128 pp.

- Buckingham, W.R., R.A. Lake and H. Melling, 1987d. Current and Sea-Level Measurements in the Northwest Passage, Volume 2, March 1983 - April 1984. Can. Data Rep. Hydrogr. Ocean Sci. No. 51: 84 pp.
- Buckingham, W.R., R.A. Lake and H. Melling, 1987e. Current and Sea-Level Measurements in the Northwest Passage, Volume 3, March 1984 - April 1985. Can. Data Rep. Hydrogr. Ocean Sci. No. 51: 139 pp.
- Campbell, N.J., 1958. The oceanography of Hudson Strait. Fish. Res. Bd. Can. MS Rept. (Oceanogr. and Limnol.). No. 12.
- Coachman, L.K. and K. Aagaard, 1974. Physical oceanography of the arctic and sub-arctic seas. In: Marine Geology and Oceanography of the Arctic Seas. Springer-Verlag, New York, N.Y.: 1-72.
- Collin, A.E., 1963. Waters of the Canadian Arctic Archipelago. In: Proceedings of the Arctic Basin Symposium, Oct. 1962. pp. 128-139. Arctic Inst. of N.A., Wash., D.C.: 313 pp.
- Collin A.E. and M.J. Dunbar, 1964. Physical Oceanography in Arctic Canada. Oceanogr. Mar. Biol. Ann. Rev. 2: 45-75.
- de Lange Boom, B.R., H. Melling and R.A. Lake, 1987. Late winter hydrography of the Northwest Passage: 1982, 1983 and 1984. Can. Tech. Rep. Hydrogr. Ocean Sci. No. 79: 165 pp.
- Fissel, D.B. and J.R. Marko, 1978. A surface current study of eastern Parry Channel, N.W.T. - summer 1977. Contr. Rep. Ser. 78-4 by Arctic Sciences Ltd., Sidney, B.C. for Institute of Ocean Sciences, Sidney, B.C.: 66 p.
- Fissel, D.B. and G.R. Wilton, 1978. Subsurface current measurements in eastern Lancaster Sound, N.W.T. - summer, 1977. Contr. Rep. Ser. 78-3 by Arctic Sciences Ltd., Sidney, B.C. for Institute of Ocean Sciences, Sidney, B.C. Unpublished manuscript: 72 pp.
- Fissel, D.B. and G.R. Wilton, 1980. Subsurface current measurements in western Baffin Bay and Lancaster Sound, 1978-1979. Data report no. 1. Unpublished manuscript. Arctic Sciences Ltd., Sidney, B.C. for Petro-Canada, Calgary, Alberta: 52 pp. plus appendices.
- Fissel, D.B., L. Cuyppers, D.D. Lemon, J.R. Birch, A.B. Cornford, R.A. Lake, B.D. Smiley, R.W. Macdonald and R.H. Herlinveaux, 1983. Arctic Data Compilation and Appraisal. Vol. 6. Queen Elizabeth Islands: Physical Oceanography - Temperature, Salinity, Currents and Water Levels. Can. Data Rep. Hydrogr. Ocean Sci. 5, (Vol. 6): 214 pp.
- Fissel, D.B., D.D. Lemon and J.R. Birch, 1981. Environmental Studies No. 25. The physical oceanography of western Baffin Bay and Lancaster Sound. Dept. of Indian and Northern Affairs, Northern Affairs Program, Ottawa: 293 pp.
- Fissel, D.B., D.D. Lemon and J.R. Birch, 1982. Major features of the near-surface circulation of western Baffin Bay, 1978 and 1979. Arctic 35: 180-200.

- Fissel, D.B., D.N. Knight and J.R. Birch, 1984. An oceanographic survey of the Canadian Arctic Archipelago, March-April 1982. Can. Contract. Rep. Hydrogr. Ocean Sci. No. 15: 415 pp.
- Greisman, P. and R.A. Lake, 1978. Current observations in the channels of the Canadian Arctic Archipelago adjacent to Bathurst Island. Pac. Mar. Sci. Rep. 78-23. Institute of Ocean Sciences, Sidney, B.C. Unpublished manuscript: 127 pp.
- Groves, G.W. and E.J. Hamman, 1968. Time series regression of sea level on weather. Review of Geophysics 6(2): 129-174.
- Juhasz, T.A., 1980. Polar Gas Pipeline Survey: ocean current measurement program, Loughheed Island to Melville Island, N.W.T. Dobrocky Seatech Ltd., Victoria, B.C. report to the Polar Gas project: 41 pp.
- Kashino, R.K., 1979. Ocean current measurement program, Dolphin and Union Strait, N.W.T. Polar Gas Pipeline Survey. Submitted to Kenting Exploration Services Ltd. by Dobrocky Seatech Ltd., Sidney, B.C. Unpublished manuscript: 183 pp.
- Killierich, A.B., 1939. The Godthaab expedition 1928 - a theoretical treatment of the hydrographical observation material. Meddelelser om Gronland 78(5): 1-148.
- LeBlond, P.H., 1980. On the surface circulation in some channels of the Canadian Arctic Archipelago. Arctic 33(1): 189-197.
- Lemon, D.D. and D.B. Fissel, 1982. Seasonal variations in currents and water properties in northwestern Baffin Bay 1978-1979. Arctic 35(1): 211-218.
- Lewis, E.L., 1980. Oceanographic instruments and deployment systems for Polar seas. Oceans '80, Seattle, Washington: 7 pp.
- MacNeil, M.R., B.R. de Lange Boom and D. Ramsden, 1978. Radar tracking of ice in the Griffith Island Area of Barrow Strait, N.W.T. Inst. of Ocean Sciences, Contr. Rep. Ser. 78-2: 105 pp.
- Marko, J.R., 1978. A satellite imagery study of eastern Parry Channel. Inst. of Ocean Sciences, Sidney, B.C., Contr. Rep. Ser. 78-5: 134 pp.
- Muench, R.D., 1971a. The physical oceanography of the northern Baffin Bay Region. Arctic Inst. of N.A., Washington, D.C. Baffin Bay-North Water Project. Sc. Rep. No. 1: 150 pp.
- Muench, R.D., 1971b. Oceanographic conditions at a fixed location in western Kane Basin, May 1969. U.S. Coast Guard, Washington, D.C., Oceanogr. Rep. No. 44: 1-5.
- Palfrey, K.M. and G. Godfrey Day, 1968. Oceanography of Baffin Bay and Nares Strait in summer of 1966 and current measurement in Smith Sound, summer 1963. U.S. Coast Guard, Washington, D.C. Oceanogr. Rep. No. 16: 204 pp.

- Peck, G.S., 1978. Arctic oceanographic data report, 1977, Viscount Melville Sound. Ocean and Aquatic Sciences, Central Region, Data Report Series No. 78-3: 150 pp. plus illustrations.
- Peck, G.S., 1980a. Arctic oceanographic data report, 1978. Vol. 2. Ocean and Aquatic Sciences, Central Region, Data Report Series No. 80-1: 163 pp. plus illustrations.
- Peck, G.S., 1980b. Arctic oceanographic data report, 1979, Sverdrup Basin. Vol. 1. Ocean and Aquatic Sciences, Central Region, Data Report Series No. 80-2: 228 pp.
- Peck, G.S., 1980c. Arctic oceanographic data report, 1979, Sverdrup Basin. Vol. 2. Ocean and Aquatic Sciences, Central Region, Data Report Series No. 80-3: 91 pp.
- Polar Gas Project, 1979. M'Clure Strait marine geophysical investigation, April 1979. Polar Gas Project, Toronto, Ontario for Combined Pipeline System Study: 73 pp.
- Prinsenbergh, S.J. and E.B. Bennett, 1987. Mixing and transports in Barrow Strait, the central part of the Northwest Passage. Cont. Shelf Res. 7: 913-935.
- Sadler, H.E., 1976a. Water, heat and salt transports through Nares Strait, Ellesmere Island. J. Fish. Res. Bd. Can. 56: 2286-2295.
- Sadler, H.E., 1976b. The flow of water and heat through Nares Strait. Def. Res. Est. Ottawa, Rep. No. 736: 184 pp.
- Sadler, H.E., H.V. Serson and R.K. Chow, 1979. The oceanography of Fury and Hecla Strait. Def. Res. Est. Pacific, Victoria, B.C., Tech. Mem. 79-11: 61 pp. plus appendices.
- Singleton, R.C., 1969. An algorithm for computing the mixed radix fast Fourier transforms. IEEE Transactions on Audio and Electro-Acoustics, 17: 93-103.
- Smith, E.H., 1931. Arctic ice, with special reference to its distribution to the North Atlantic Ocean; the Marion expedition to Davis Strait and Baffin Bay, 1928. United States Coast Guard Bulletin 19 (3): 1-221.
- Smith, M. and B. Rigby, 1981. Distribution of polynyas in the Canadian Arctic. In Polynyas in The Canadian Arctic, Sterling I. and H. Cleaton (ed.). Occ. Paper No. 45, Can. Wildlife Service: 7-28.
- Stronach, J.A., J.A. Helbig, S.S. Salvador, H. Melling and R.A. Lake, 1987. Tidal elevations and tidal currents in the Northwest Passage, Can. Tech. Rep. Hydrogr. Ocean Sci. No. 97: 329 pp.

- Todoroff, S.W., 1983. Circulation characteristics of Barrow Strait in the Northwest Passage. Fish. and Oceans, internal report, Ocean. Sci. and Survey, Bayfield Lab., Manuscript Rep. Series No. 16. Unpublished manuscript (M.A.Sc. Civ. Eng., Univ. Waterloo): 104 pp.
- Verrall, R.I., J.H. Ganton and A.R. Milne, 1974. An ice drift measurement in western Parry Channel. Arctic 27(1): 47-52.
- Waddell, S., 1985. Low frequency flow in the Canadian Arctic Archipelago. Ph.D. Thesis, Dept. of Oceanography, Dalhousie University, Halifax, N.S.: 203 pp.
- Walker, E.R., 1977. Aspects of oceanography in the archipelago. Inst. of Ocean Sciences, Sidney, B.C. Note 3: 186 pp.

FIGURES



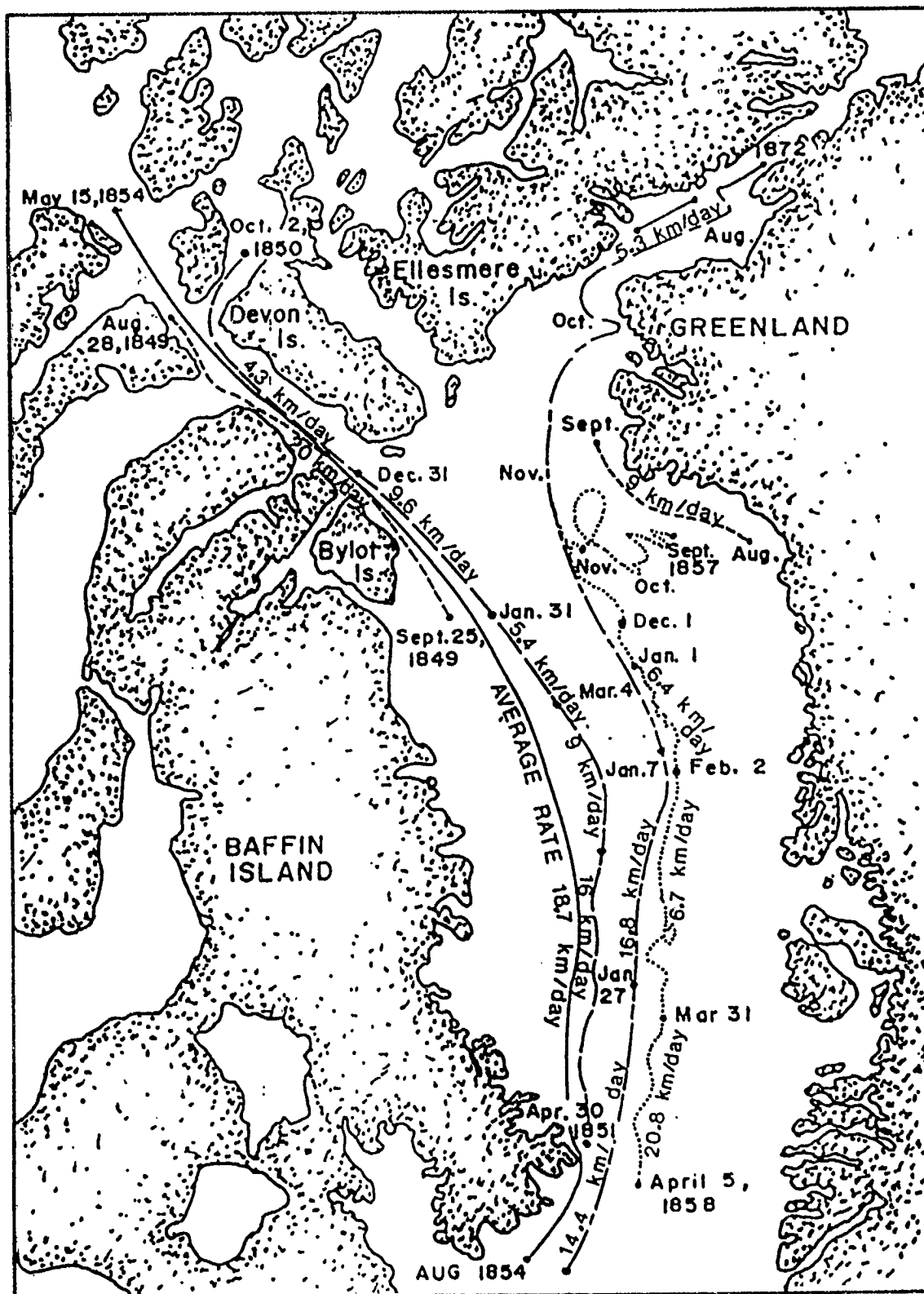


Figure 1.3-1: Trajectories of several ice-beset vessels and of the *Polaris* ice-floe party (Smith, 1931). Average net speeds are indicated for major segments of each track (from Fissel, Lemon and Birch, 1981).

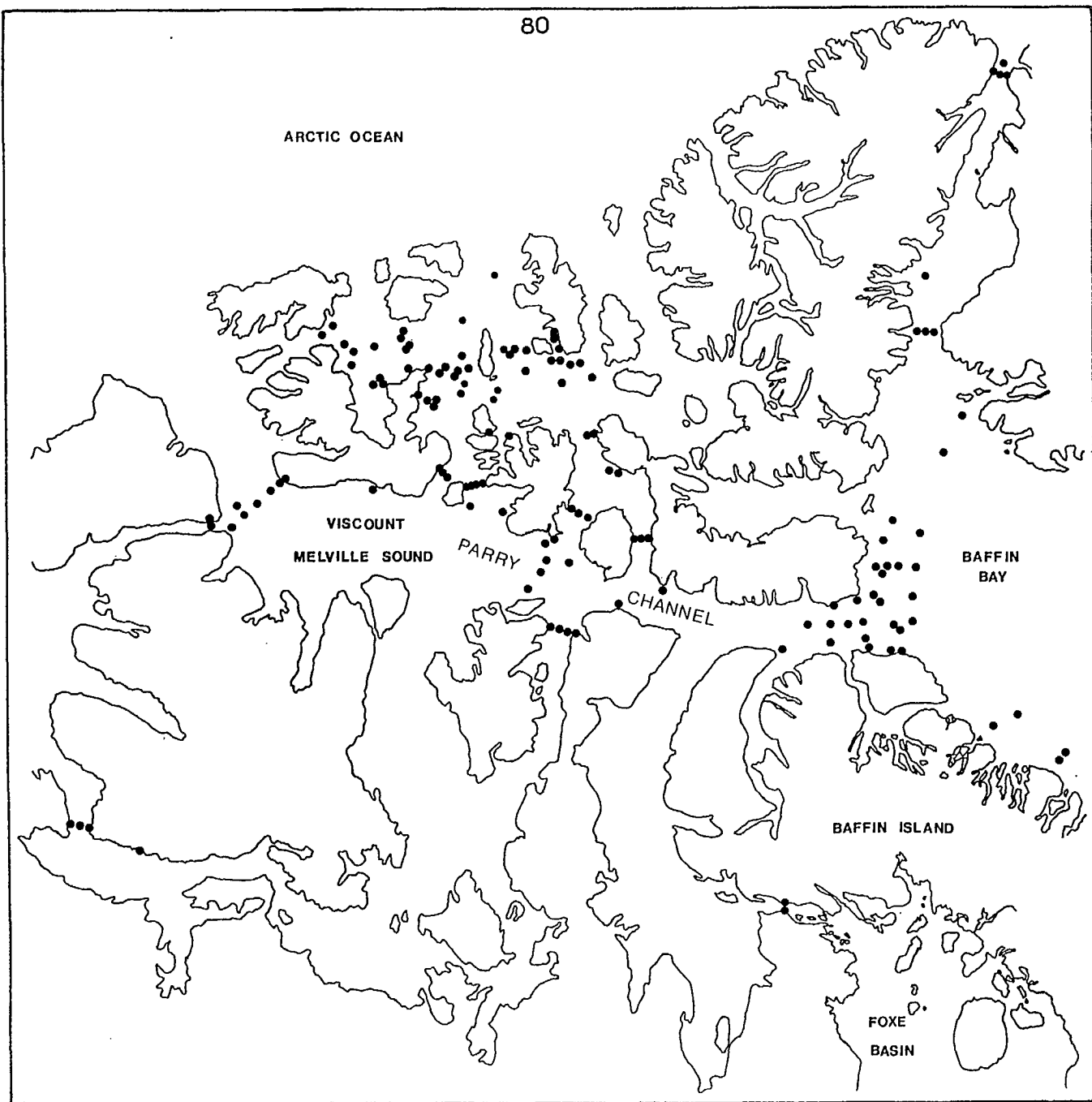


Figure 1.3-2: Locations of all moored-current-meter data obtained in the Canadian Arctic Archipelago prior to 1982 (from Fissel et al., 1983; Birch et al., 1983, 1987).

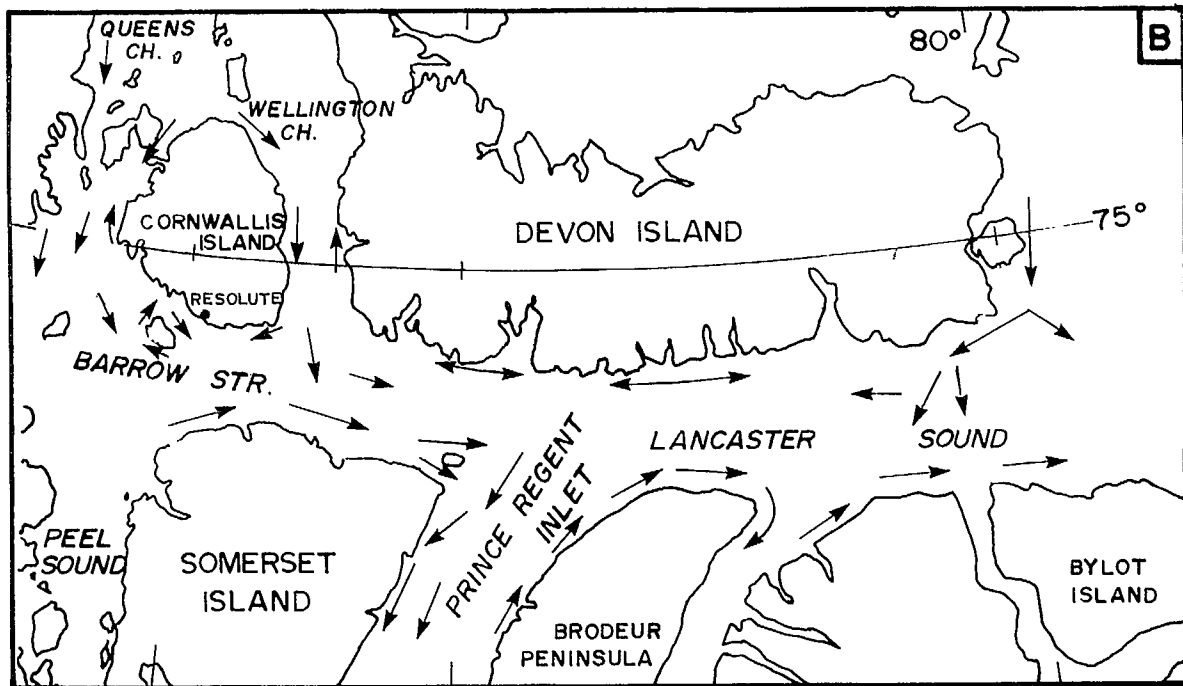
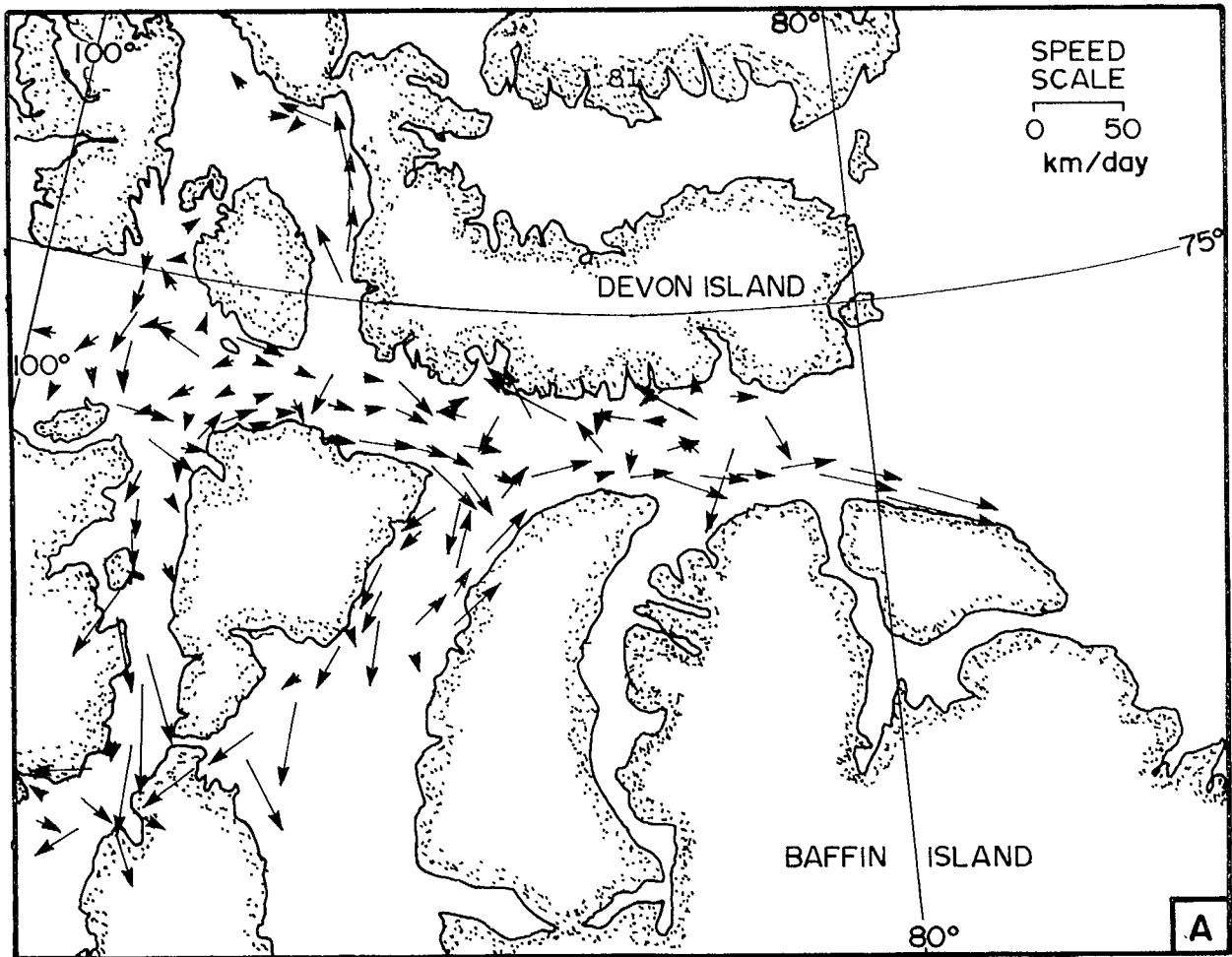


Figure 1.3-3: a) Vector-averaged velocities from drogued-drifter measurements in eastern Parry Channel, July–November, 1977. The averaging is applied over rectangles of size 0.2° latitude by 0.8° longitude (from Fissel and Marko, 1978).
 b) Observed directions of summer ice movements in eastern Parry Channel, 1973–1977. Arrow length is approximately proportional to observed ice speed (from Marko, 1978).

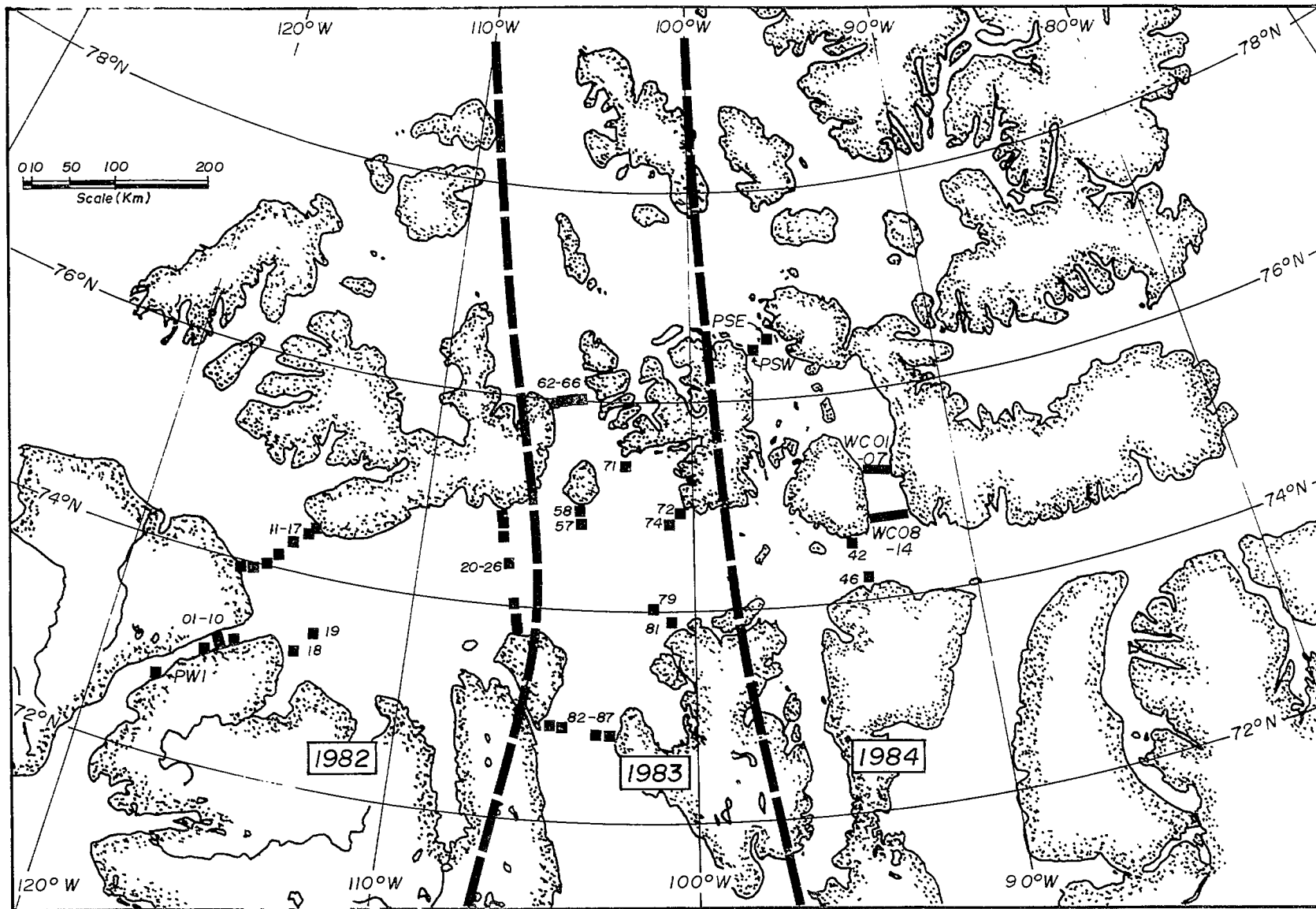


Figure 2.1-1: Institute of Ocean Sciences current measurement sites in 1982, 1983 and 1984.

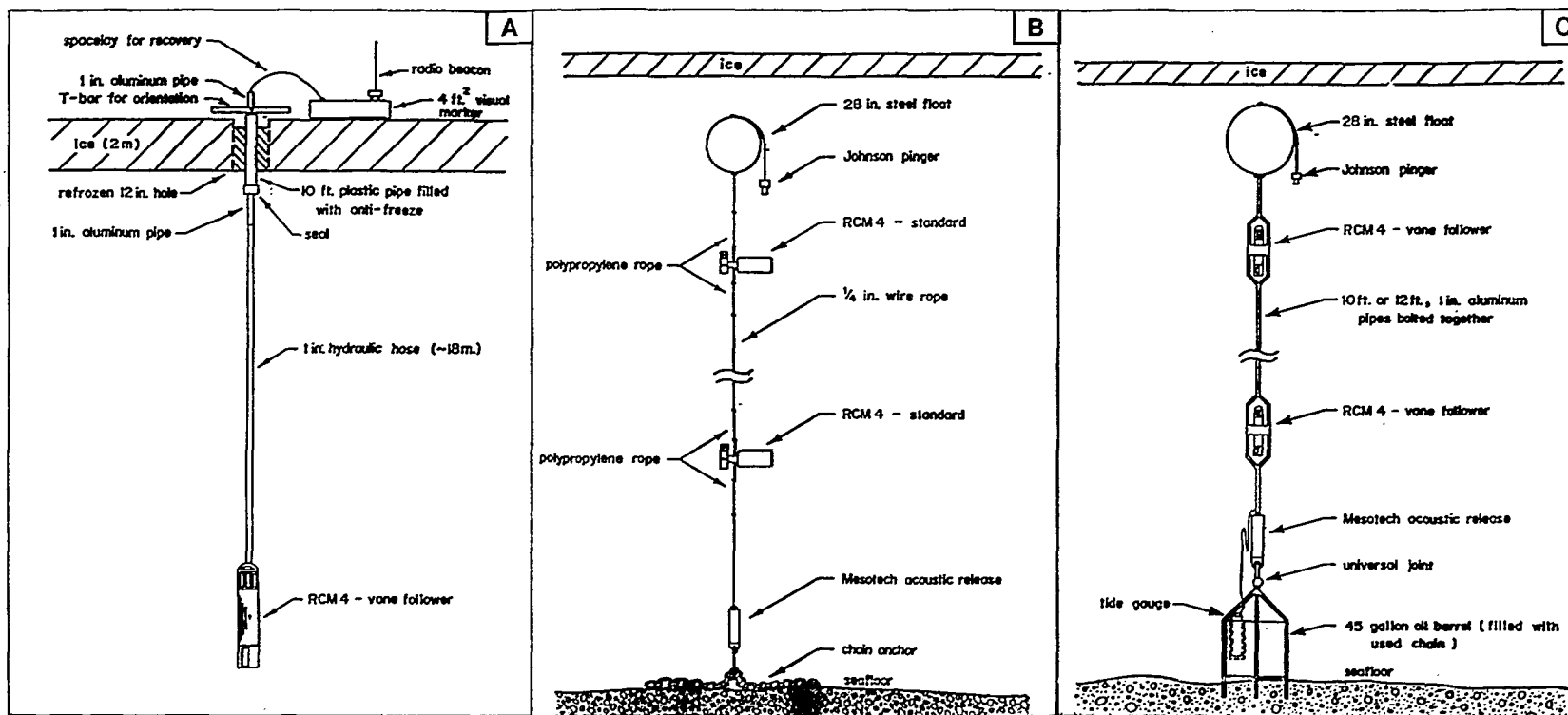


Figure 2.1-2a: Vane-follower current meters suspended from the sea-ice on hydraulic hose (from Buckingham, Lake and Melling, 1987c).

Figure 2.1-2b: Standard configuration current meter on a taut-line mooring (from Buckingham, Lake and Melling, 1987c).

Figure 2.1-2c: Bottom-founded mooring with vane-follower current meters (from Buckingham, Lake and Melling, 1987c).

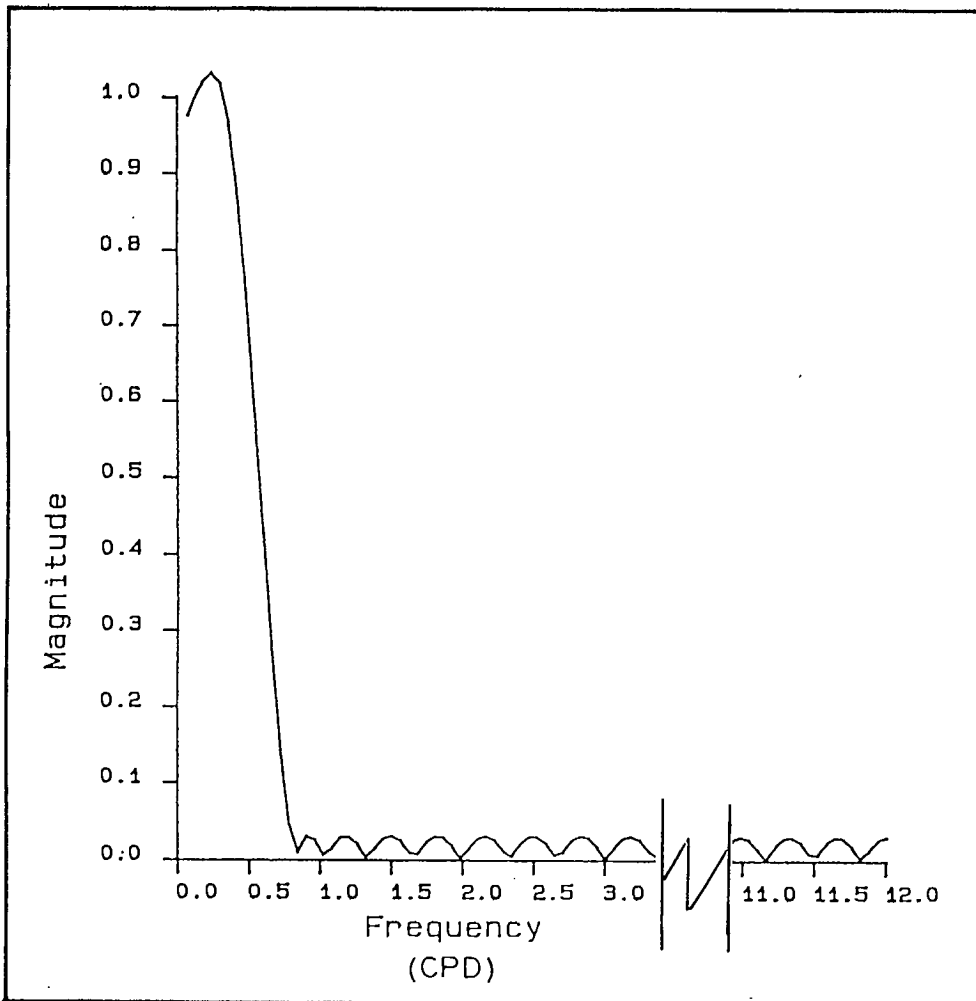


Figure 2.2-1: Response curve of the low-pass filter used to isolate the residual component of the current record. The filter has 72 coefficients, resulting in a data loss of 1.5 days at each end of the record.

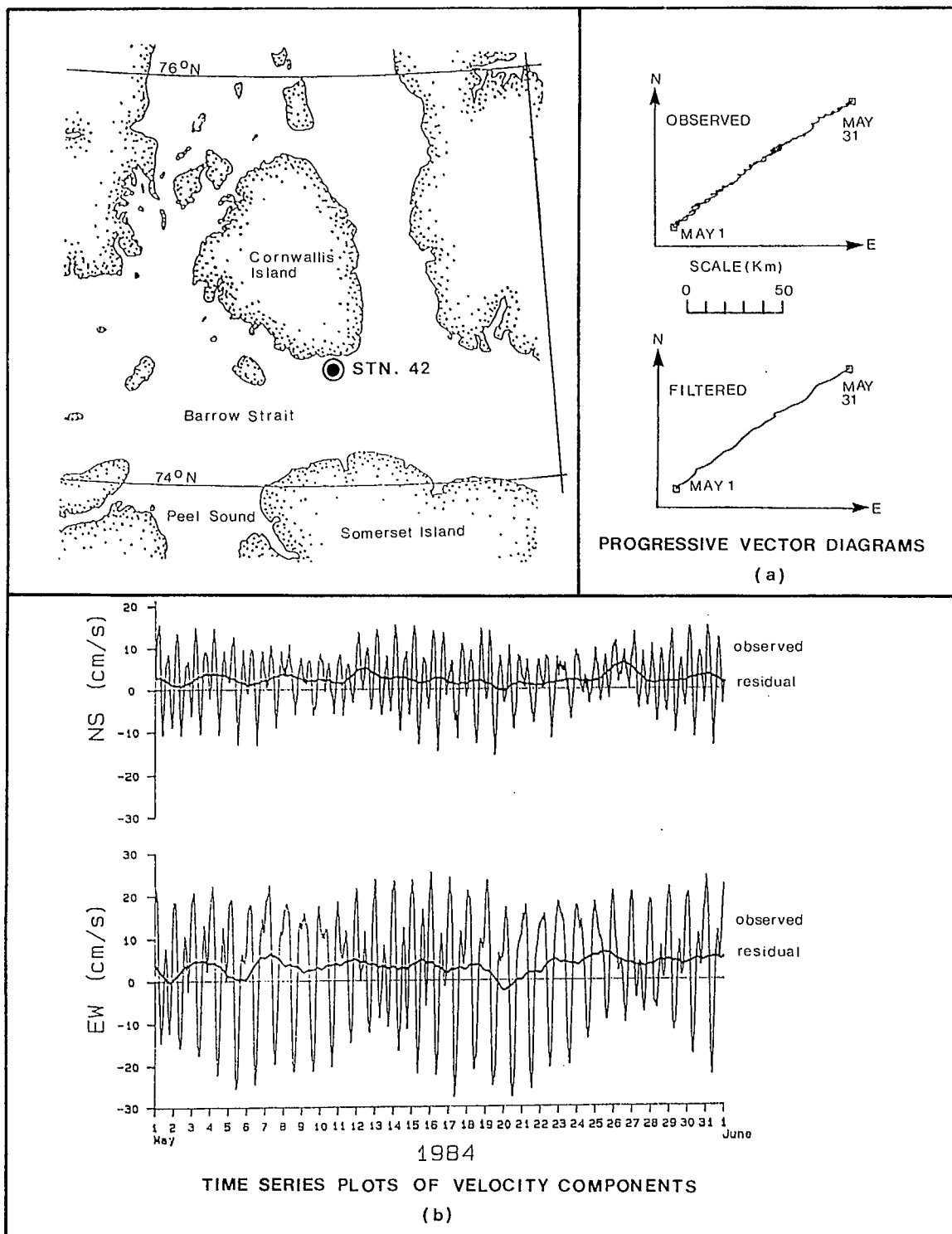


Figure 2.2-2: Observed and low-pass filtered currents at Station 42, May 1984. The observed currents oscillate between southwesterly (flood tide) and northeasterly (ebb tide), although the residual flow is to the north and east. The progressive vector diagrams are not trajectories but represent the cumulative displacement due to the current observed at Station 42.

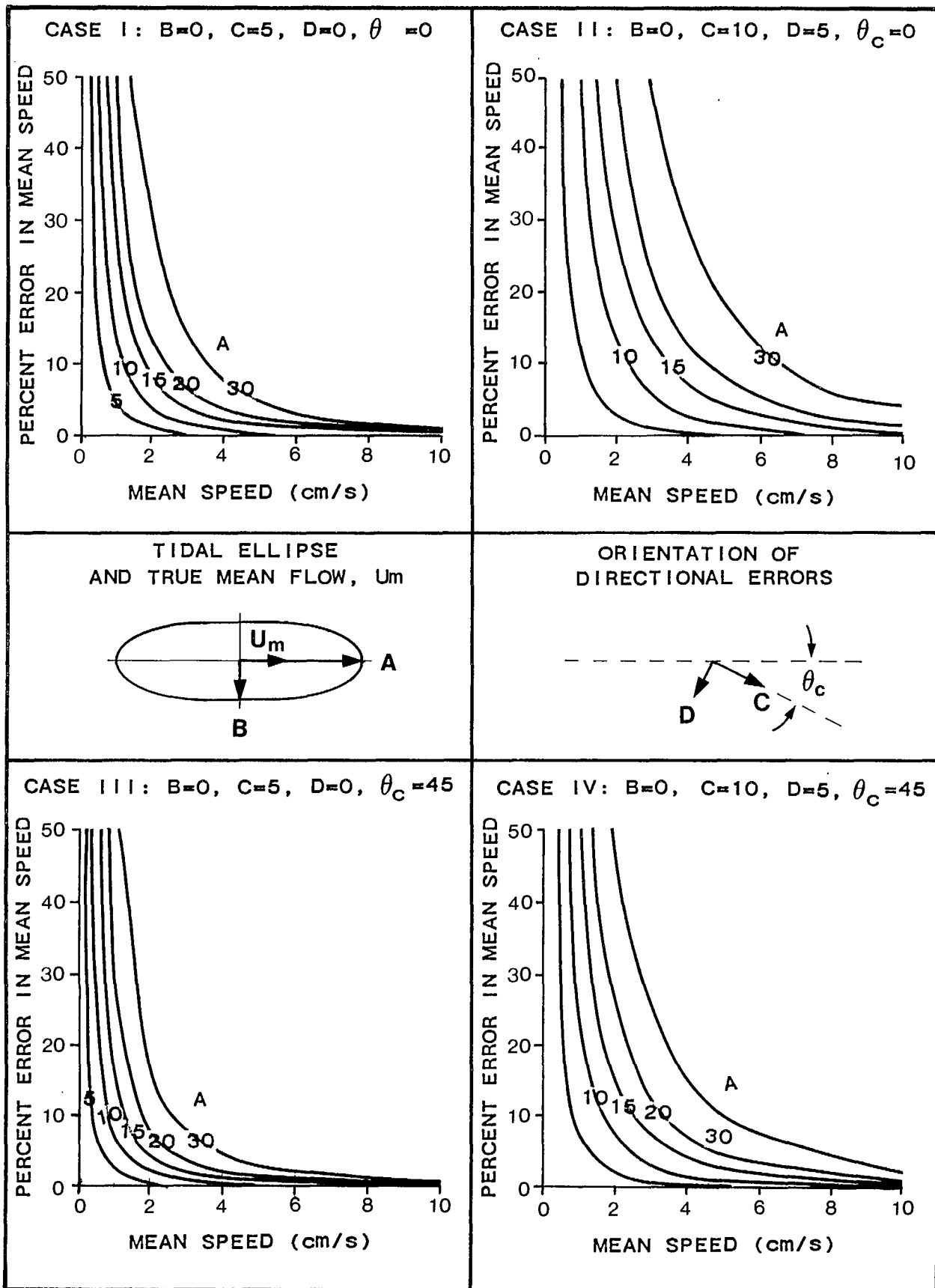


Figure 2.3-1: Estimates of the percent error in measured mean speed, for various tidal signals and compass calibration errors.

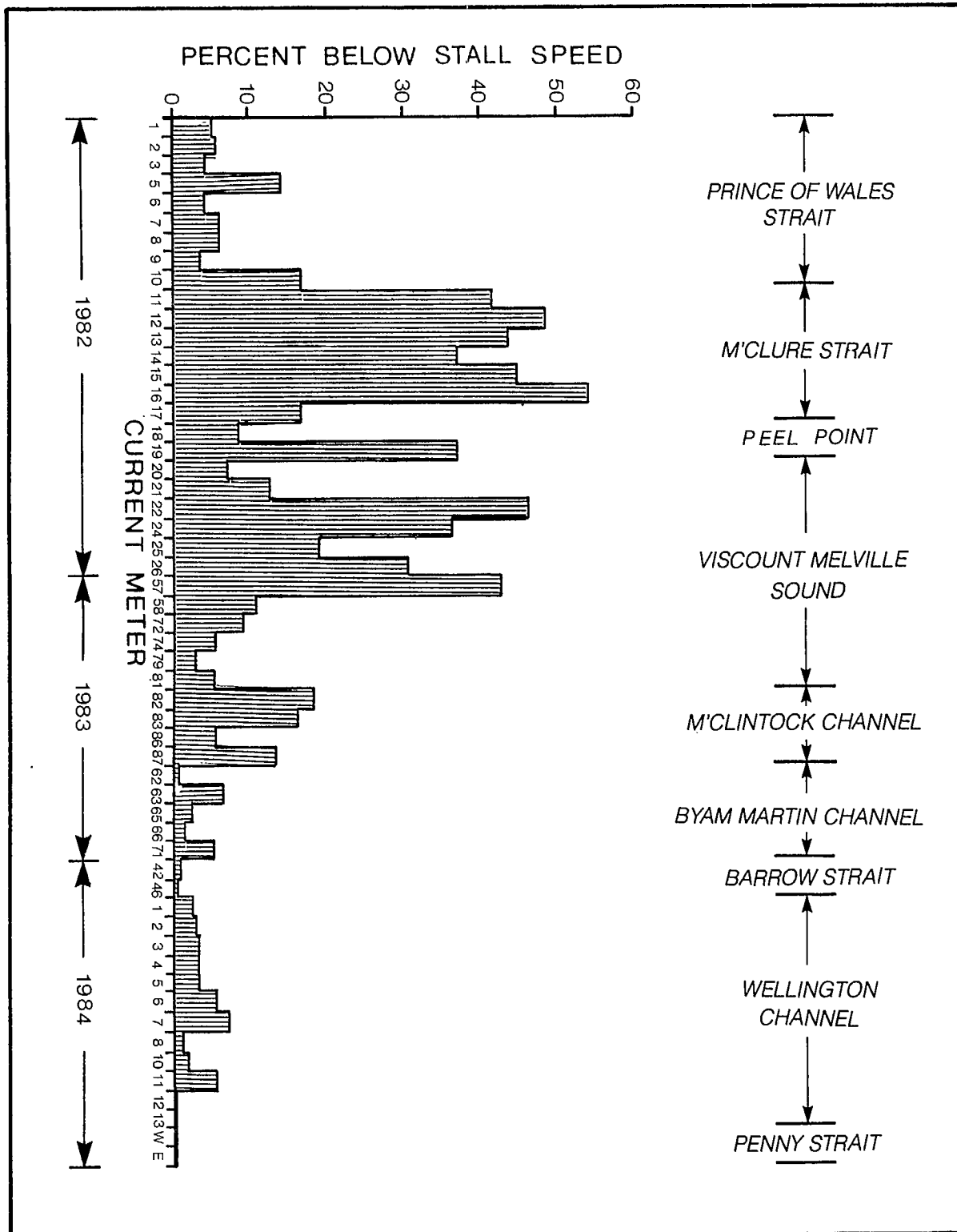


Figure 2.3-2: Percent of recorded speeds below stall speed, summarized according to site identification and area.

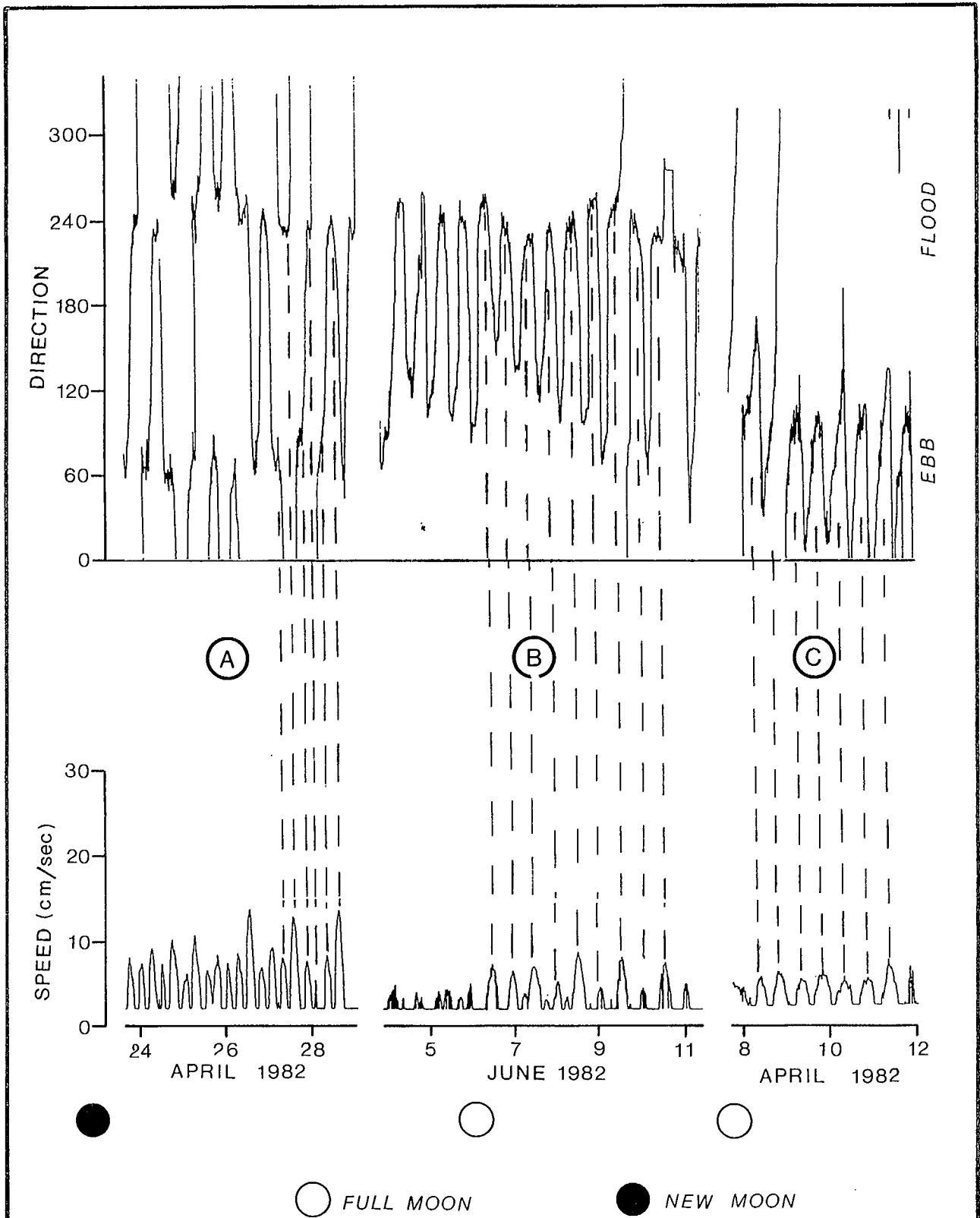


Figure 2.3-3: Three cases illustrating occurrences of subthreshold currents in M'Clure Strait. A - Rotor stalled for 1-2 hours at both high and low tide; B - Rotor stalled during slack high tide and following ebb; C - Rotor stalled during slack low tide and subsequent flood.

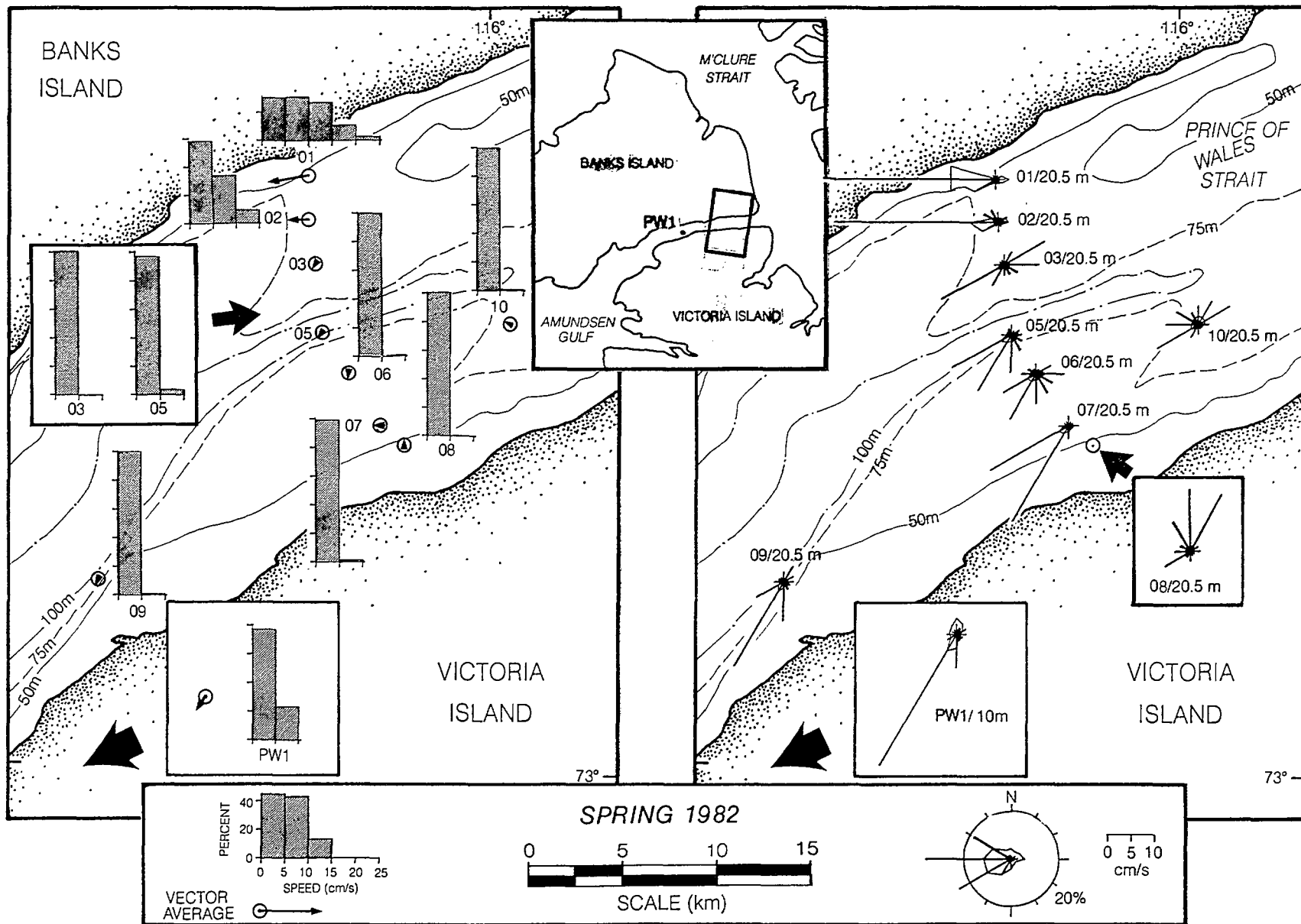


Figure 3.1-1: Speed and directional distribution, and vector average of near-surface (20 m) residual currents in Prince of Wales Strait, spring 1982. The radial sticks (right-hand side) represent the percentage of values whose directions fall within the given 30° class, while the mean residual speed for each directional class is indicated by the point of intersection of the encircling line and the radial stick. Distribution and vector average of residual speed are provided on the left-hand side. Vector averages less than 2 cm/s have tail-less arrows. Each site is identified by site number/instrument depth.

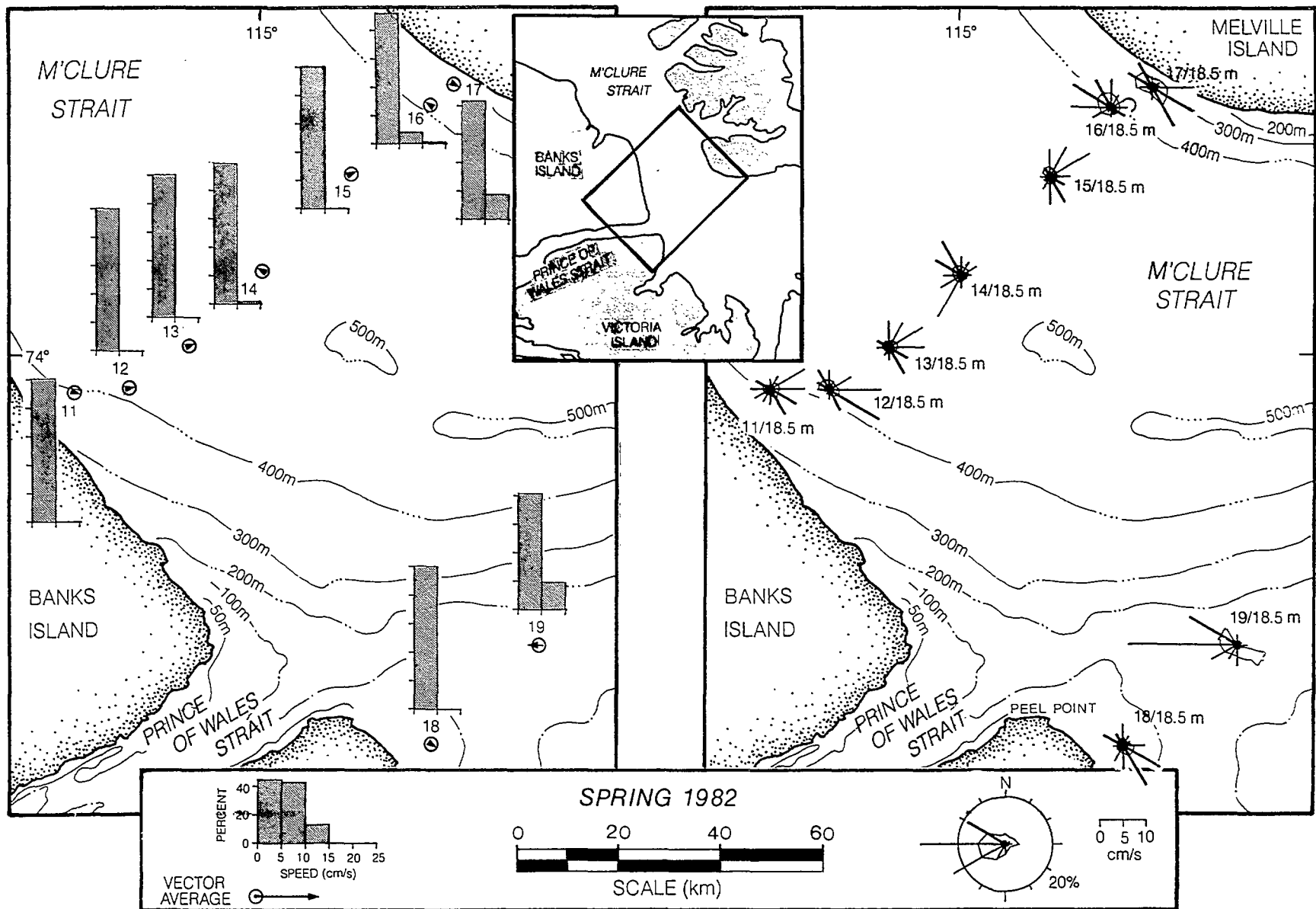


Figure 3.1-2: Speed and directional distribution, and vector average of near-surface (20 m) residual currents in M'Clure Strait, spring 1982. Presentation as for Figure 3.1-1.

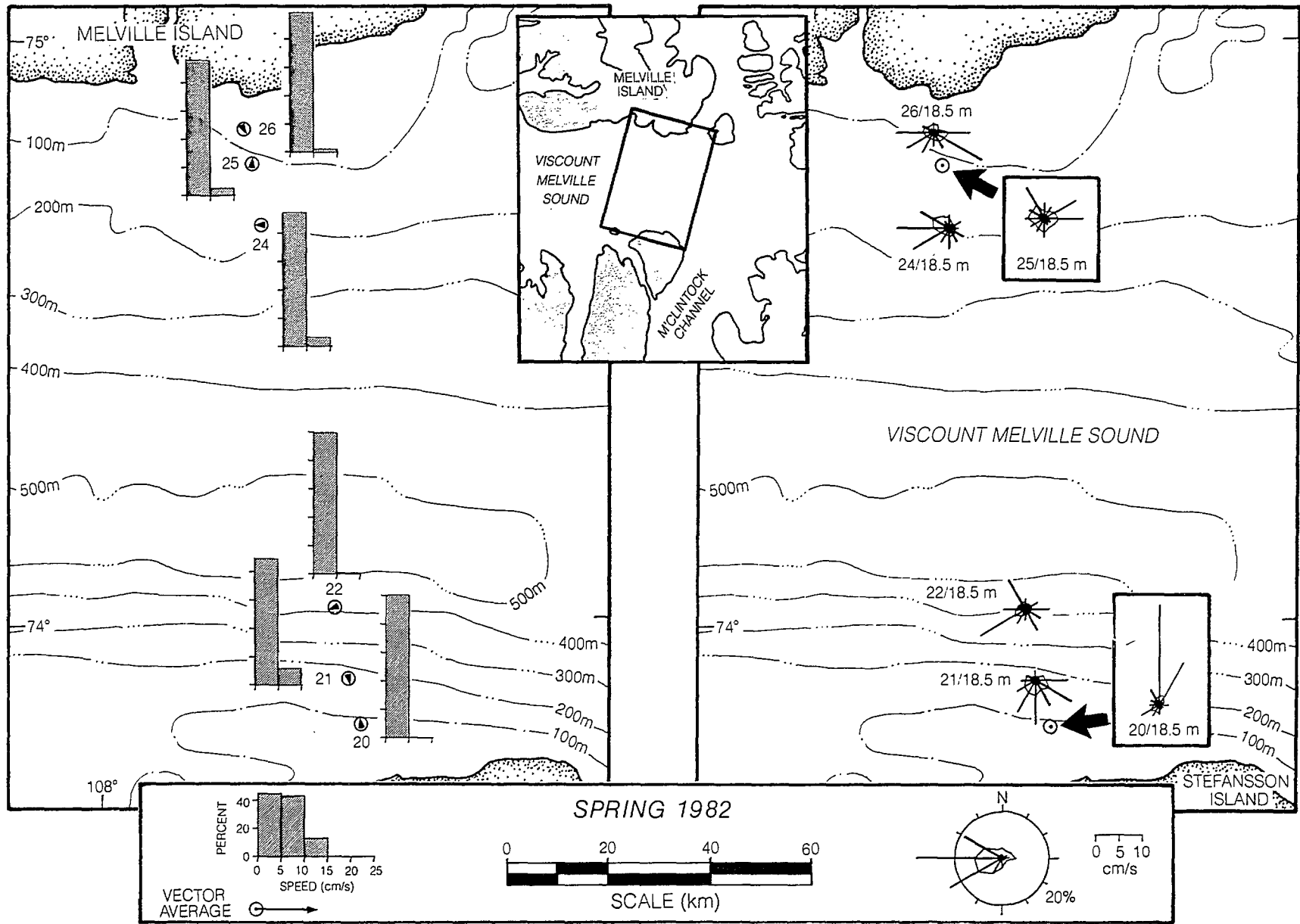


Figure 3.1-3: Speed and directional distribution, and vector average of near-surface (20 m) residual currents in central Viscount Melville Sound, spring 1982. Presentation as for Figure 3.1-1.

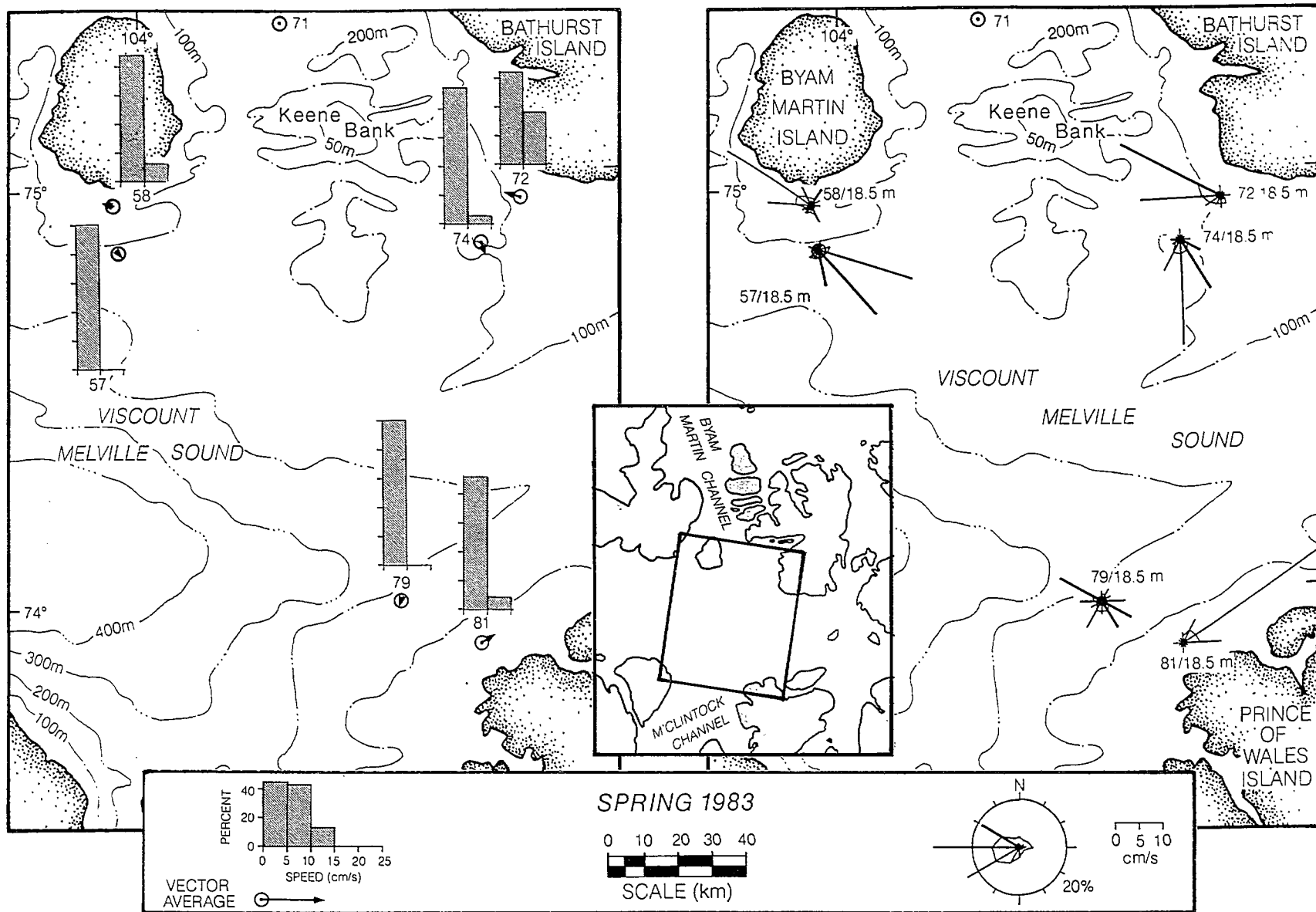


Figure 3.1-4: Speed and directional distribution, and vector average of near-surface (20 m) residual currents in eastern Viscount Melville Sound, spring 1983. Presentation as for Figure 3.1-1.

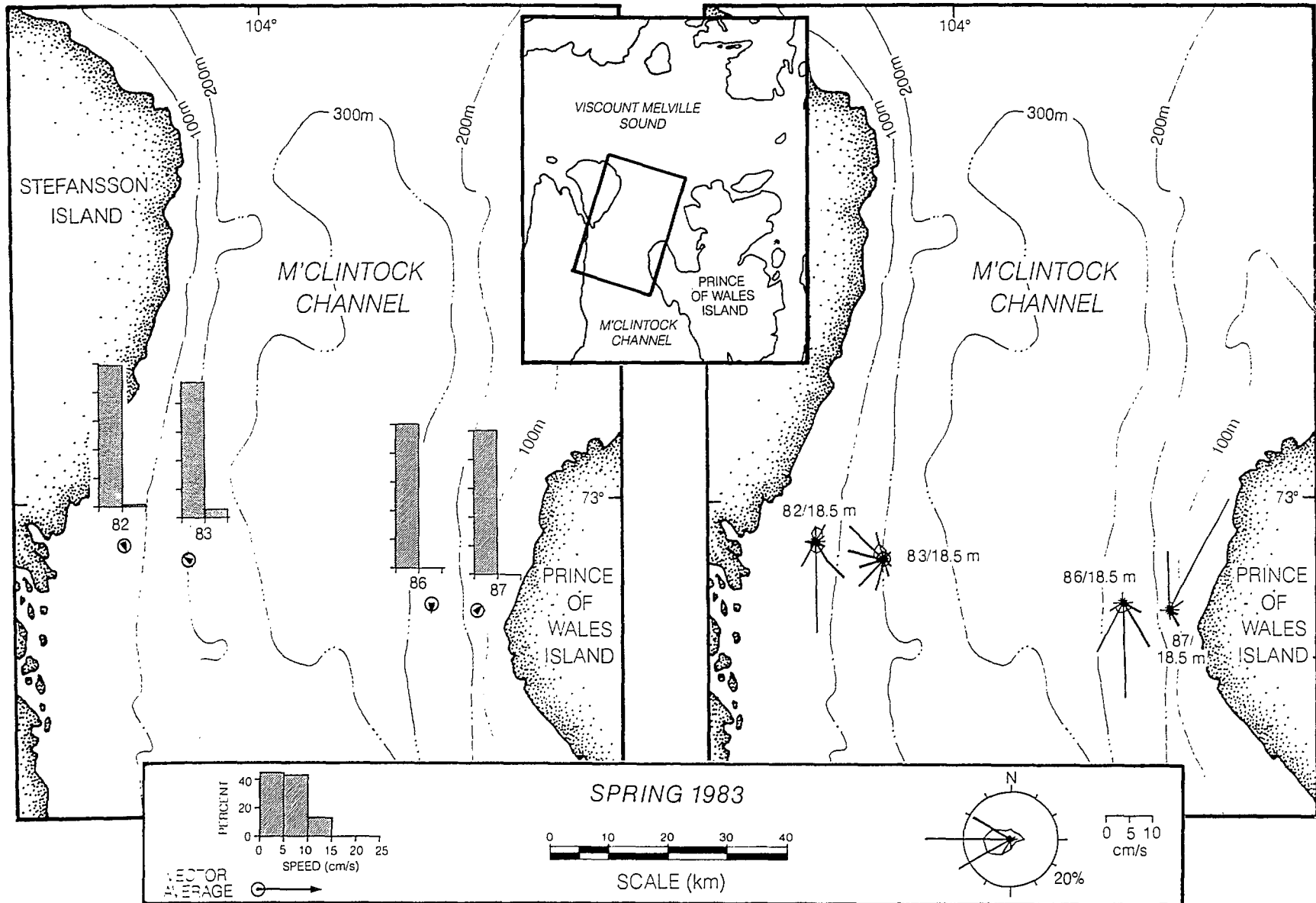


Figure 3.1-5: Speed and directional distribution, and vector average of near-surface (20 m) residual currents in M'Clintock Channel, spring 1983. Presentation as for Figure 3.1-1.

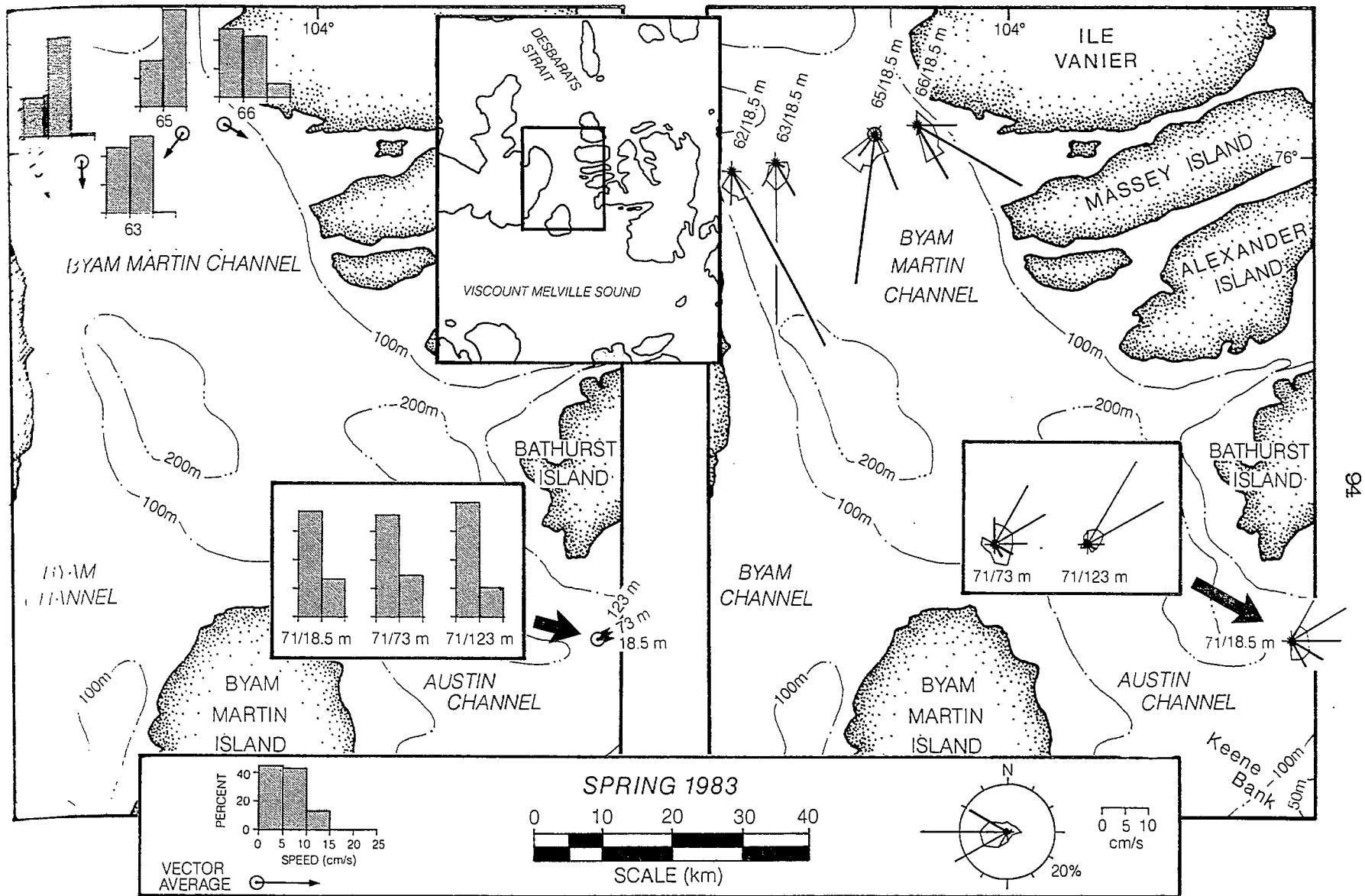


Figure 3.1-6: Speed and directional distribution, and vector average of near-surface (20 m) residual currents in Byam Martin Channel and Austin Channel, spring 1983. Presentation as for Figure 3.1-1.

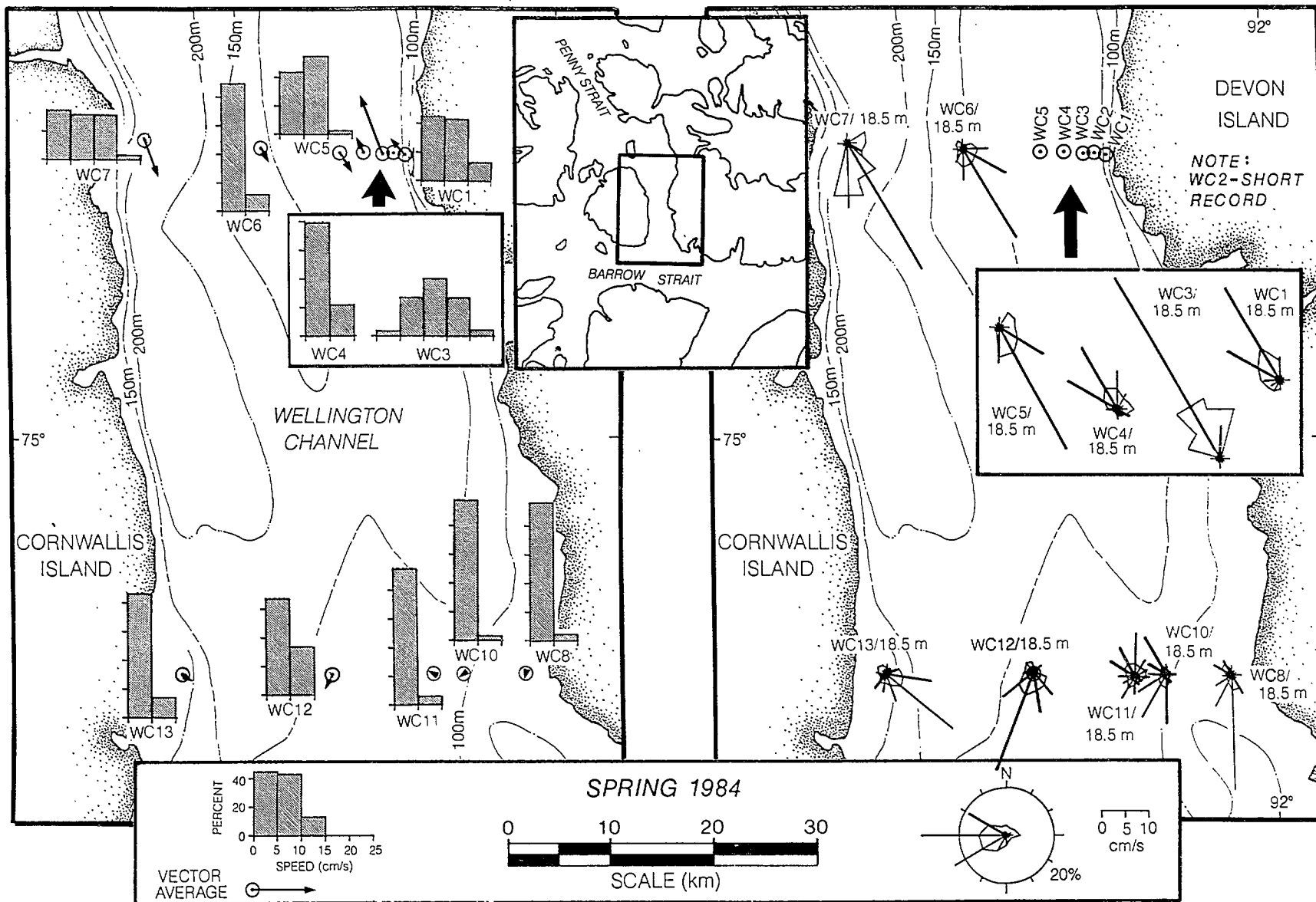


Figure 3.1-8: Speed and directional distribution, and vector average of near-surface (20 m) residual currents in Wellington Channel, spring 1984. Presentation as for Figure 3.1-1.

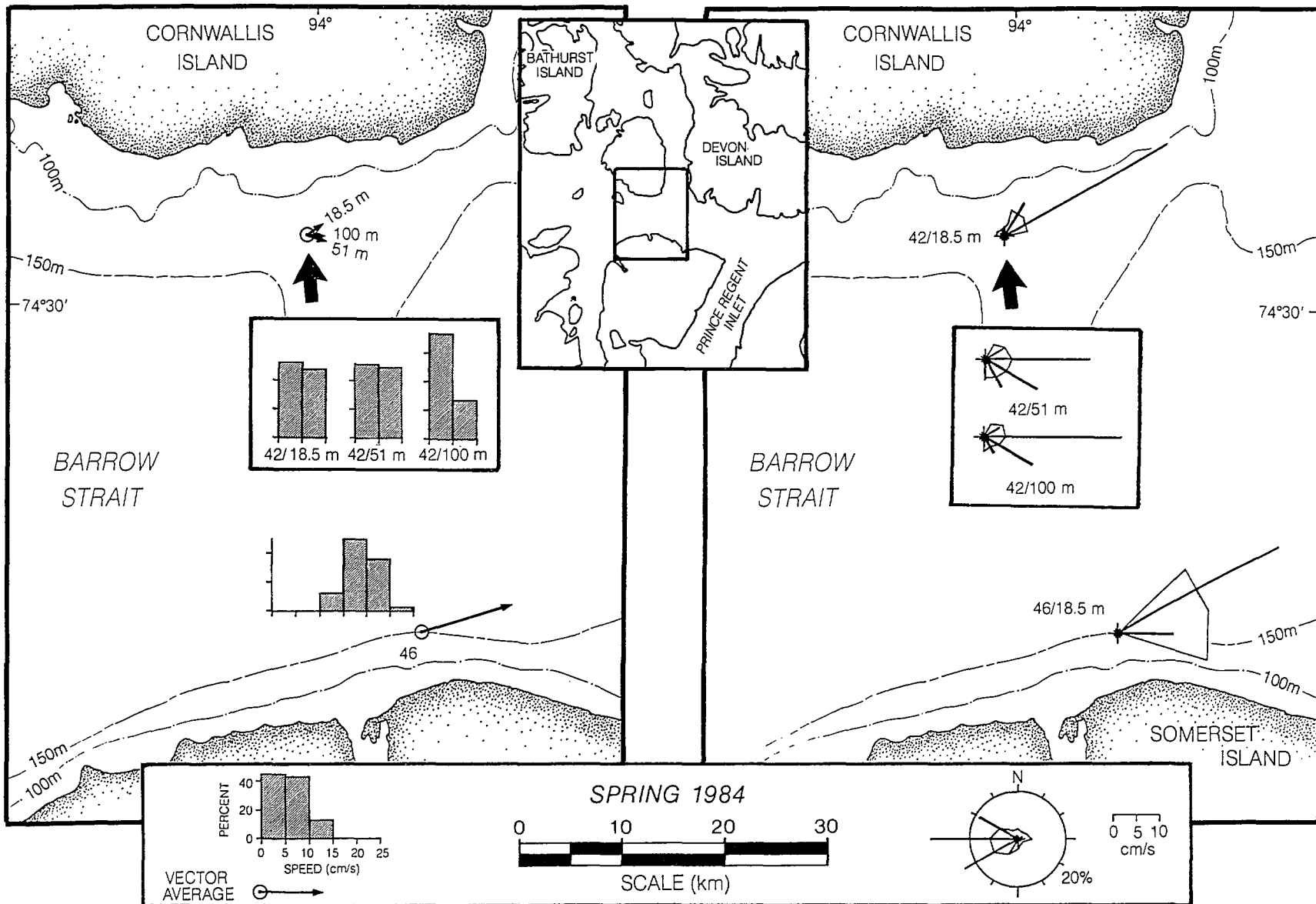


Figure 3.1-9: Speed and directional distribution, and vector average of residual currents in Barrow Strait, spring 1984. Presentation as for Figure 3.1-1.

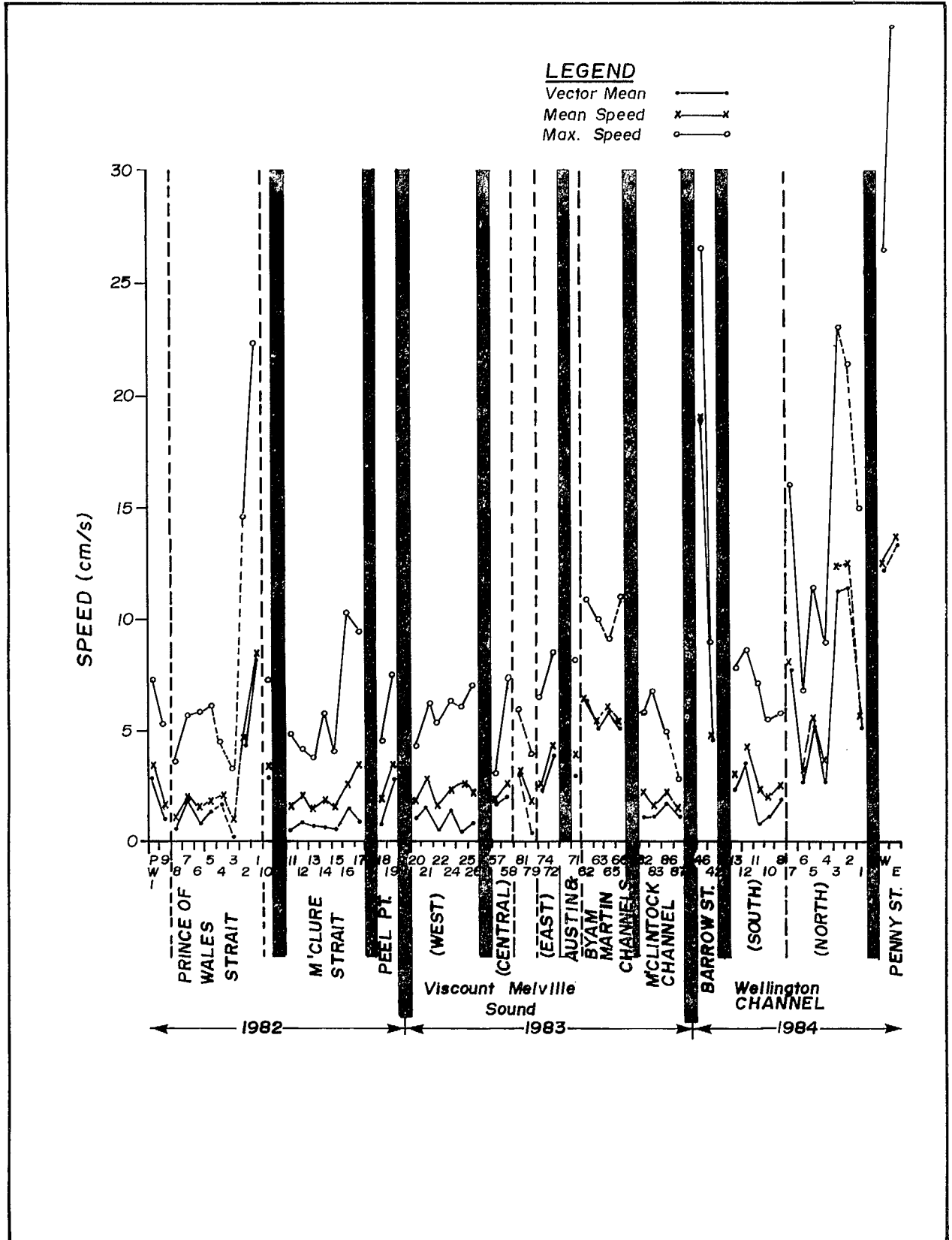


Figure 3.1-10: Computed residual current velocity parameters including vector mean, mean speed and maximum speed (cm/s) for all springtime data sets, 1982-1984.

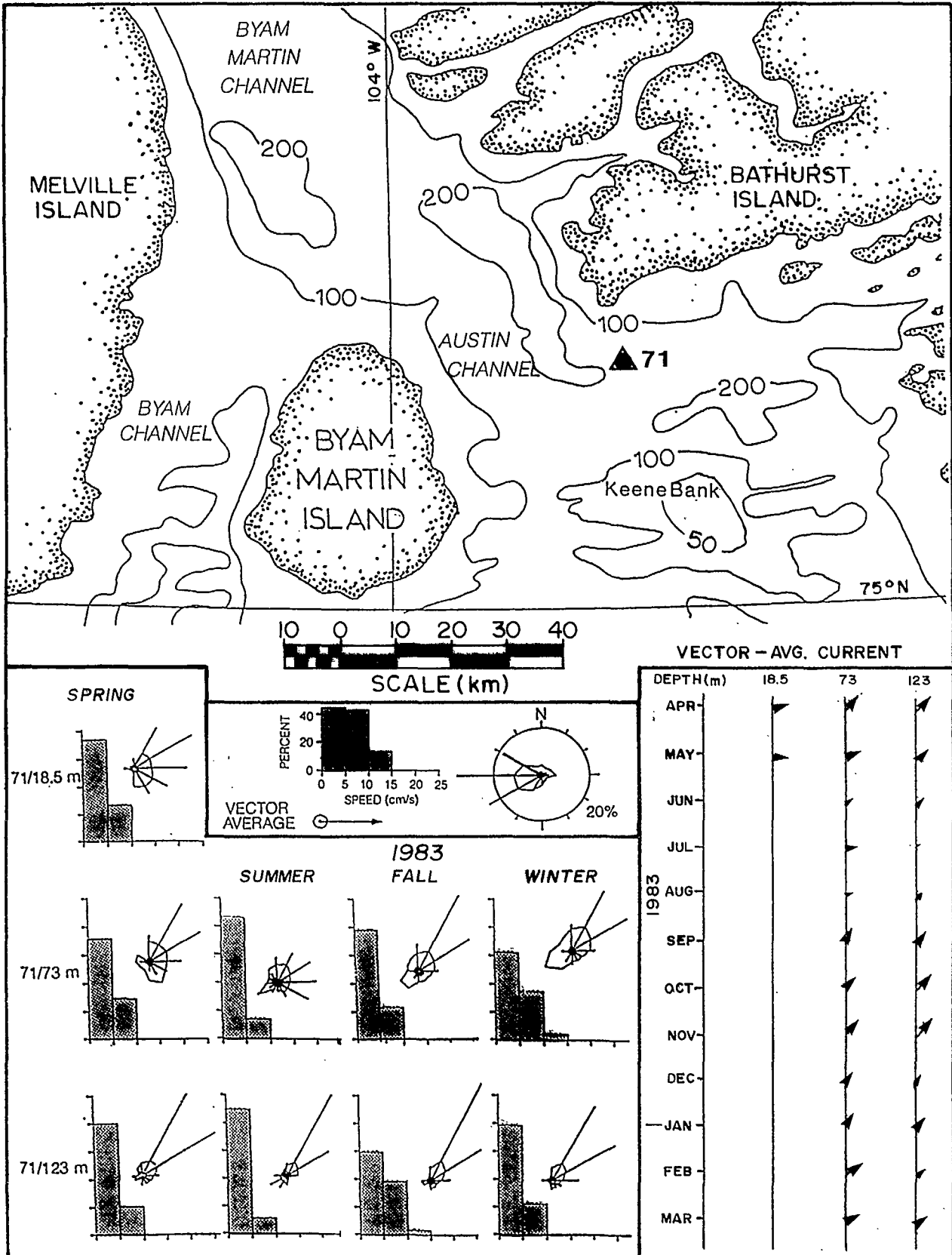


Figure 3.1-11: Seasonal variability in the residual currents at site 71 in Austin Channel. The speed-histogram and direction-distribution format is the same as was used for the springtime data. The plot of vector averaged velocities is based on monthly values. If there were not at least 15 days of data then no value was plotted for that month.

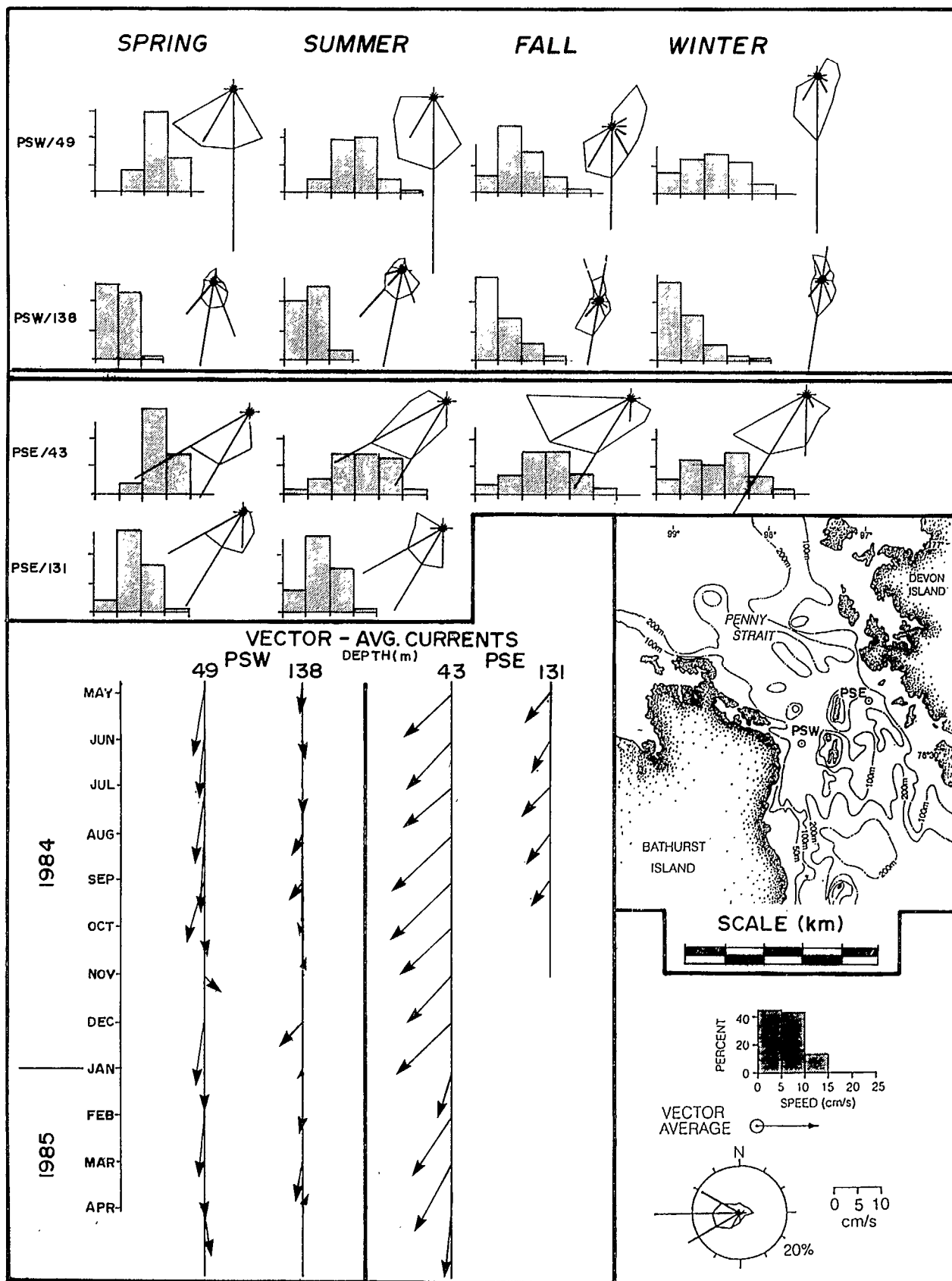


Figure 3.1-12: Seasonal variability in the residual currents at sites PSE and PSW in Penny Strait. The speed-histogram and direction-distribution format is the same as was used for the springtime data. The plot of vector averaged velocities is based on monthly values. If there were not at least 15 days of data then no value is plotted for that month.

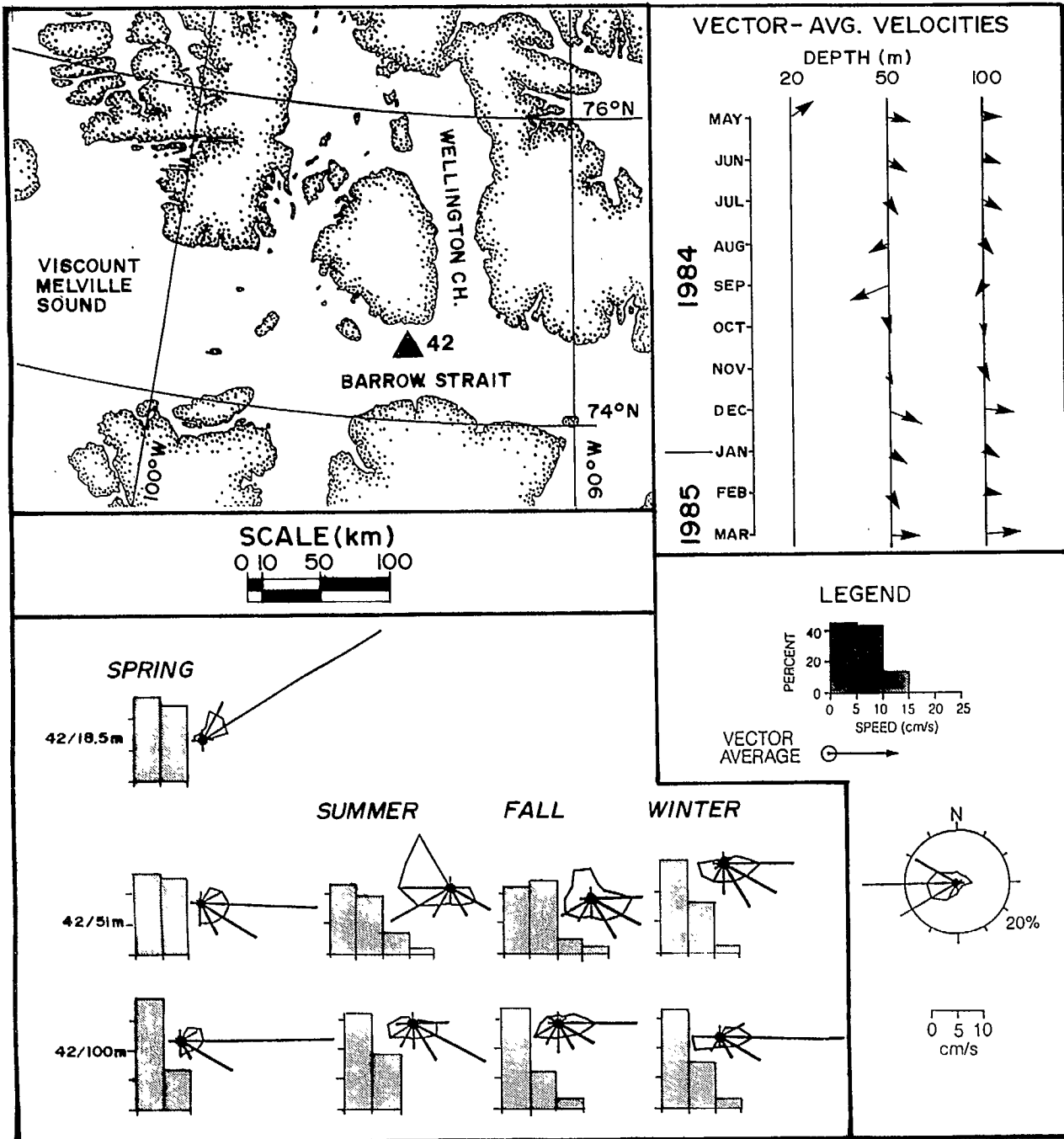


Figure 3.1-13: Seasonal variability in the residual currents at site 42 in Barrow Strait. The speed-histogram and direction-distribution format is the same as was used for the springtime data. The plot of vector averaged velocities is based on monthly values. If there were not at least 15 days of data then no value is plotted for that month.

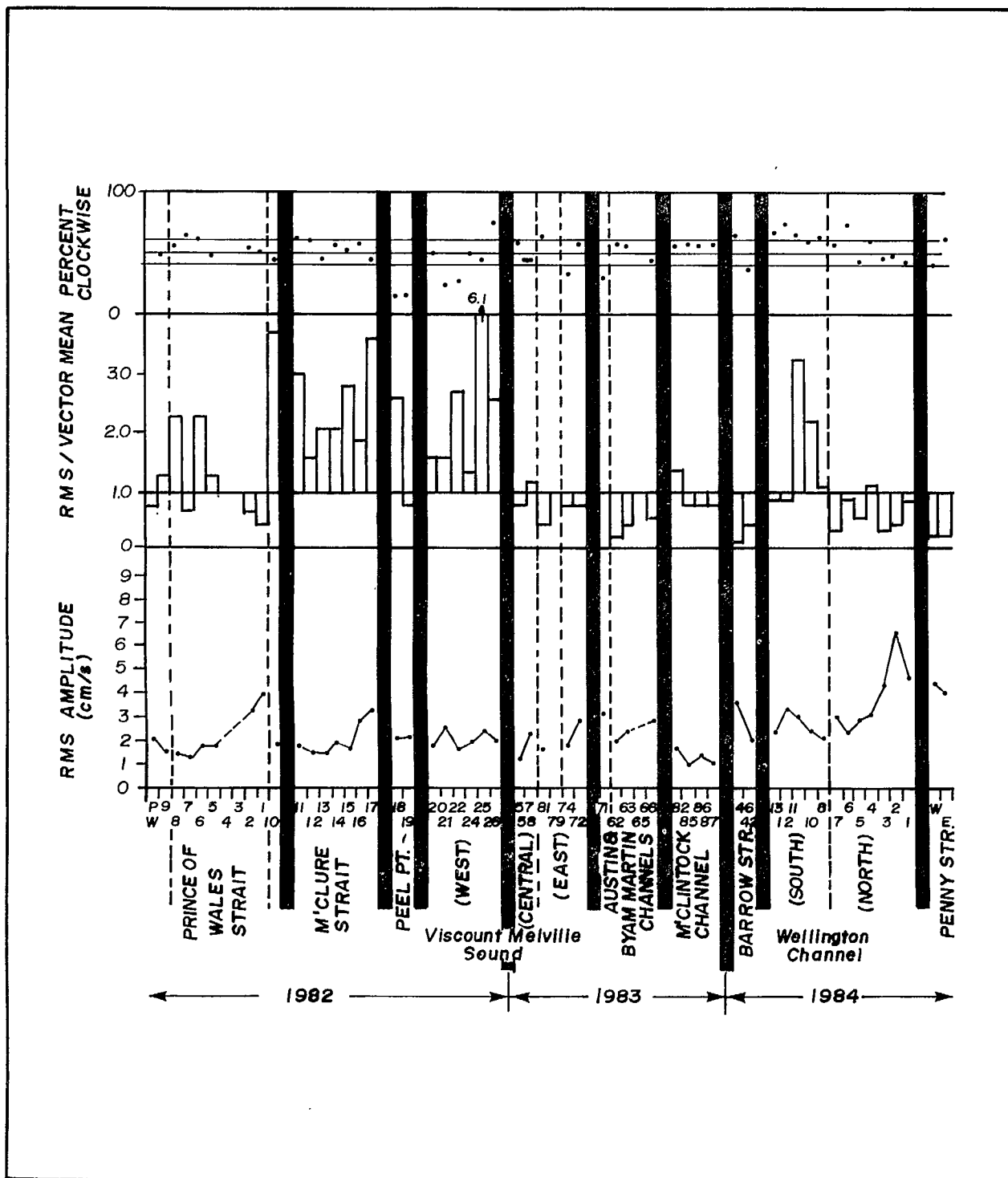


Figure 3.2-1: Residual flow parameters derived from auto-spectral analyses for all springtime data sets:
 - root-mean-square (RMS) amplitude of fluctuations (cm/s)
 - ratio of RMS to vector average
 - percent of total auto-spectral density having clockwise rotation.

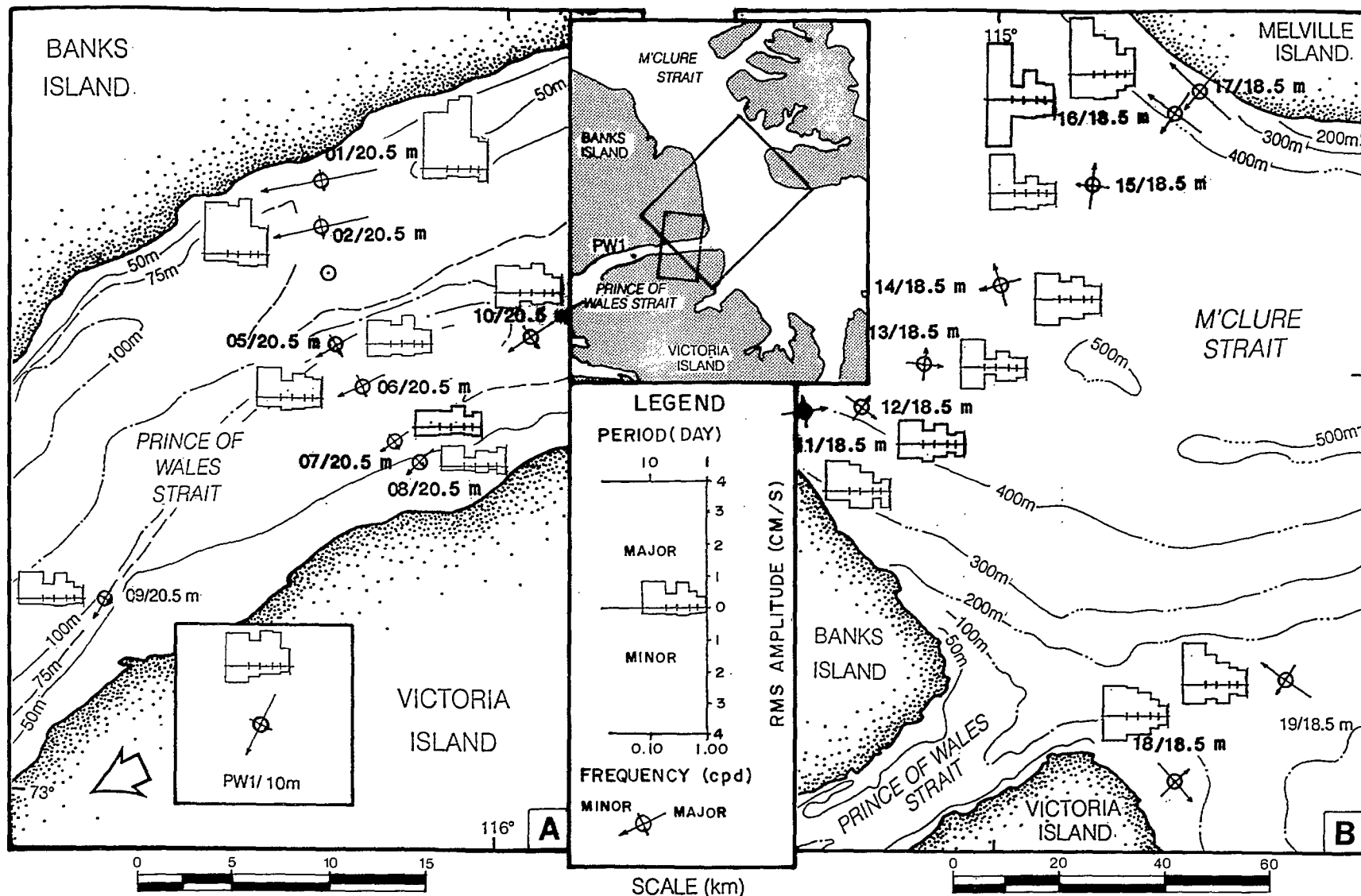


Figure 3.2-2: Auto-spectral densities for major and minor components of the residual currents measured in 1982 at sites in (a) Prince of Wales Strait and (b) M'Clure Strait.

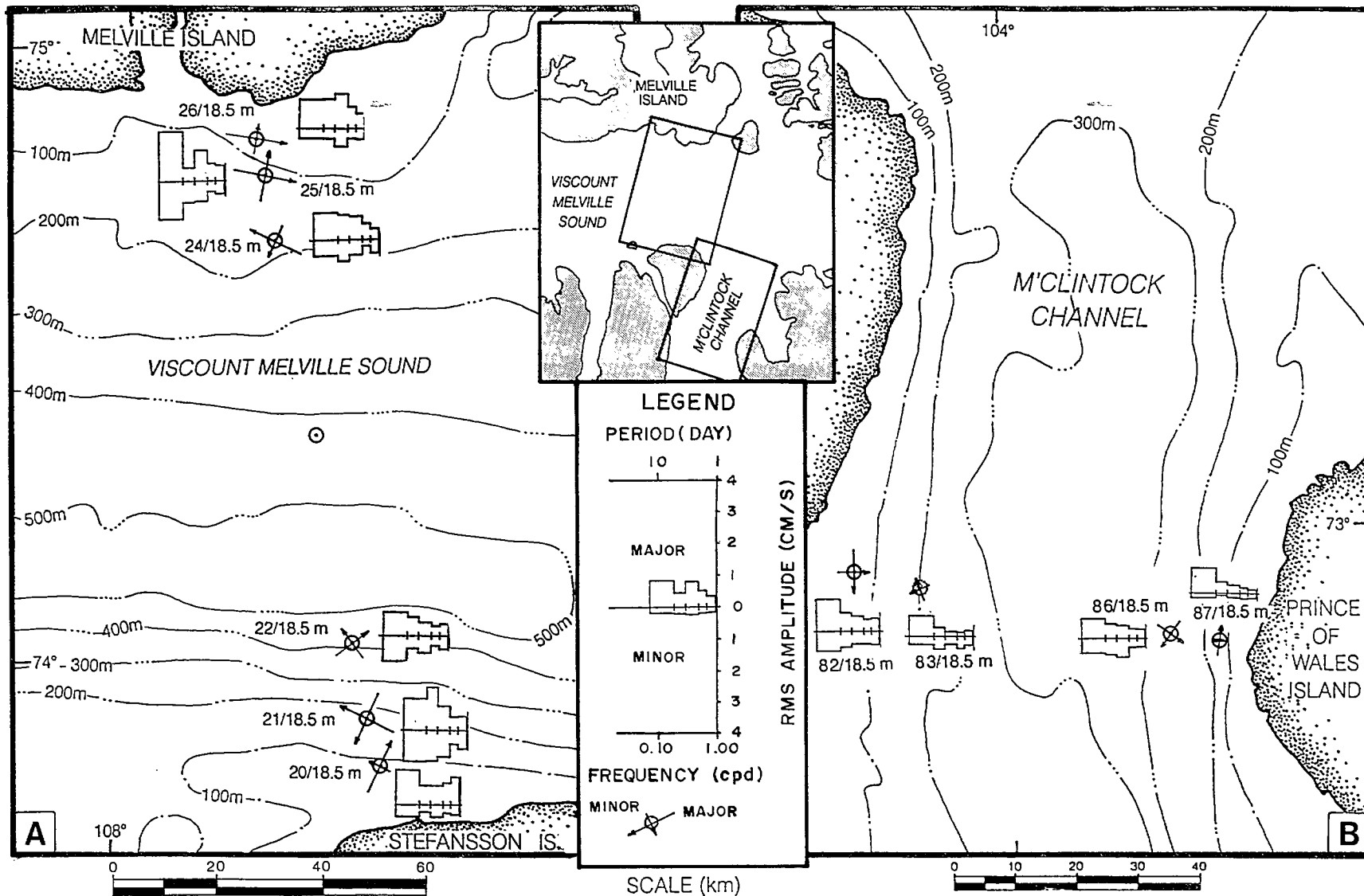


Figure 3.2-3: Auto-spectral densities for major and minor components of the residual currents measured in 1982 at sites in (a) Central Viscount Melville Sound and (b) M'Clintock Channel.

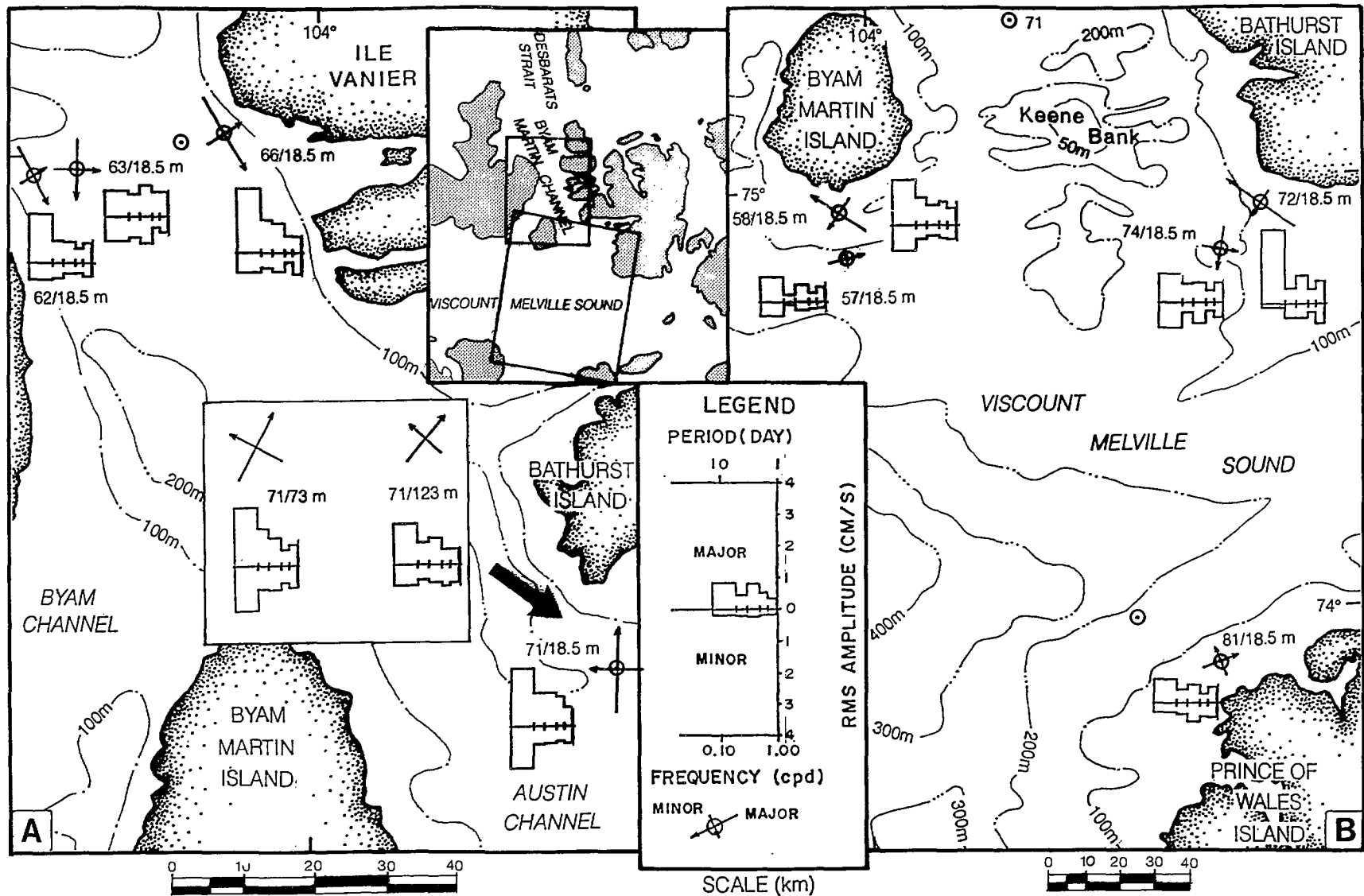


Figure 3.2-4: Auto-spectral densities for major and minor components of the residual currents measured in 1983 at sites in (a) Byam Martin and Austin Channels and (b) Eastern Viscount Melville Sound.

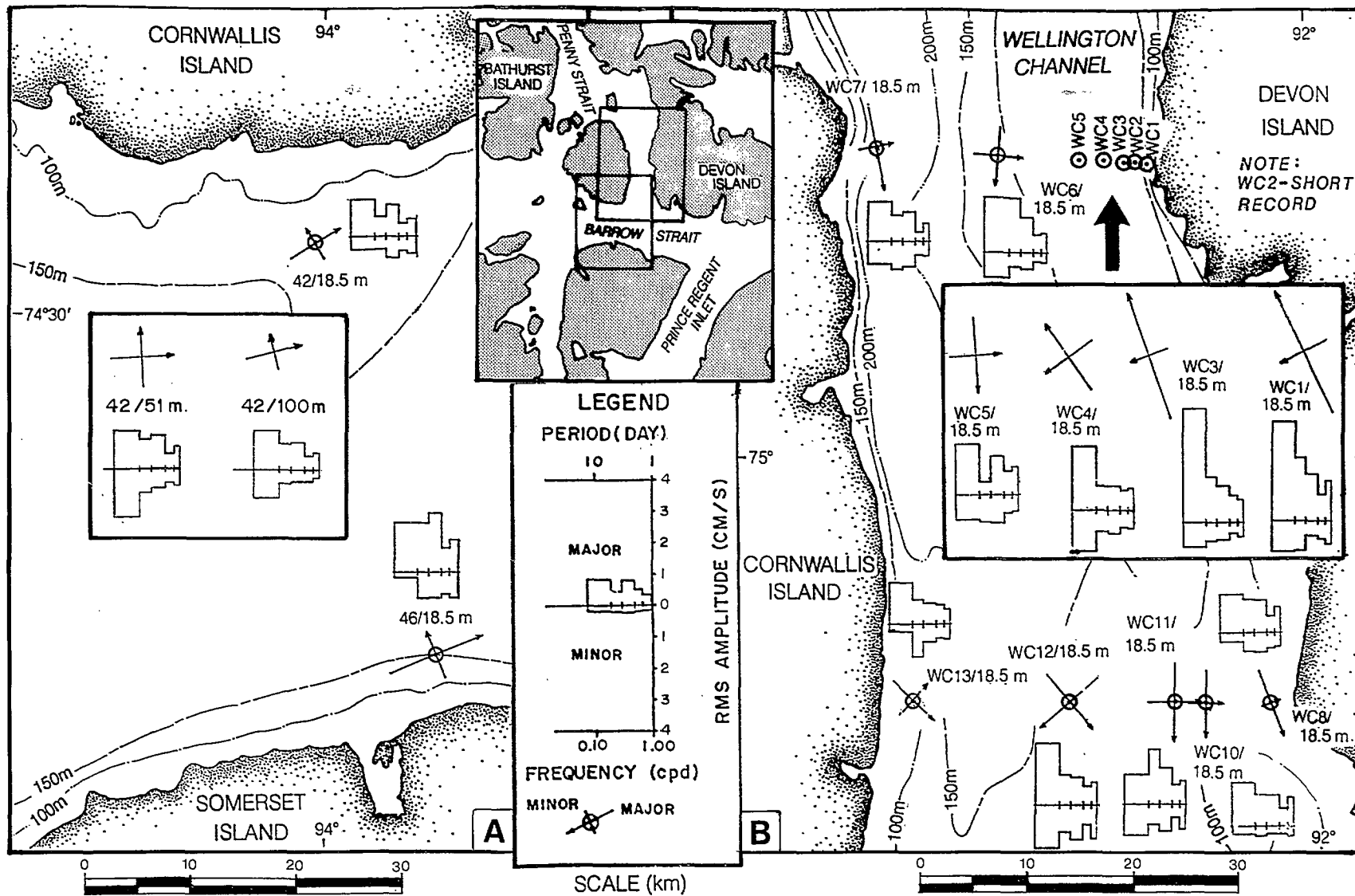


Figure 3.2-5: Auto-spectral densities for major and minor components of the residual currents measured in 1984 at sites in; (a) Barrow Strait; (b) Wellington Channel.

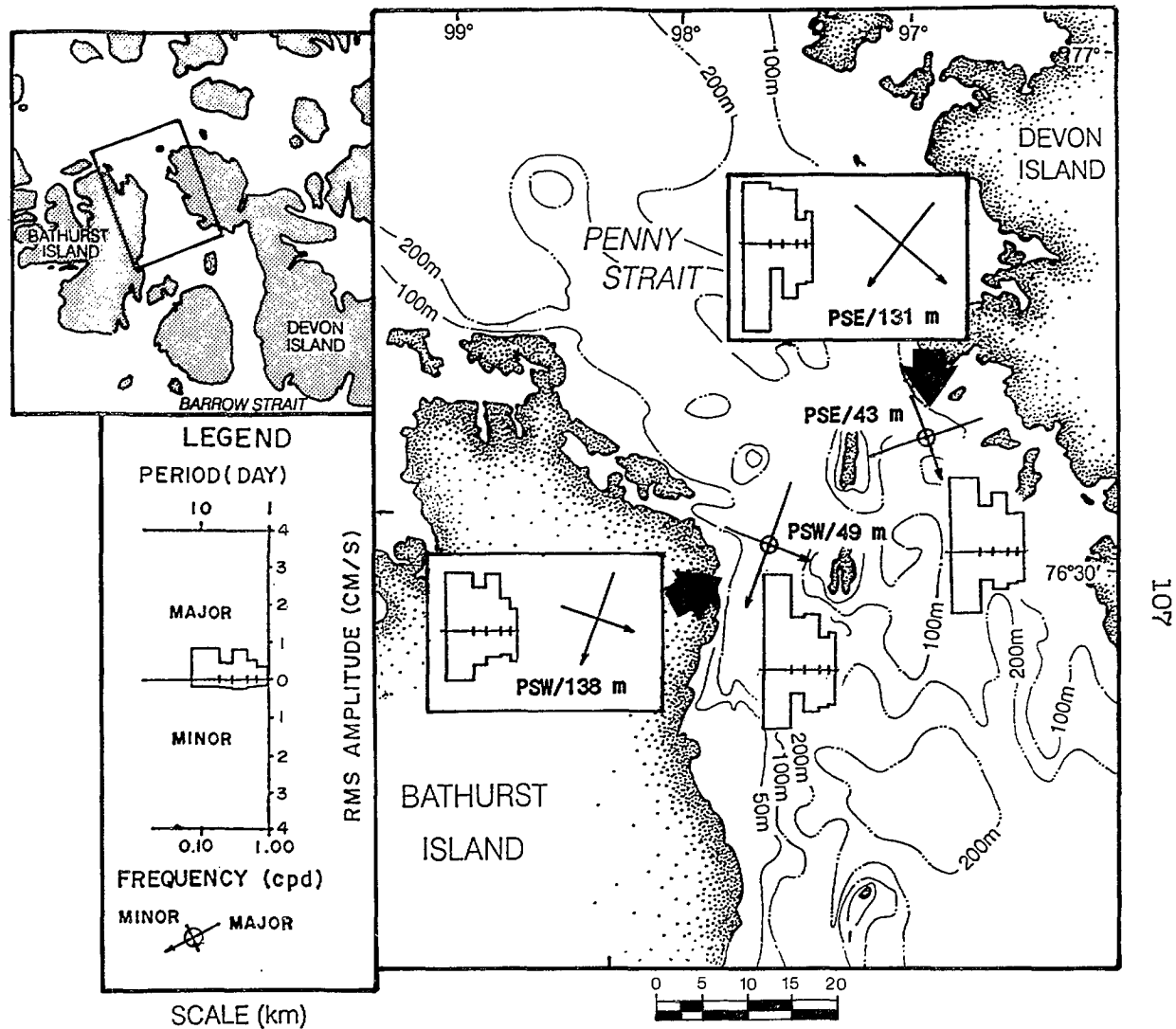


Figure 3.2-6: Auto-spectral densities for major and minor components of the residual currents measured in 1984 at sites in Penny Strait.

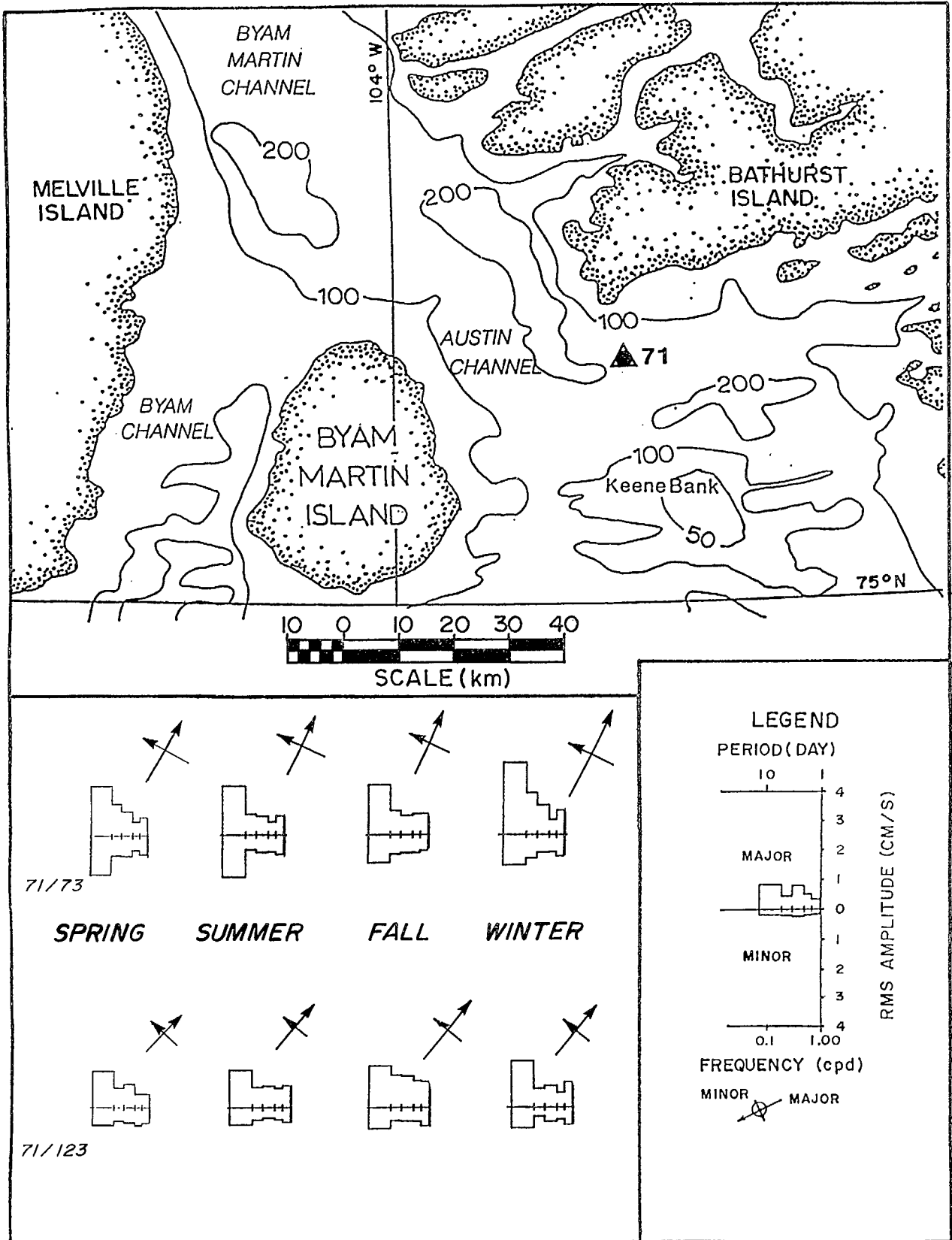


Figure 3.2-7: Seasonal auto-spectra computed for year-long data in Austin Channel.

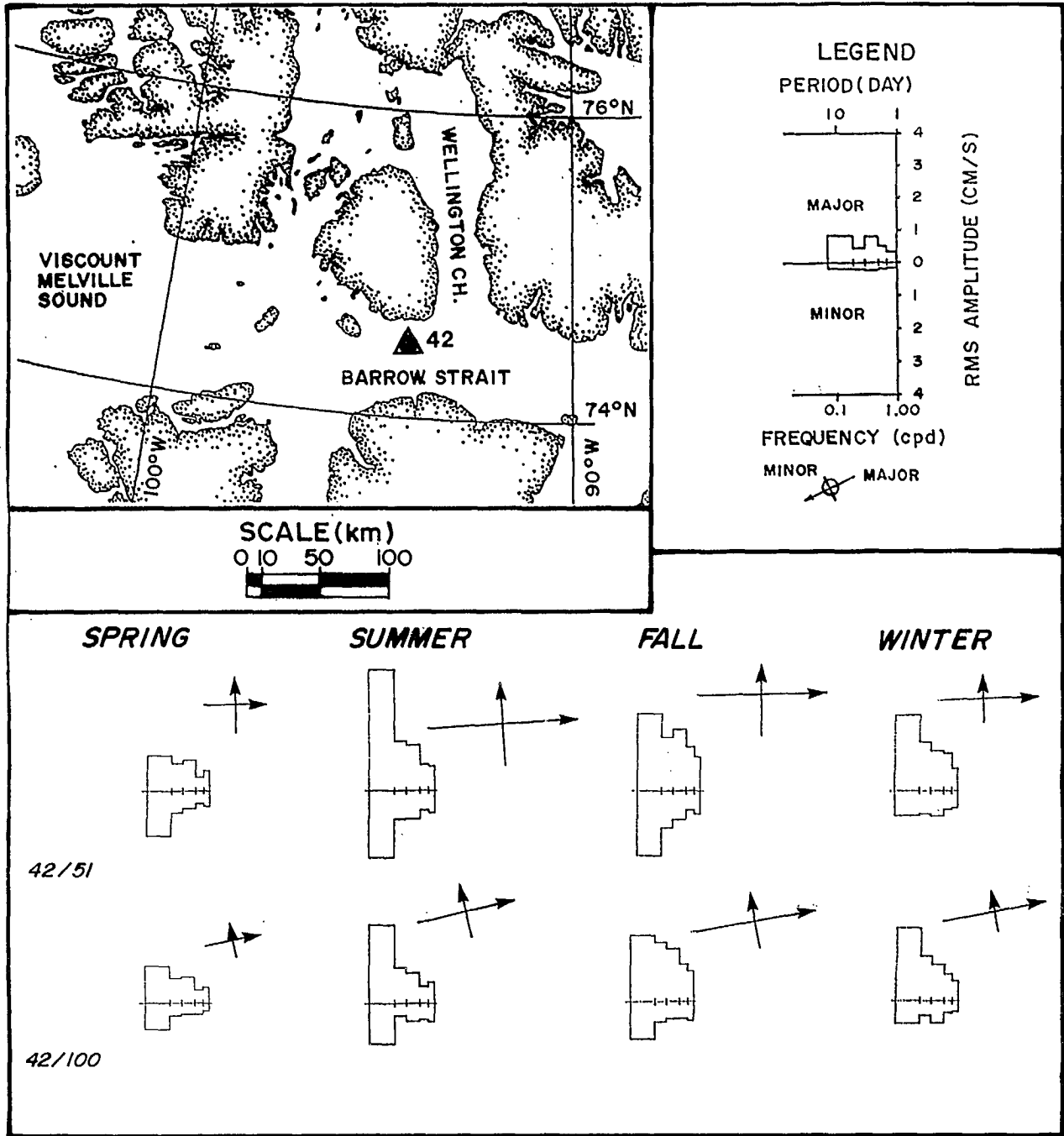


Figure 3.2-8: Seasonal auto-spectra computed for year-long data in Barrow Strait.

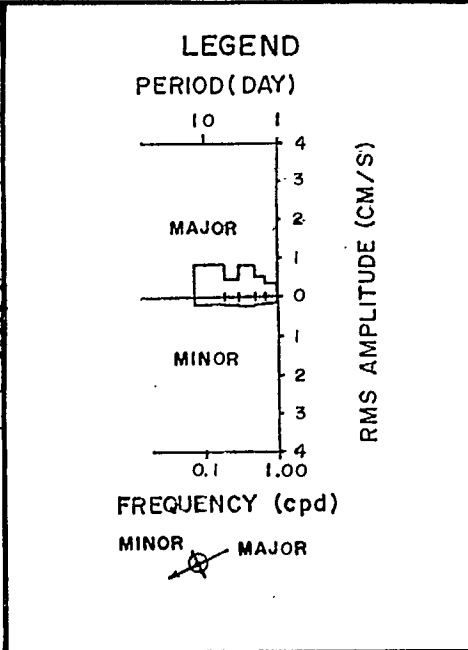
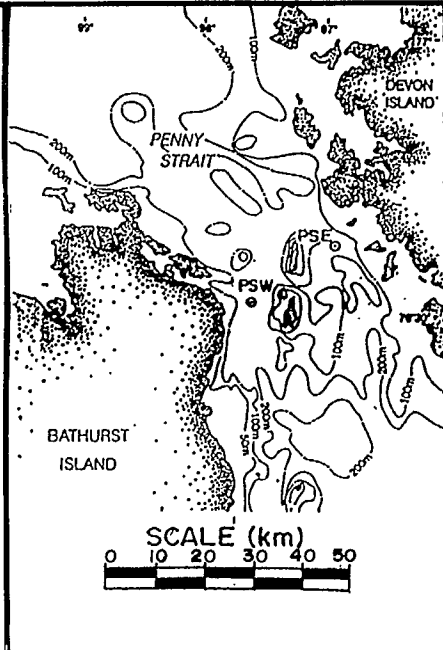
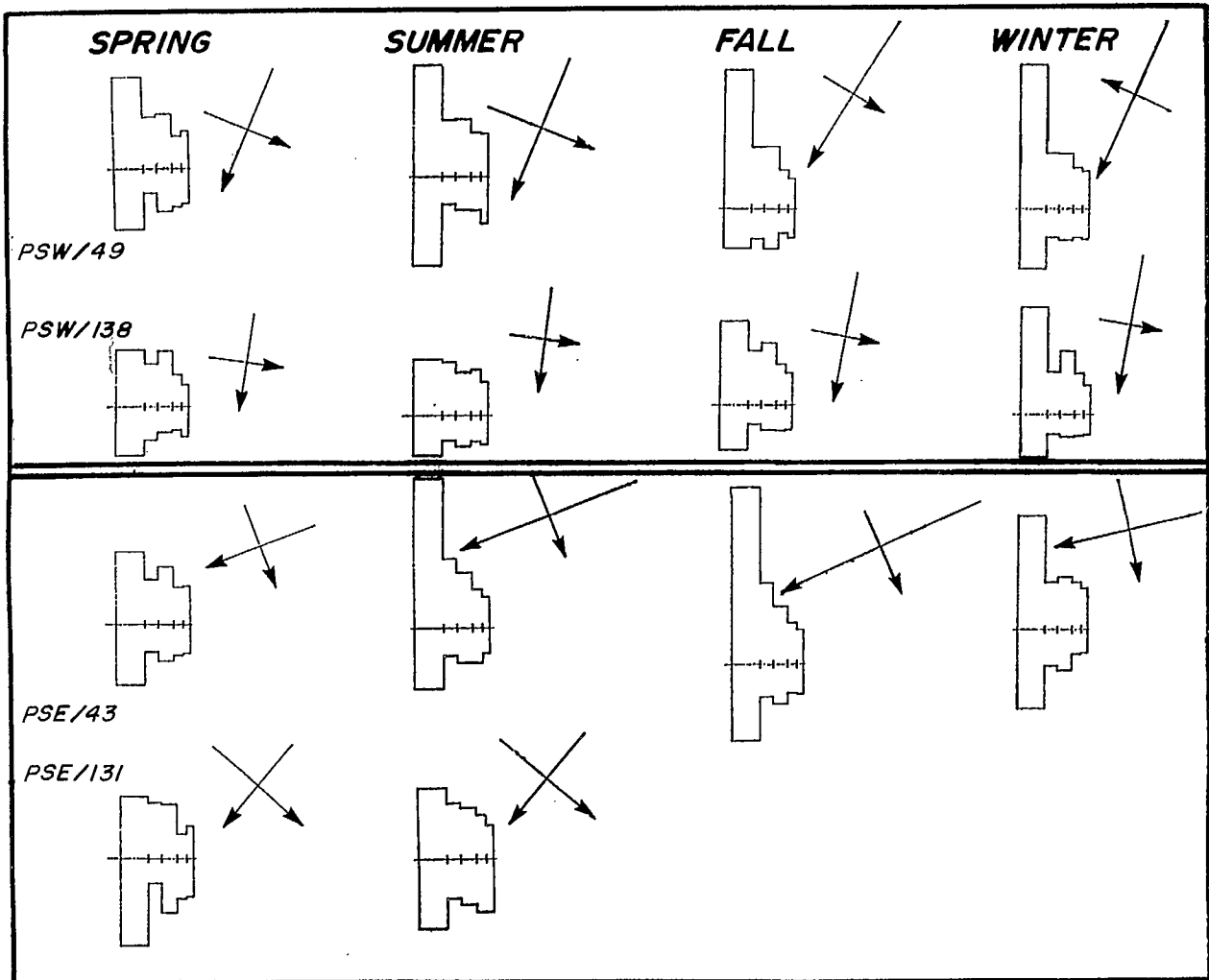


Figure 3.2-9: Seasonal auto-spectra computed for year-long data in Penny Strait.

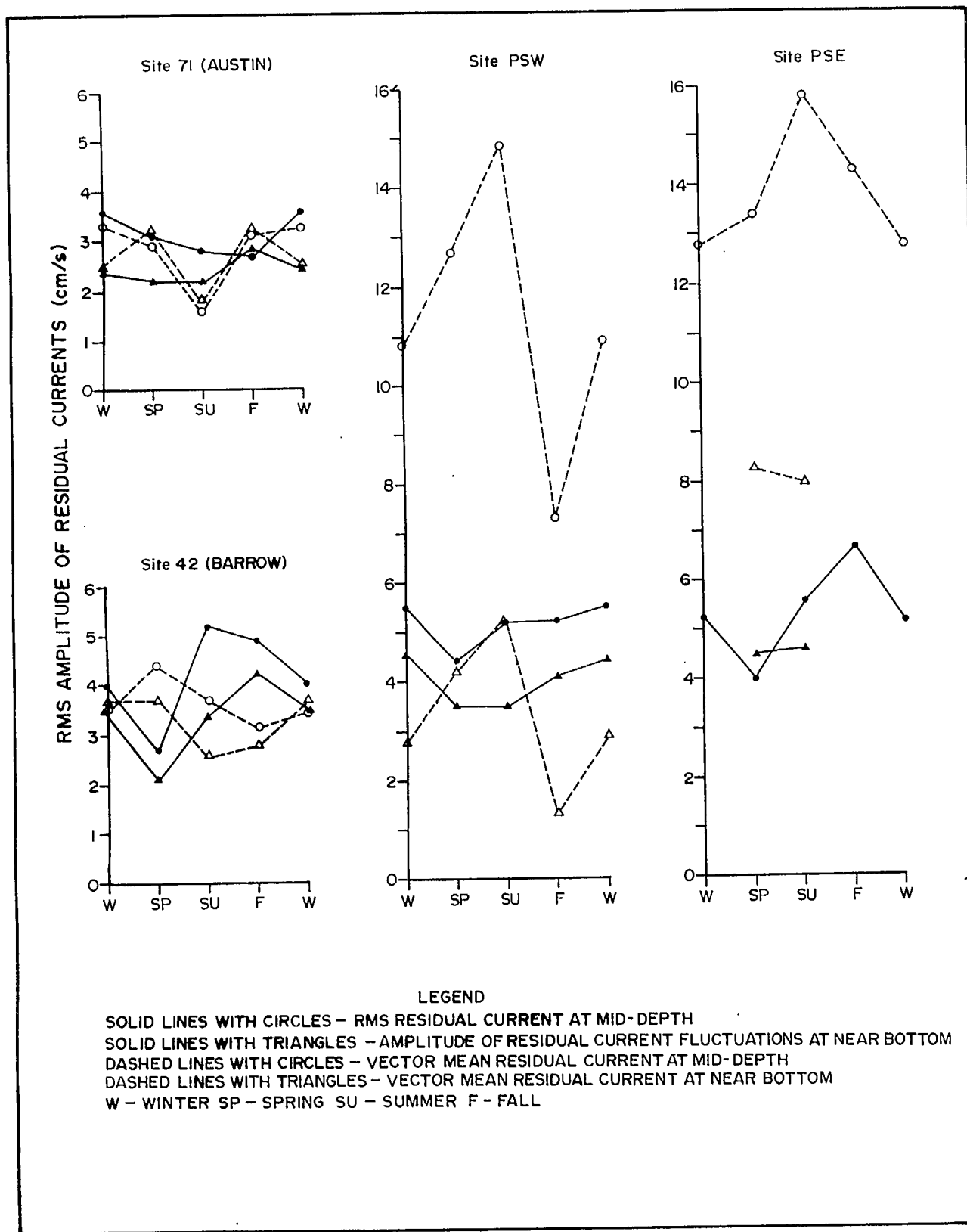


Figure 3.2-10: The seasonal root-mean-square (RMS) amplitudes of residual current fluctuations, along with vector average magnitude.

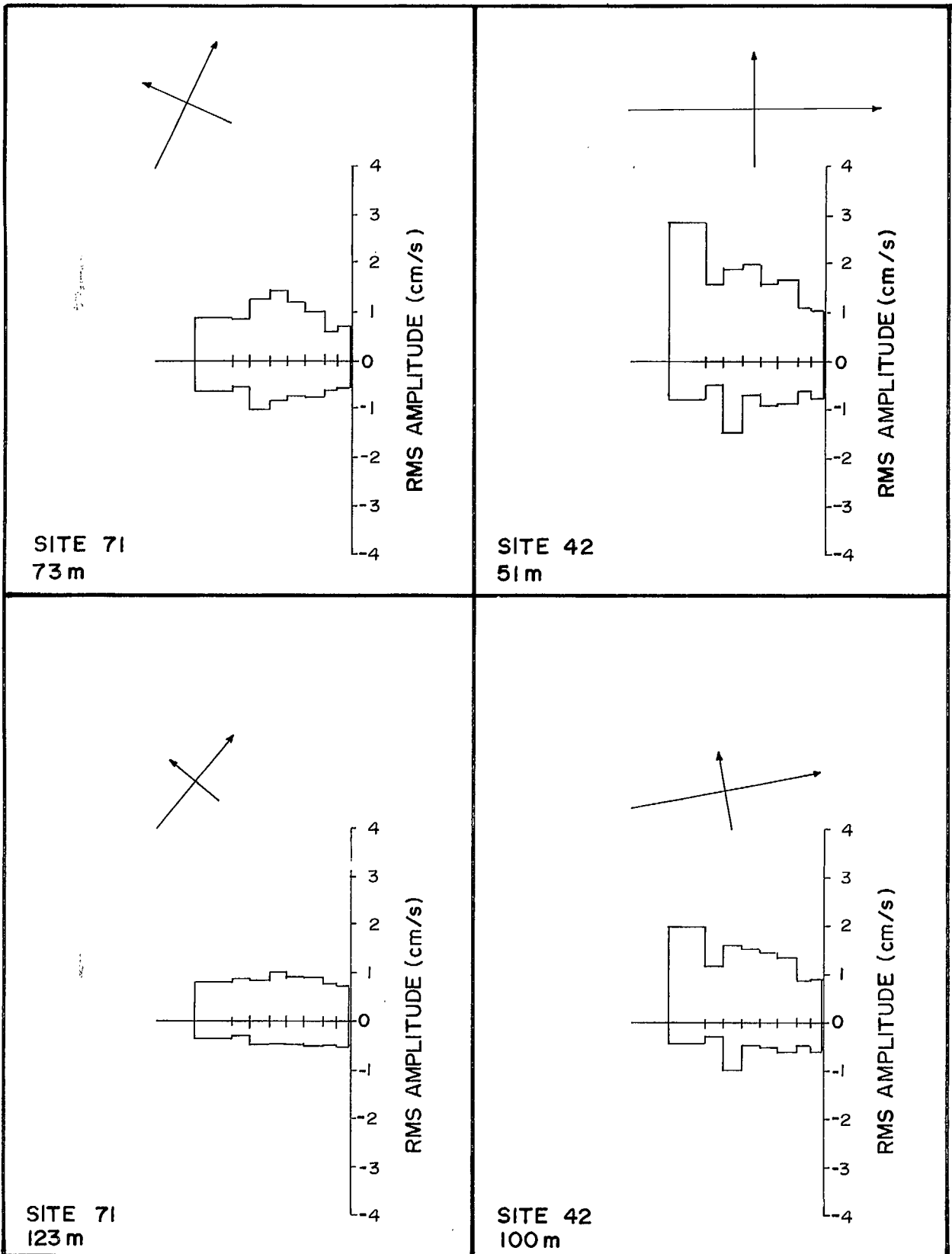


Figure 3.2-11: Auto-spectra computed from the full year-long current-meter data in; (a) Austin Channel (Site 71); (b) Barrow Strait (Site 42).

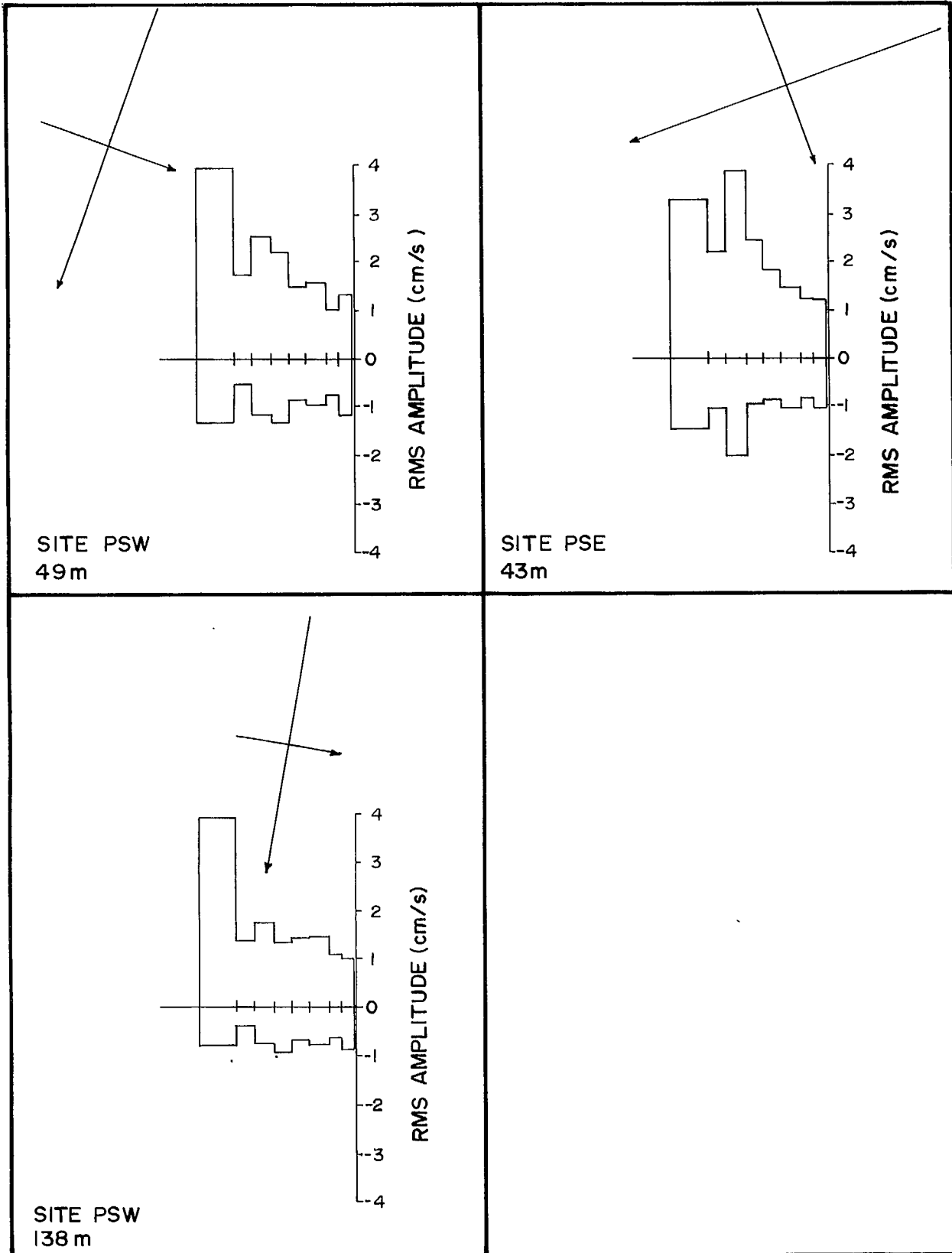


Figure 3.2-12: Auto-spectra computed from the full year-long current-meter data in Penny Strait (Sites PSW and PSE).

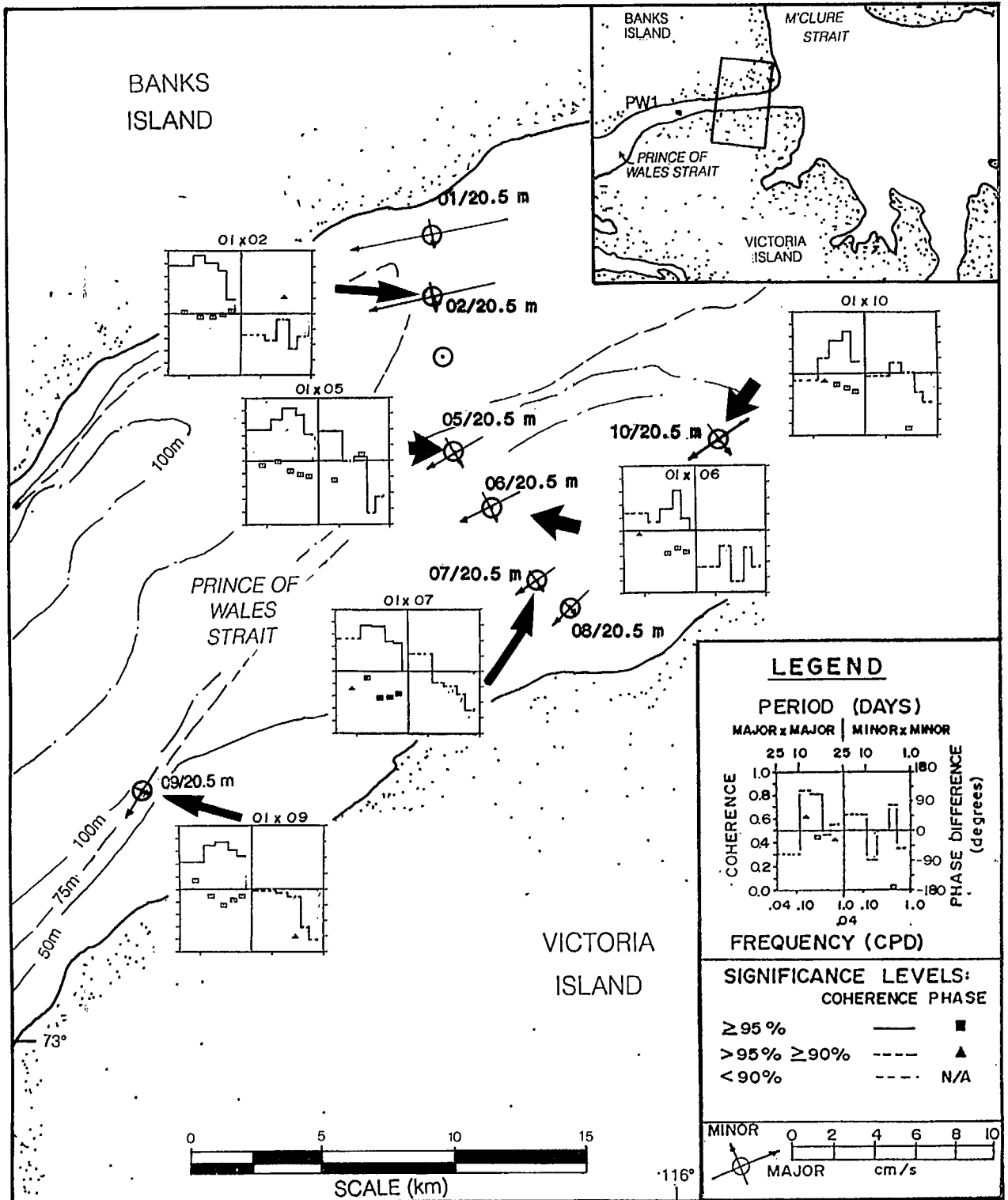


Figure 3.3-1: Cross-spectra computed for pairs of current-meter records in Prince of Wales Strait.

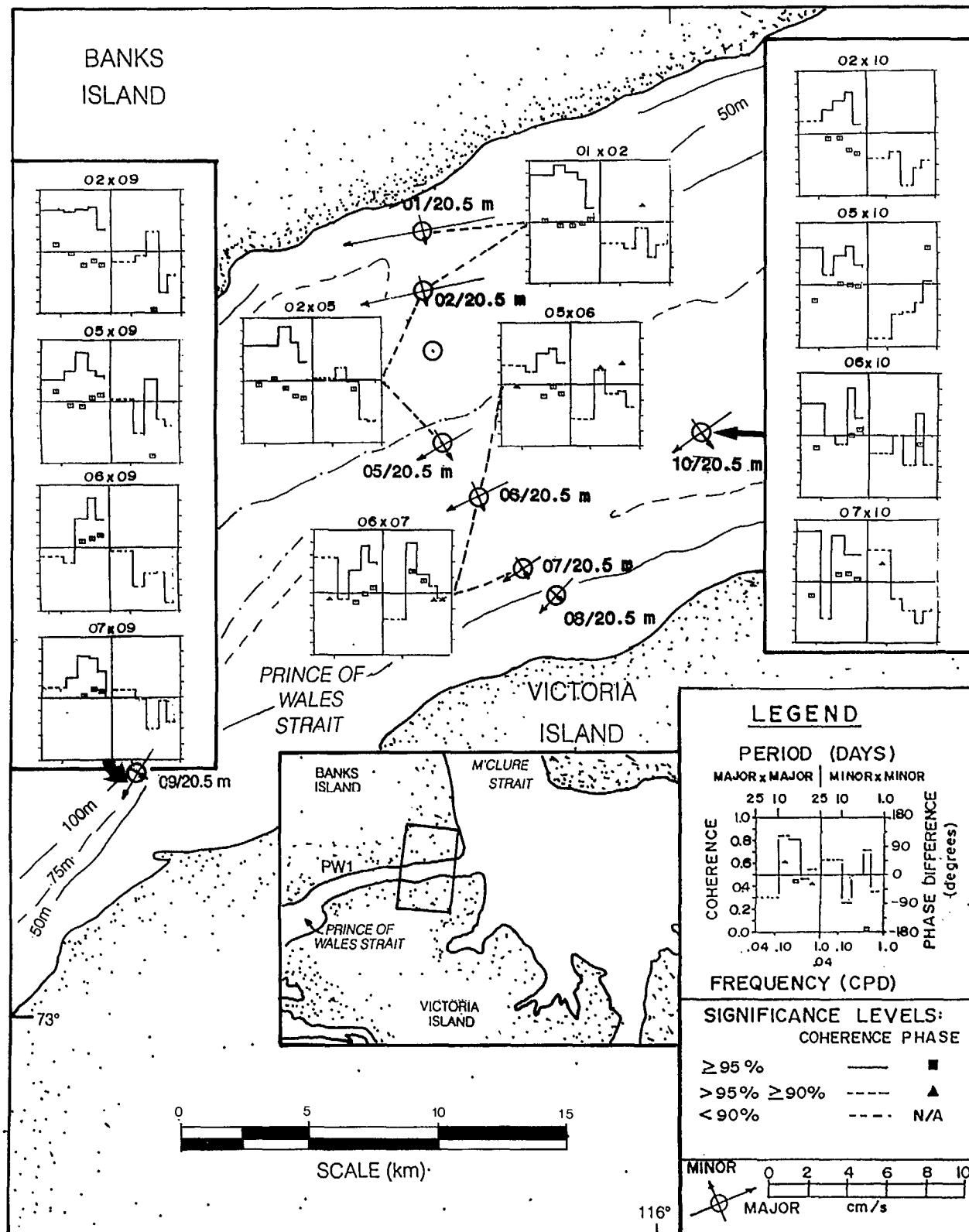


Figure 3.3-2: Cross-spectra computed for pairs of current-meter records in Prince of Wales Strait.

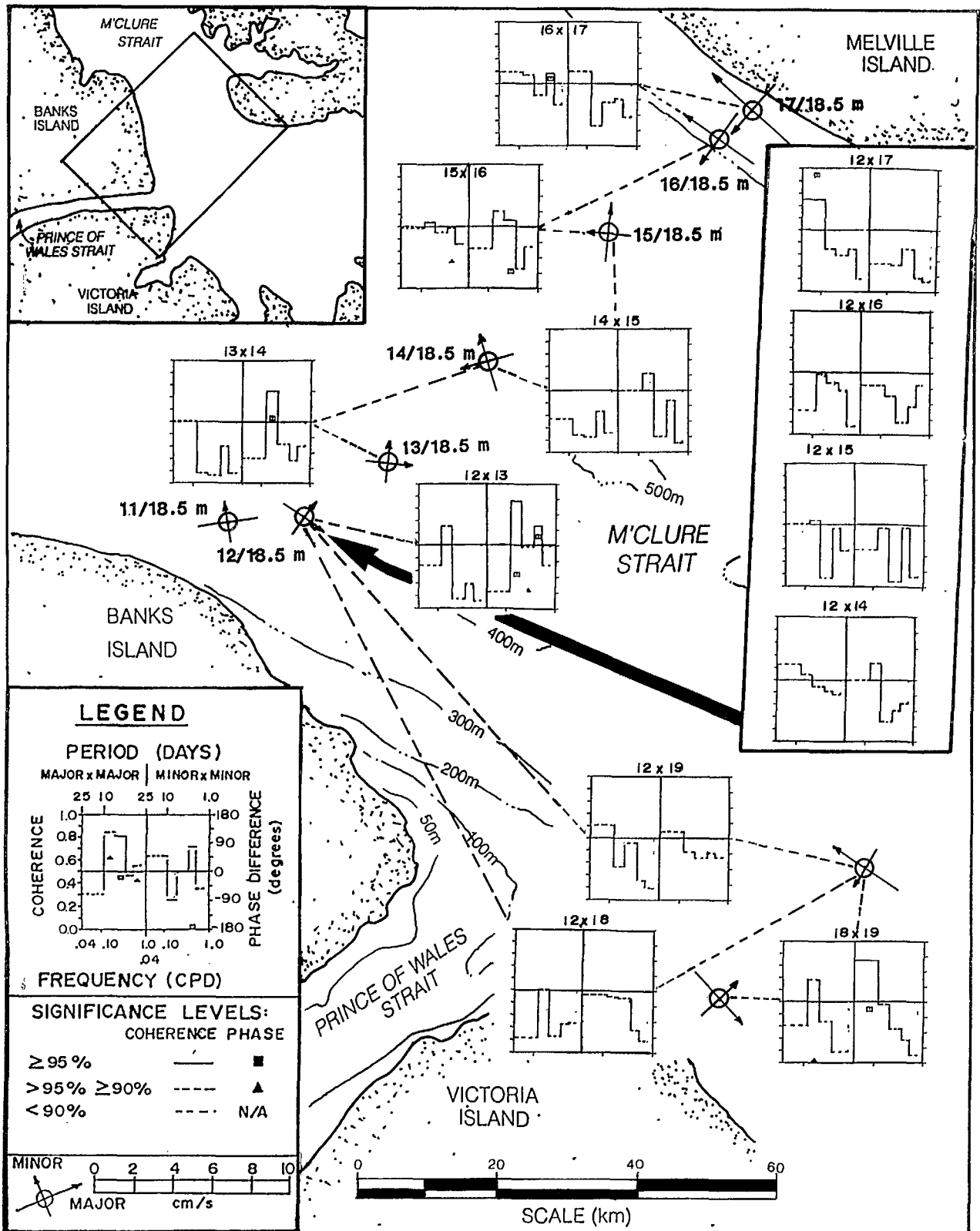


Figure 3.3-3: Cross-spectra computed for pairs of current-meter records in M'Clure Strait.

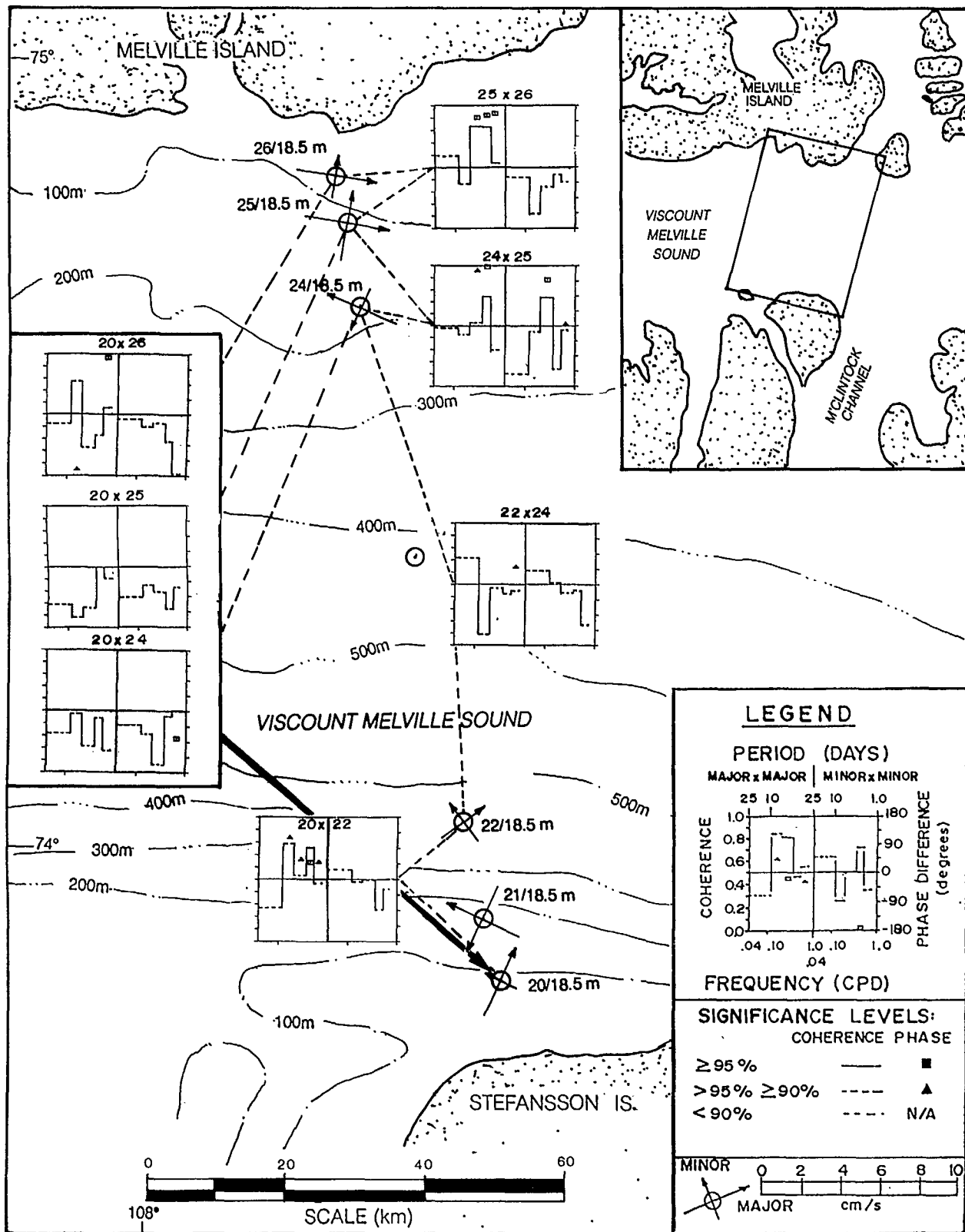


Figure 3.3-4: Cross-spectra computed for pairs of current-meter records in Central Viscount Melville Sound.

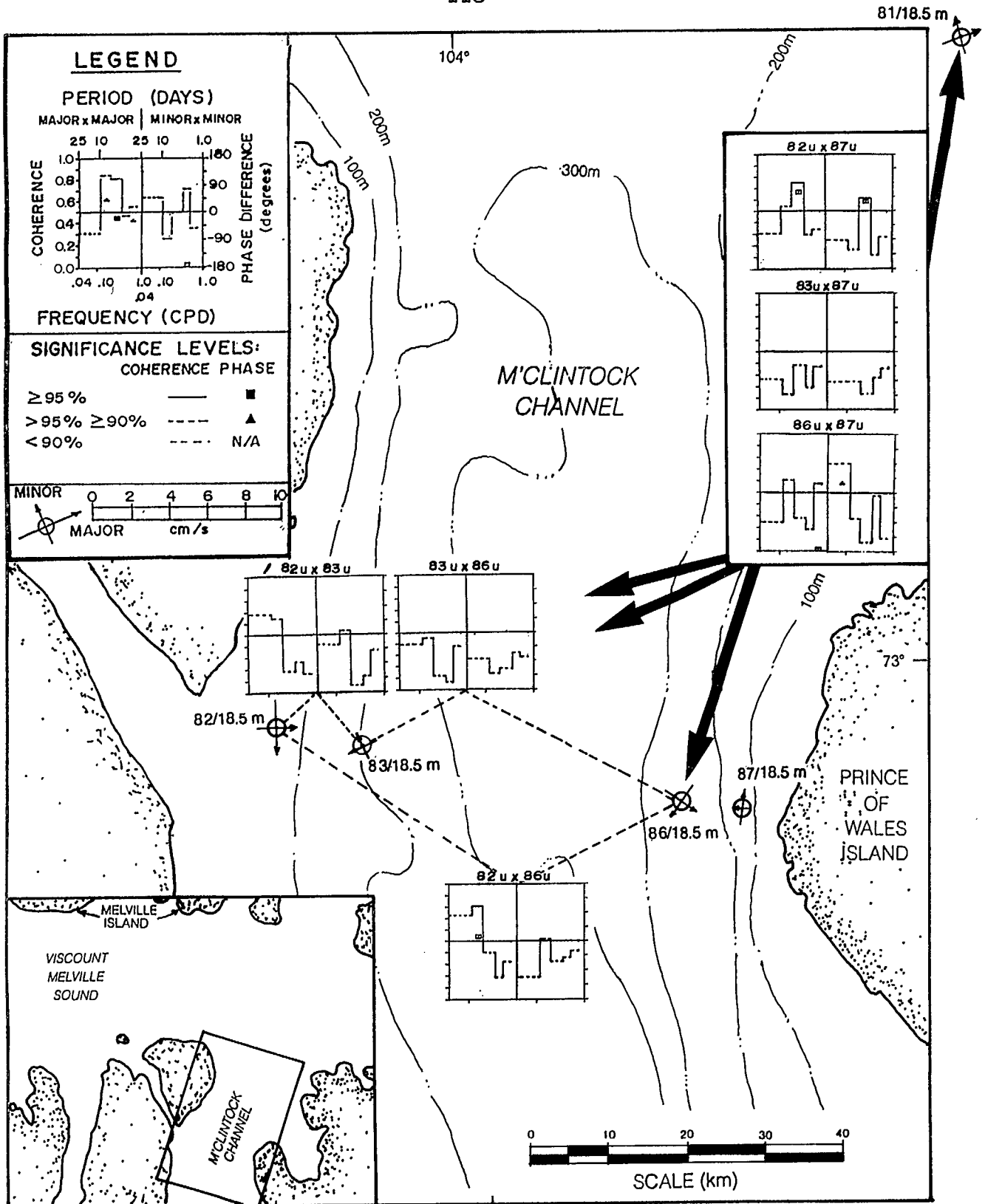


Figure 3.3-5: Cross-spectra computed for pairs of current-meter records in M'Clintock Channel.

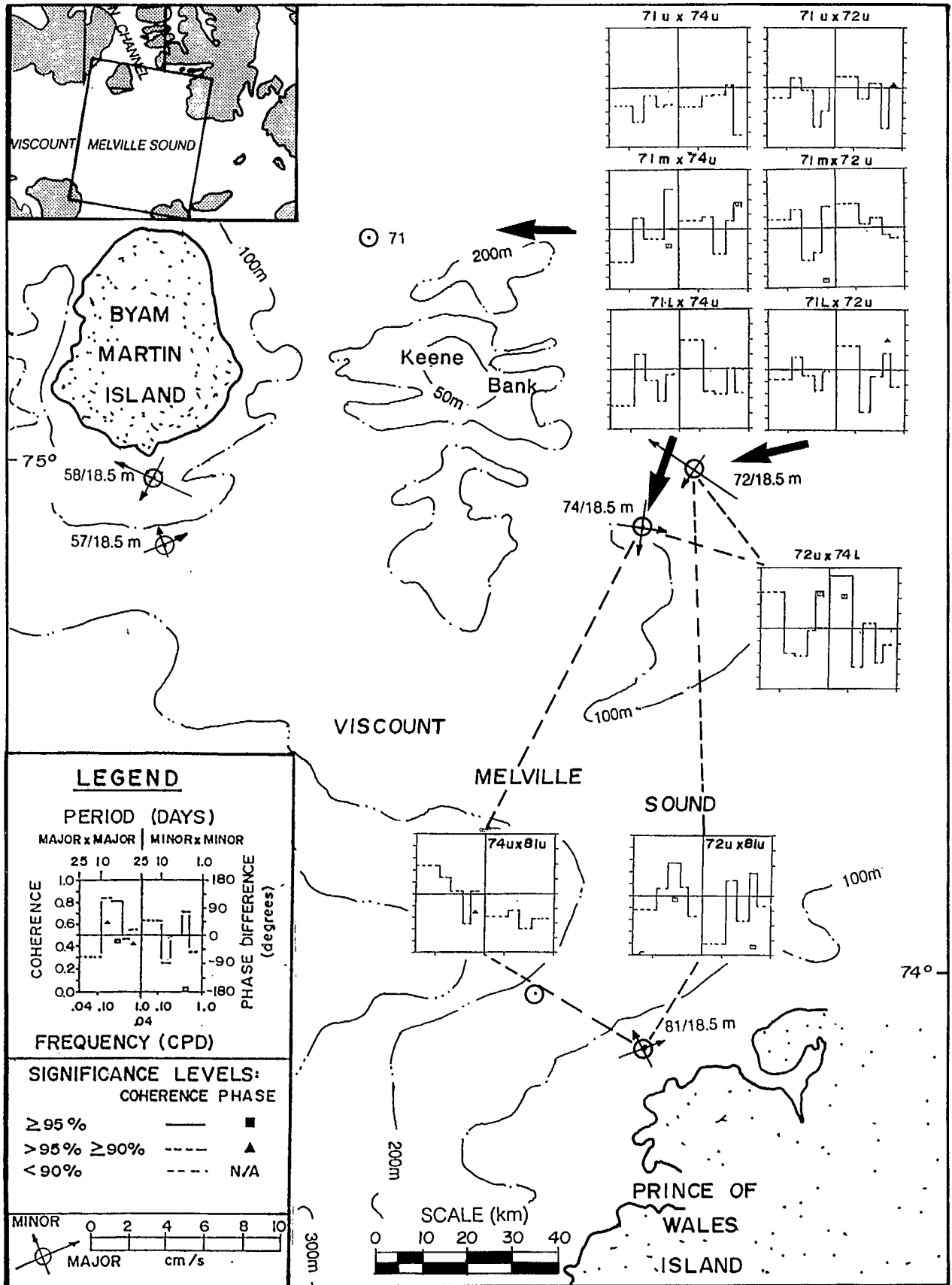


Figure 3.3-6: Cross-spectra computed for pairs of current-meter records in Eastern Viscount Melville Sound.

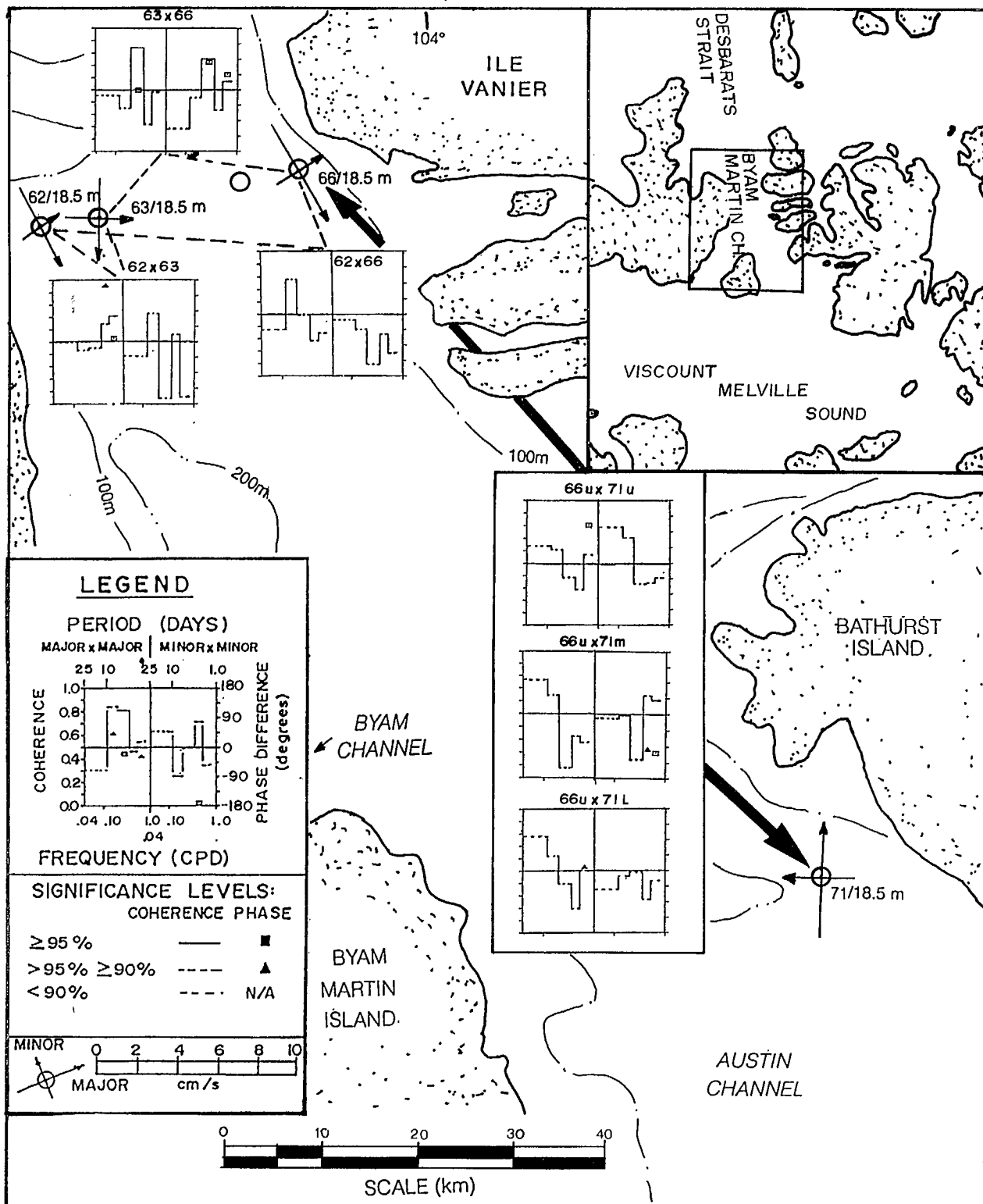


Figure 3.3-7: Cross-spectra computed for pairs of current-meter records in Byam Martin and Austin Channels.

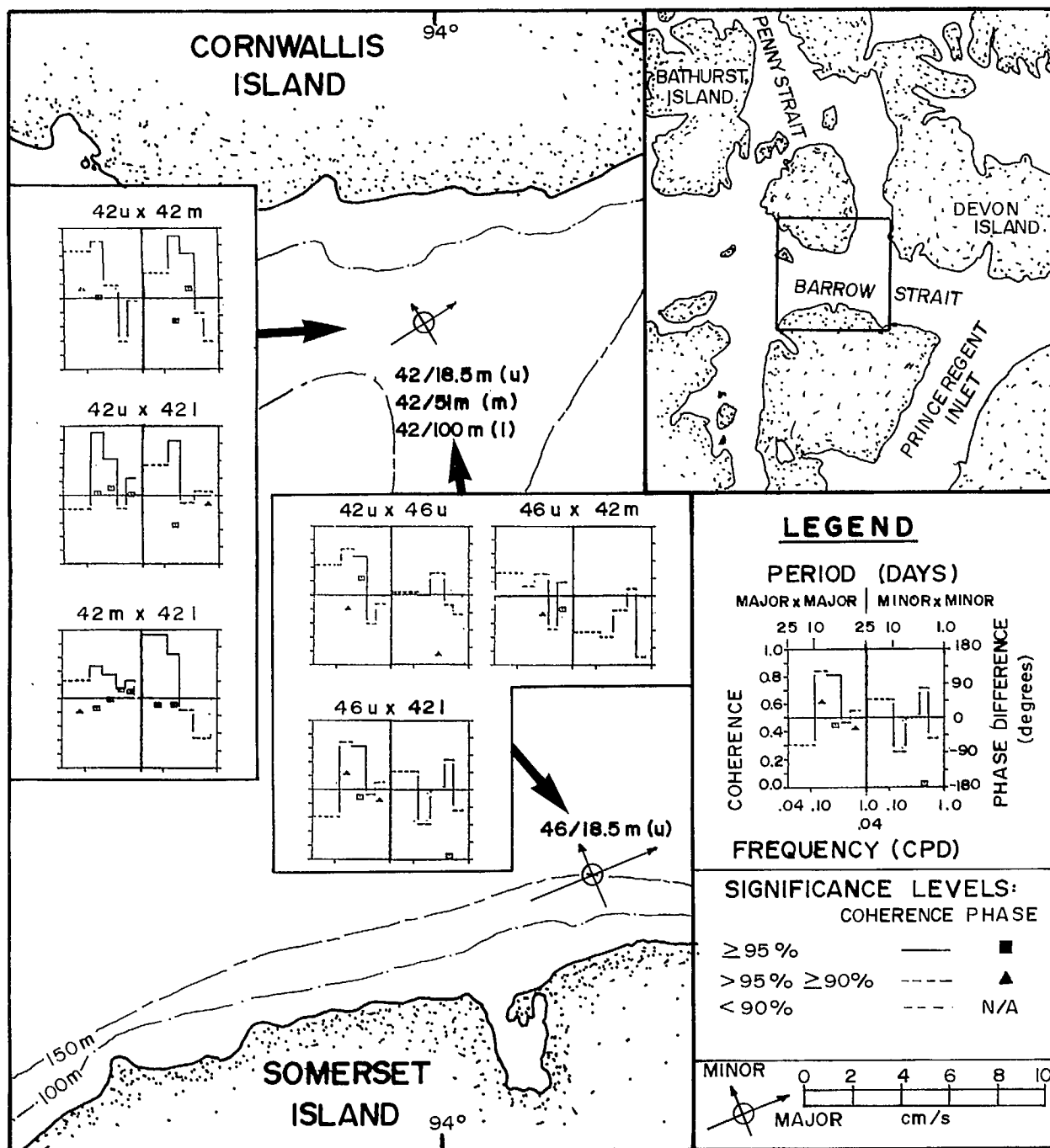


Figure 3.3-8: Cross-spectra computed for pairs of current-meter records in Barrow Strait.

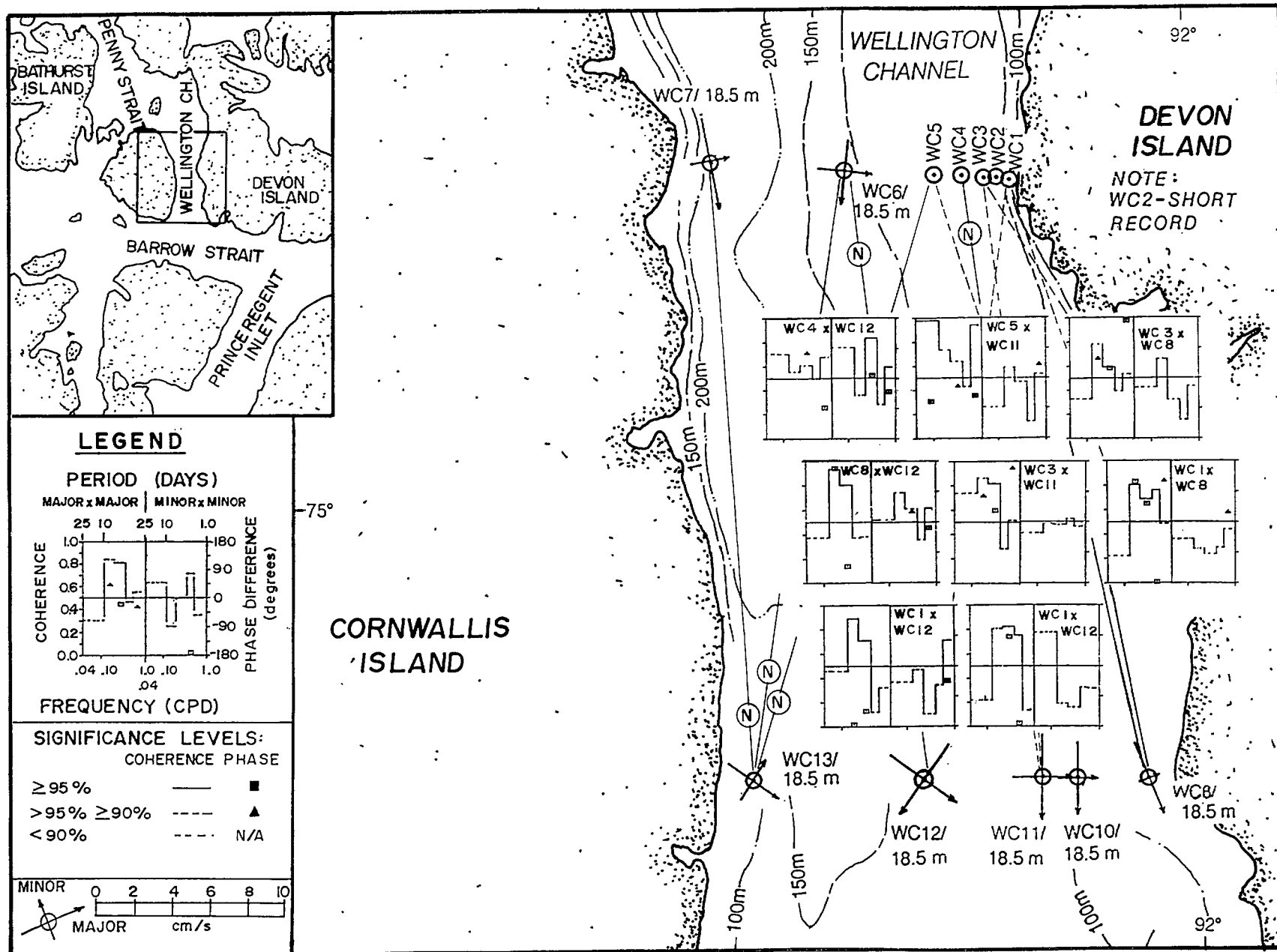
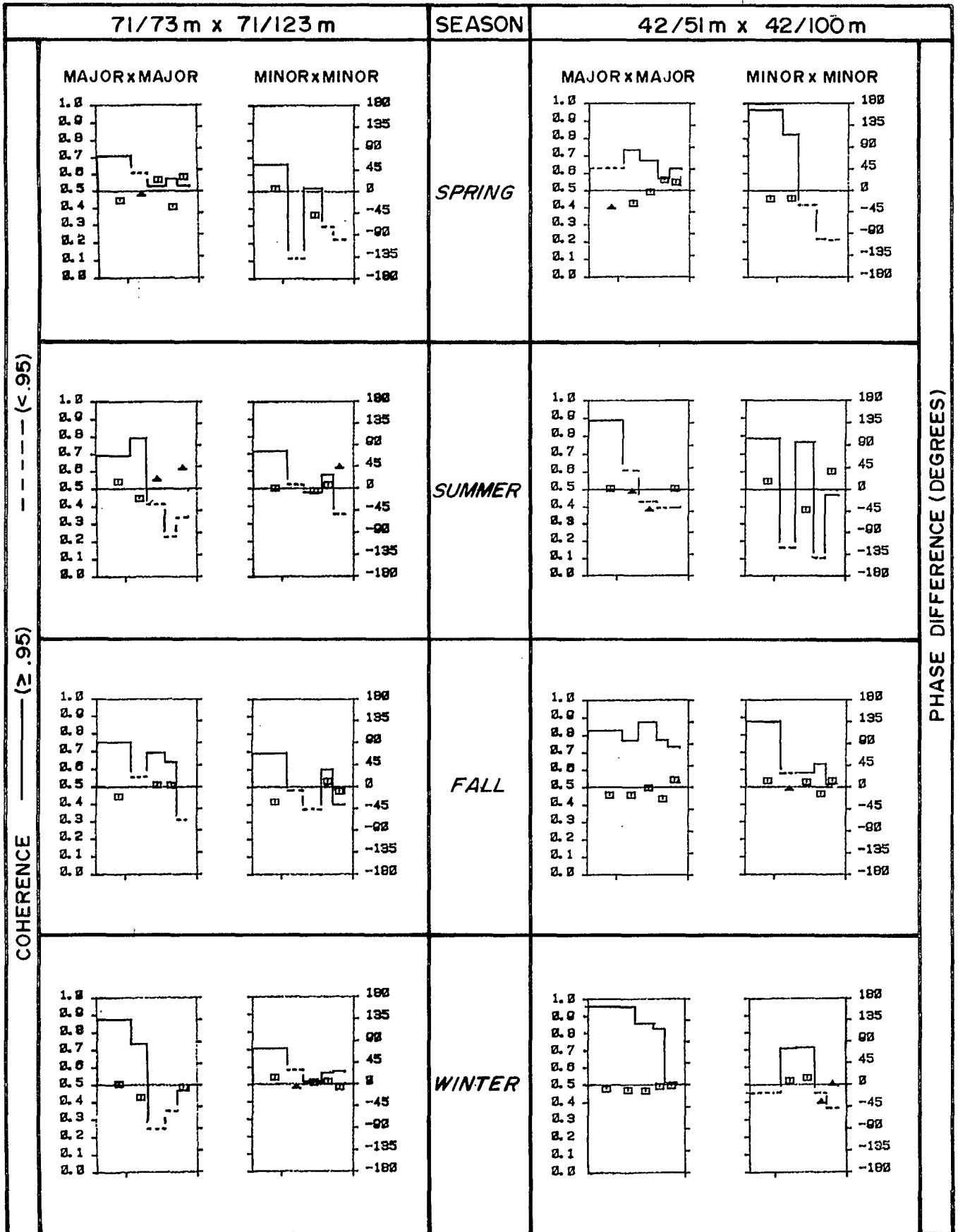


Figure 3.3-10: Cross-spectra computed for pairs of current-meter records in Wellington Channel.



COHERENCE

— (≥ .95)
 - - - (< .95)

PHASE DIFFERENCE (DEGREES)

Figure 3.3-11: Cross-spectra computed for each season from vertically-separated current-meter records in; (a) Austin Channel (Site 71); (b) Barrow Strait (Site 42).

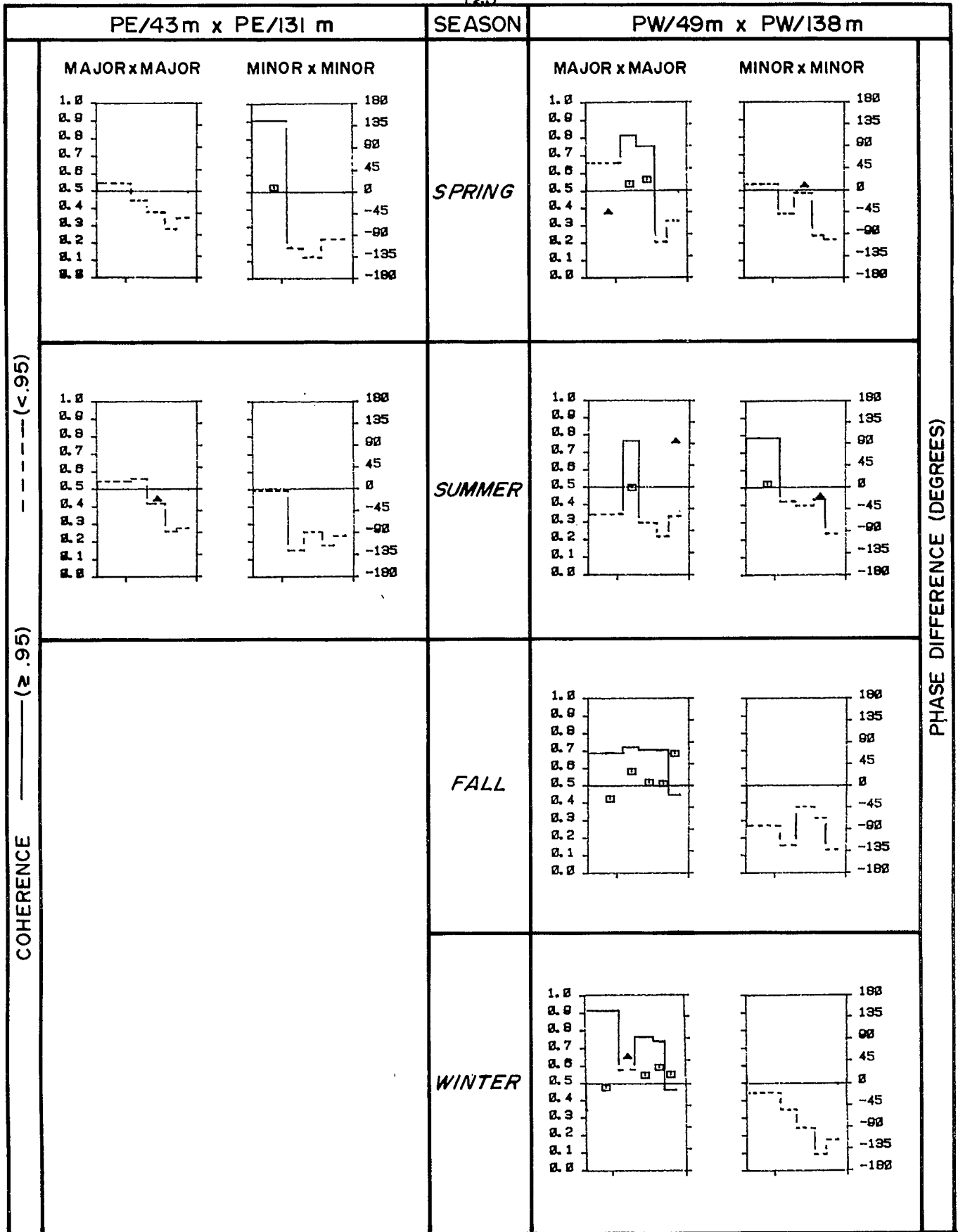


Figure 3.3-12: Cross-spectra computed for each season from vertically-separated current-meter records in Penny Strait (Sites PSW and PSE).

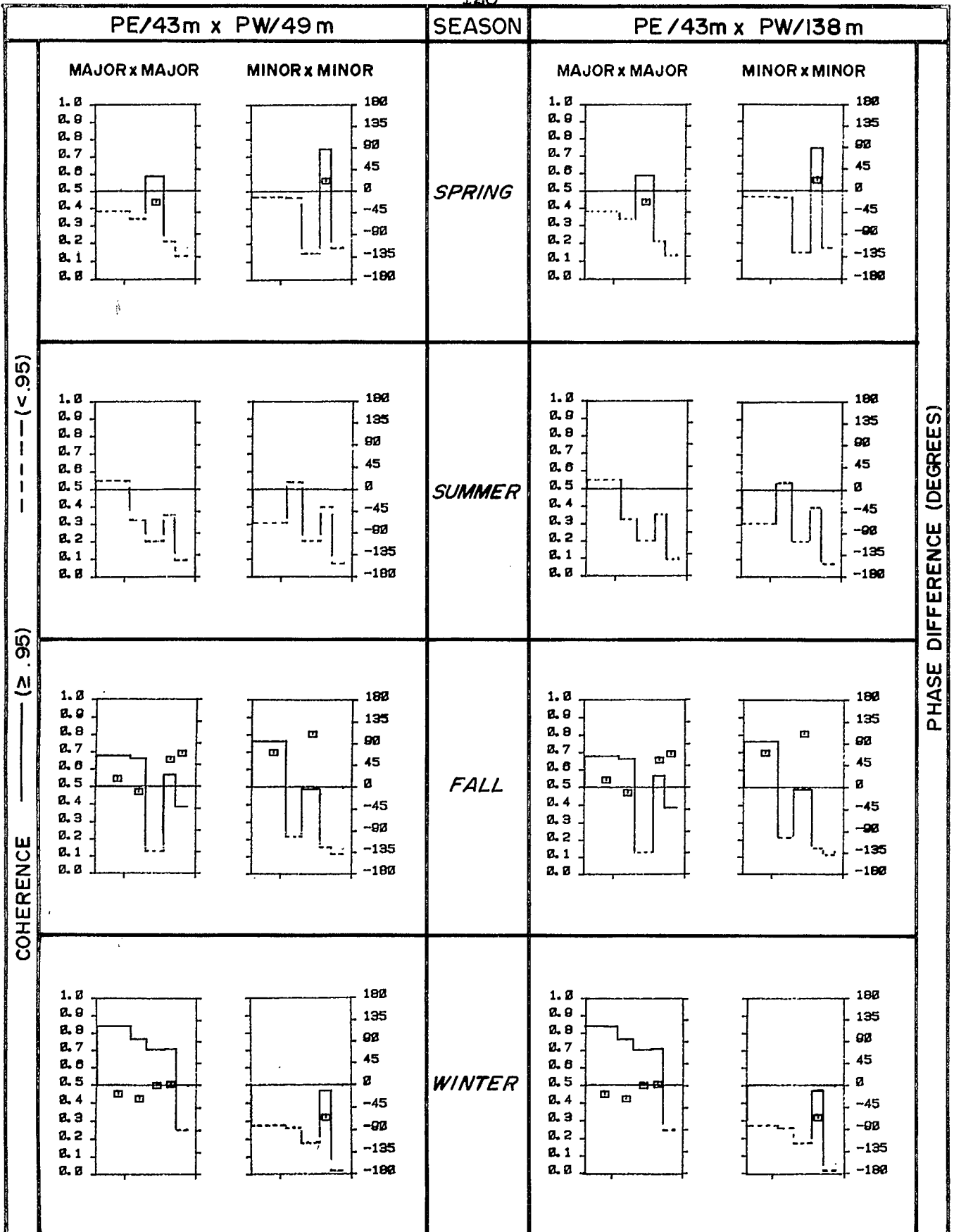
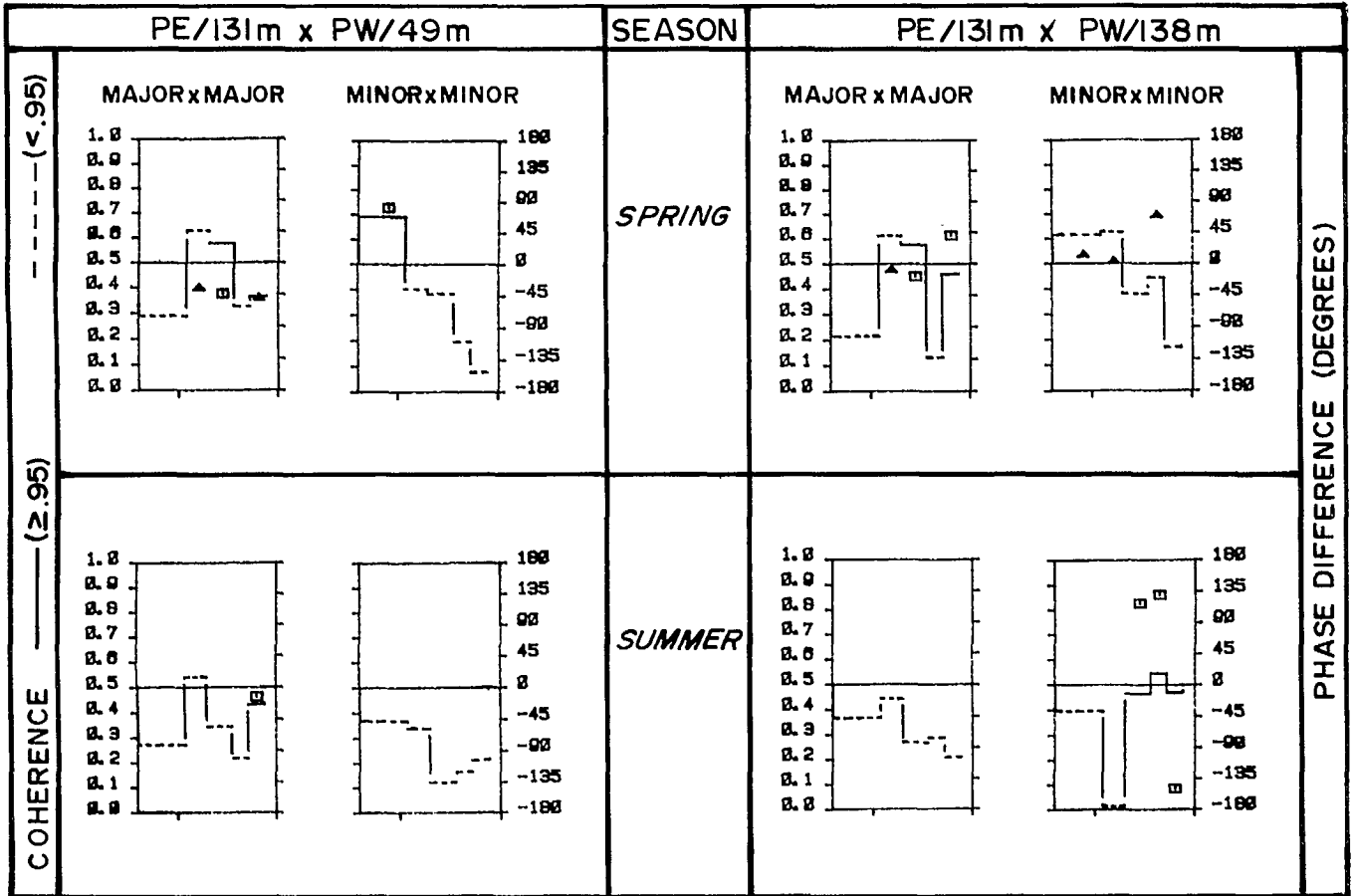


Figure 3.3-13: Seasonal cross-spectra computed for horizontally-separated station pairs in Penny Strait, using Site PSE mid-depth.



PHASE DIFFERENCE (DEGREES)

Figure 3.3-14: Seasonal cross-spectra computed for horizontally separated station pairs in Penny Strait, using Site PSE lower current meter.

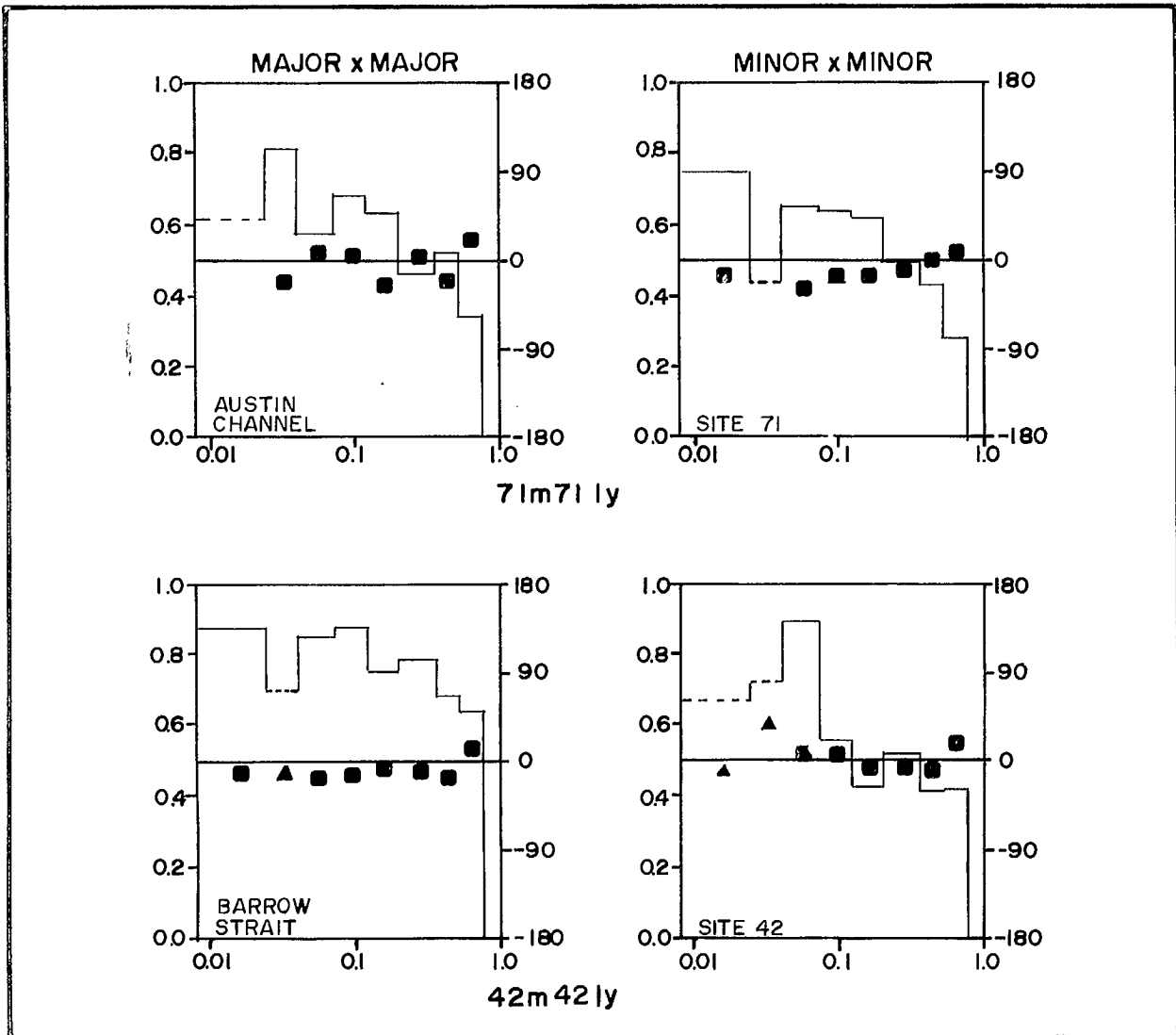


Figure 3.3-15: Cross-spectra computed from full year-long data sets in; (a) Austin Channel; (b) Barrow Strait.

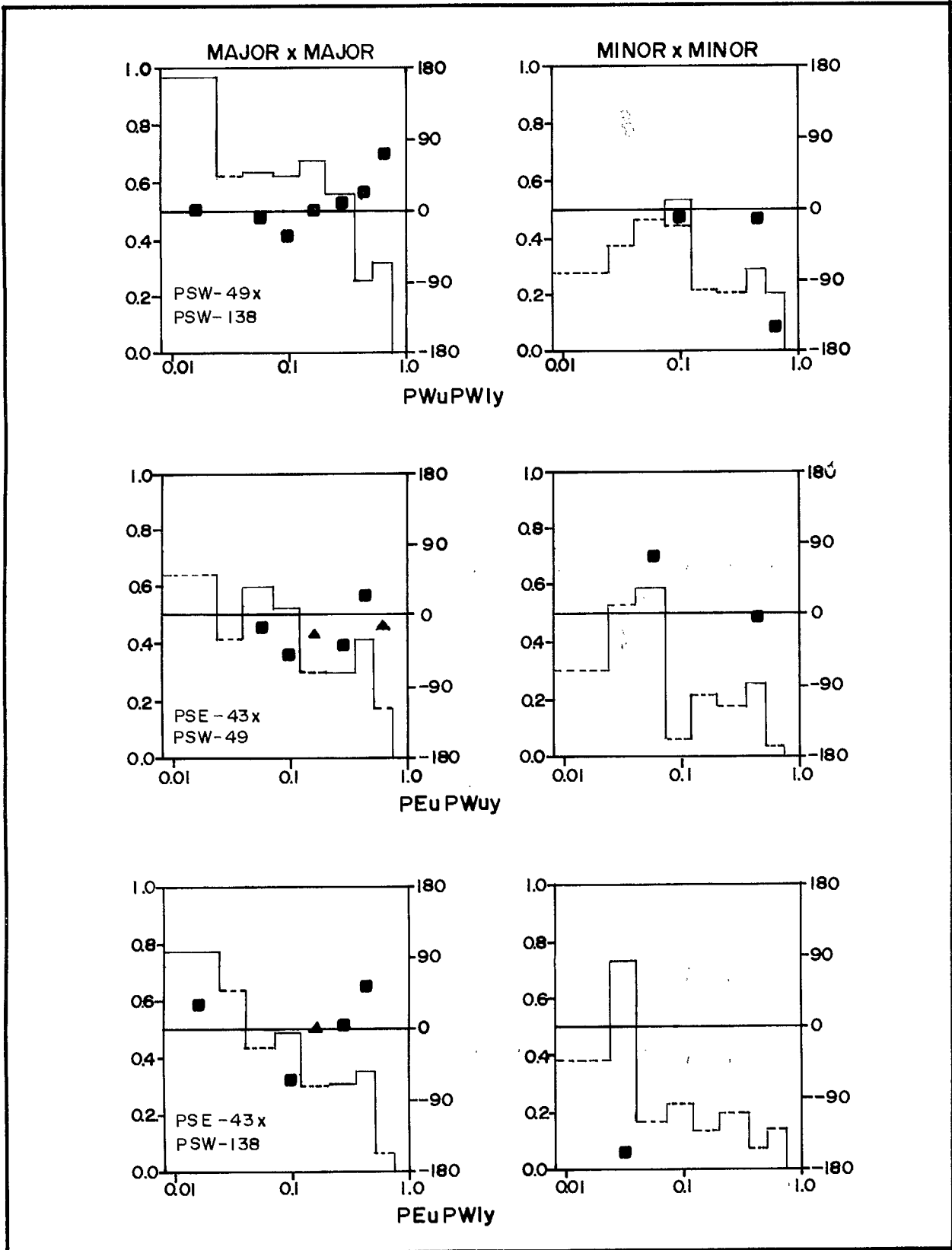


Figure 3.3-16: Cross-spectra computed from full year-long data sets in Penny Strait.

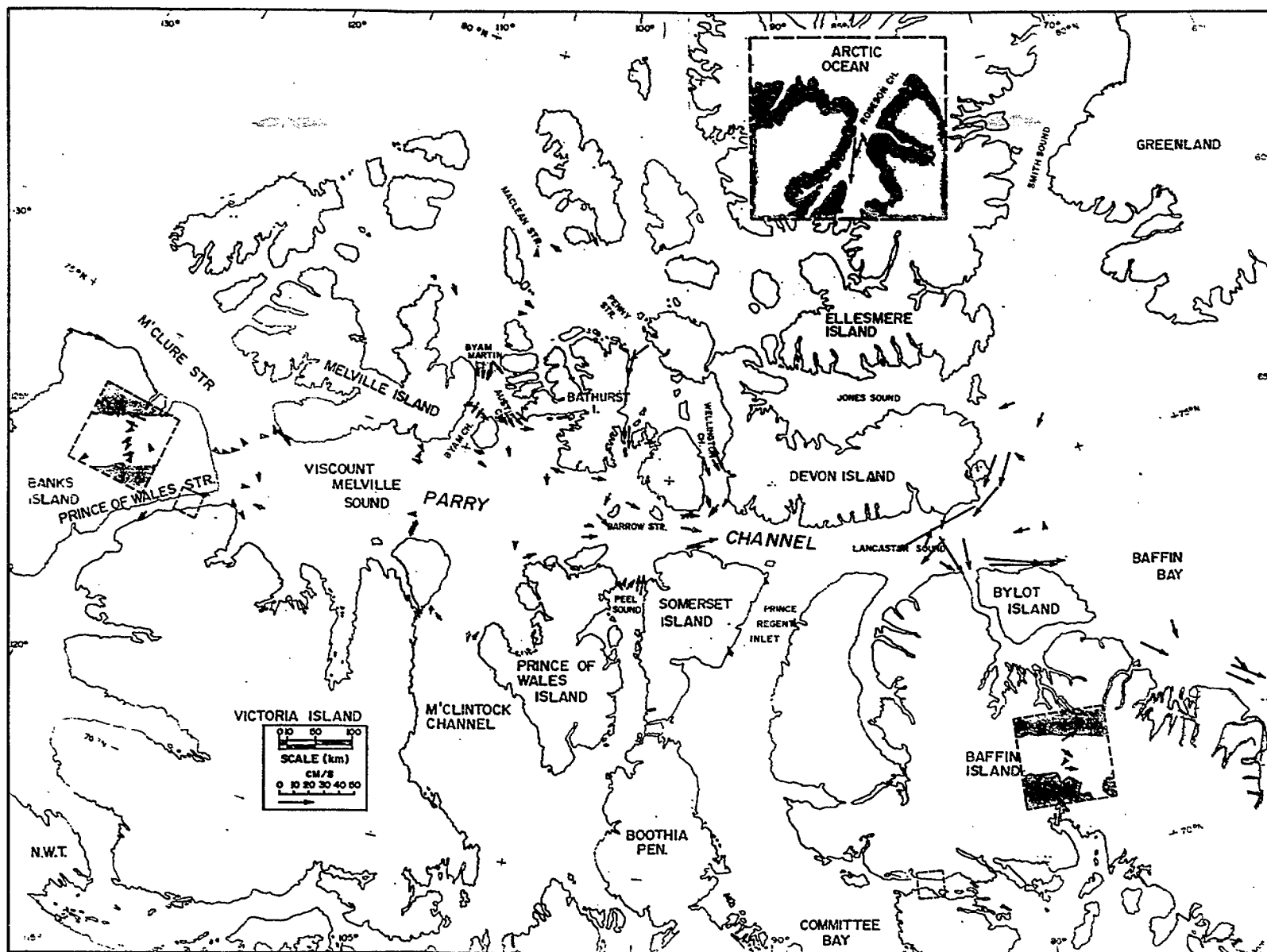


Figure 4-1: Summary plot of near-surface vector averaged residual currents, based on the 1982-1985 data obtained by IOS, and the data identified in Appendix 2. The arrowhead provides the direction of the flow; the speed is given by the length of the tail of each vector, scaled as in the legend. Vectors having an arrowhead but no tail indicate speeds less than 1 cm/s. The dashed vector along the northwest coast of Banks Island indicates a strong flow there, the actual magnitude of which is not available at this time.

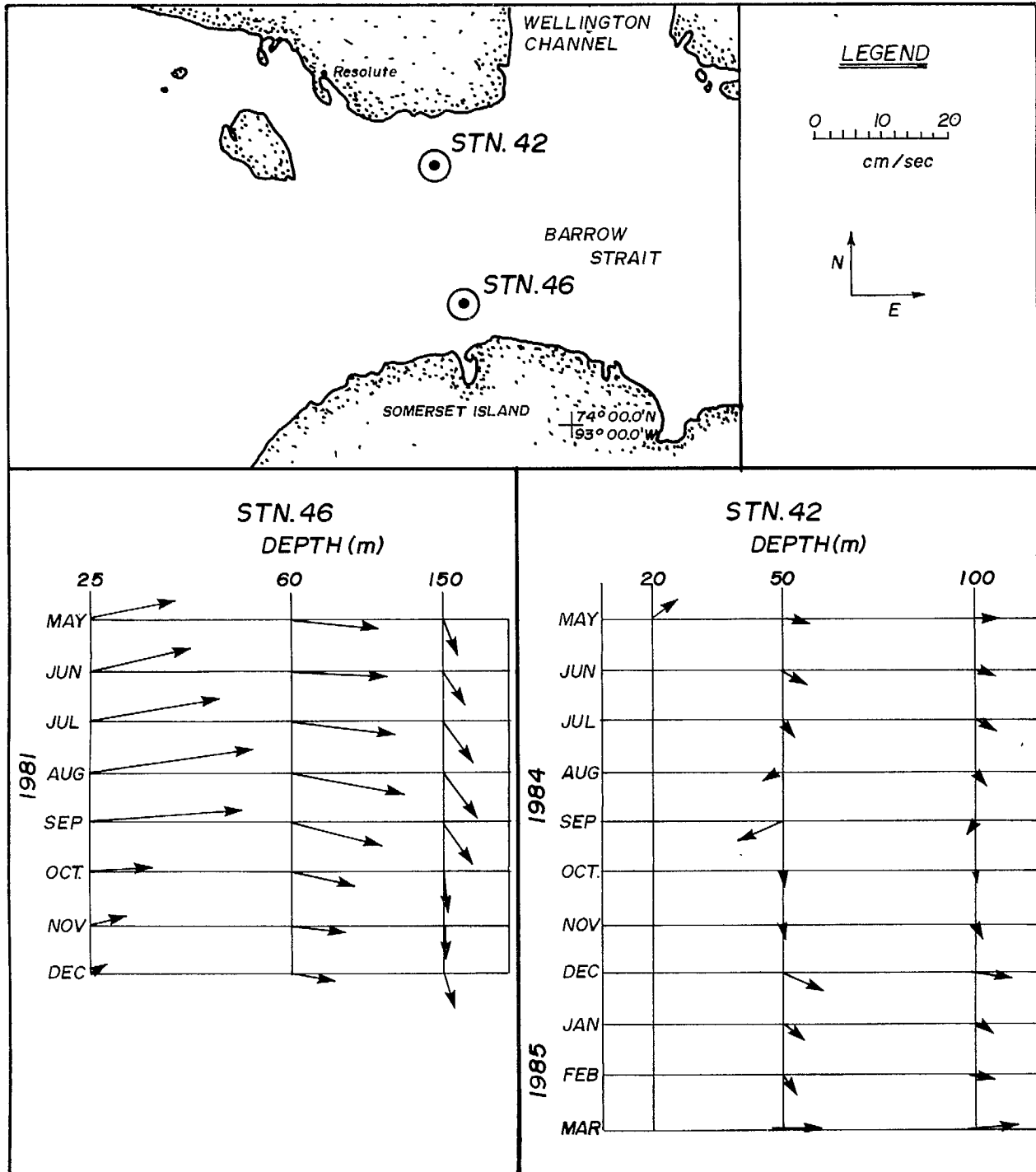


Figure 4-2: Monthly vector averaged velocities at stations 46 in 1981 and 42 in 1984. Although the data are from different years, the increased flow at station 46 during the summer correlates with a reversal from easterly to westerly flow at station 42.

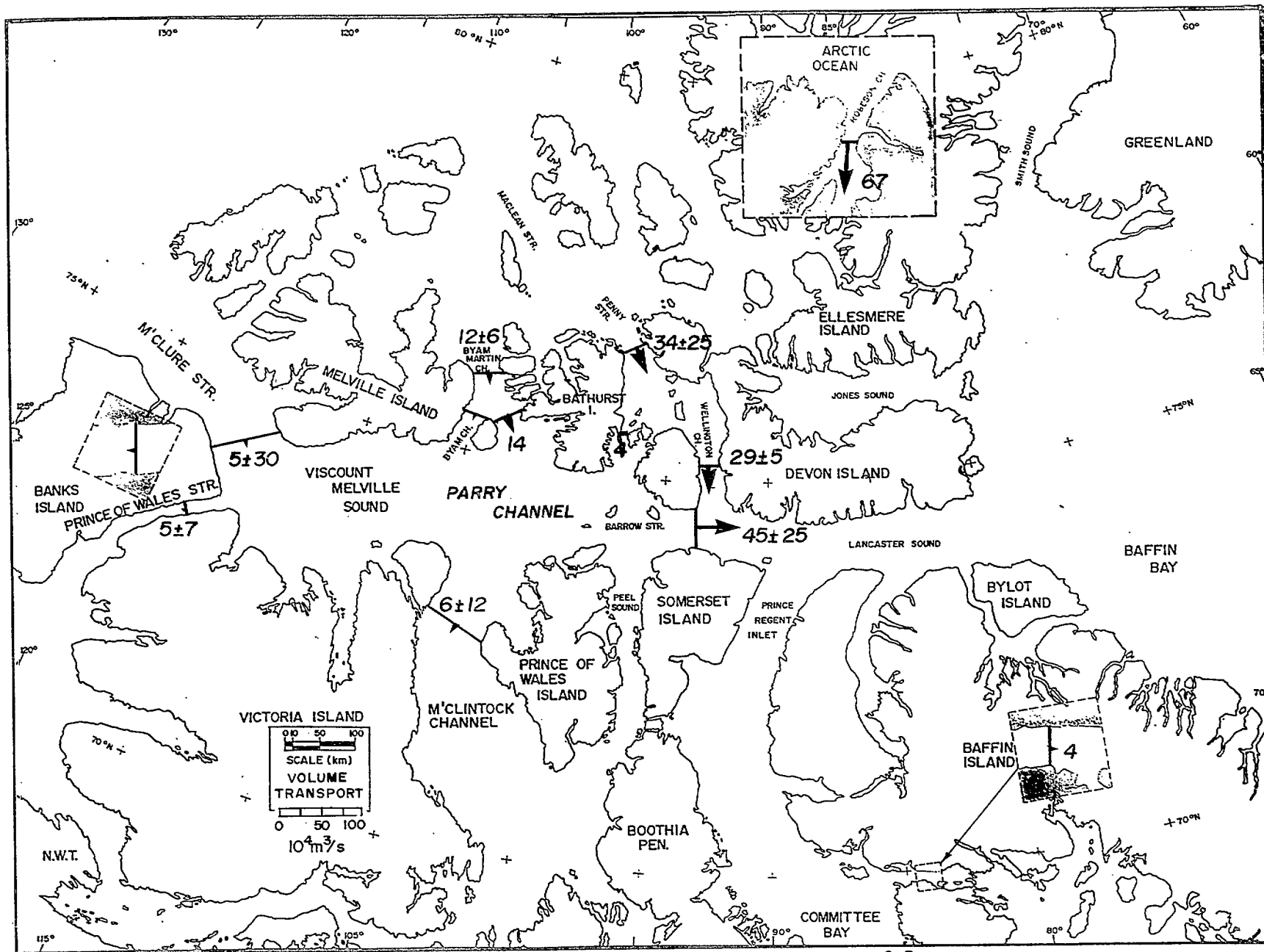


Figure 4-3: Estimated transport, in hundredth's of Sverdrups ($1 \text{ Sv} = 10^6 \text{ m}^3/\text{s}$), through the channels of the Canadian Archipelago. Sources are the 1982-1985 IOS data and others specified in Appendix 2.

APPENDICES



APPENDIX 1

DATA SETS CONTAINING CURRENT MEASUREMENTS WHICH MAY BE USEFUL
IN DETERMINING RESIDUAL CIRCULATION PATTERNS IN THE CANADIAN ARCHIPELAGO

Period [IOS I.D. #]	Area	Collecting Agency	Comments
1. 1969 May 3-20 [69-0005]	Kane Basin	Arctic Inst. of N. America	Sixteen days of current data from 50 m depth indicated a weak southerly net flow. Speed and direction histograms, but no means, are reported by Muench (1971).
2. 1971, 1972 and 1975	Robeson Channel	DREP & DREO	Springtime measurements in the 3 years indicated a net southerly transport of $0.67 \times 10^6 \text{ m}^3/\text{s}$ (Sadler, 1976a,b).
3. 1976 Apr-May [76-0007]	Fury & Hecla Strait	DREP	Line of current meters extending north-south across the Strait. Effective length of records, typically 20-30 days. Data status: processed and reported (Sadler, Serson and Chow, 1979). Calculated transport of $1.2 \times 10^{12} \text{ m}^3/\text{year}$ to the east.
4. 1976 Apr-Jul [76-0017]	Byam Channel & Austin Channel	Frozen Sea Research Group	Seventeen current meters; surface, mid-depth and near-bottom. Effective length of records typically 40-70 days. Detailed analyses in Greisman and Lake (1978).
5. 1977 Apr-May [77-0012]	M'Clure Strait & Prince of Wales Strait	CCIW	Near-surface current meters. Effective lengths 10-40 days. Detailed analyses in Peck (1978).
6. 1977-1978 Mar-Mar [77-0026]	Crozier Strait & Pullen Strait	Frozen Sea Research Group	Six moorings in Crozier Strait, one in Pullen Strait. Effective lengths of records typically 50-70 days. Detailed analyses in Greisman and Lake (1978). Two deep meters in Crozier Strait provided records of nearly one-year duration.

	Period [IOS I.D. #]	Area	Collecting Agency	Comments
7.	1977 Aug-Oct [77-0013]	Lancaster Sound	IOS	Three moorings off Borden Peninsula. Maximum record lengths of 65 days. Detailed analyses in Fissel and Wilton (1978).
8.	1978 Mar-Apr [78-0007]	Barrow Strait & Austin Channel	CCIW	Five moorings across Barrow Strait and three in Austin Channel. Effective lengths typically 20-40 days. Barrow Strait moorings had instruments at 5 and 50 m depth. Detailed analyses in Peck (1980a).
9.	1978 Apr-Jul [78-0012]	Wellington Channel	Frozen Sea Research Group	Four moorings in an east-west line across the channel. Instruments at 12 and 100 m. Reference IOS (unpubl. data report, 1981).
10.	1978 Aug-Sep [78-0005]	Lancaster Sound	Petro-Canada/ Arctic Sciences	Three moorings running north-south across the sound. Effective lengths 20-46 days. Detailed analyses in Fissel and Wilton (1980).
11.	1979 Aug-Sep [79-0011]	Lancaster Sound & Lady Ann Strait	Petro-Canada/ Arctic Sciences	Seven moorings in Lancaster Sound, one in Lady Ann Strait. Effective lengths typically 50 days. Detailed analyses in Fissel and Wilton (1980).
12.	1979 Mar-Apr [79-0013]	M'Clure Strait	Polar Gas/ Dobrocky Seatech	Five moorings across M'Clure Strait. Meters typically at near-surface, 250 m, and 500 m. Directional information at near-surface meters only. Reference Polar Gas Project (1979).
13.	1979 Apr-May [79-0019]	Desbarats Strait & Maclean Strait	CCIW	Seven moorings with eight meters providing records of 10 to 30 days. Detailed analyses in Peck (1980b,c).

	Period [IOS I.D. #]	Area	Collecting Agency	Comments
14.	1979 Aug-Sep [79-0012]	Dolphin & Union Strait	Polar Gas/ Dobrocky Seatech	Five moorings extending across the strait. Effective record lengths typically 15 days. Analyses in Kashino (1979).
15.	1980 Apr [80-0014]	Desbarats Strait	Polar Gas/ Dobrocky Seatech	15-20 day records at 10 m, three sites. Reference Juhasz (1980).
16.	1981 Mar-Apr [81-0007]	Barrow Strait & Peel Sound	CCIW	Five moorings across Peel Sound. The mooring in southern Barrow Strait recorded data from April through December. No report; contact Dr. S. Prinsenberg at BIO (902-426-6598).
17.	1982 Mar-Jun [82-0002]	Barrow Strait	CCIW	Three moorings across Barrow Strait (22-34 days). Data analyzed but not reported; contact Dr. S. Prinsenberg at BIO (902-426-6598).
18.	1983 Apr [83-0009]	Barrow Strait	CCIW	Two moorings (42A, 46A). Effective lengths 7-30 days. Data analyzed but not reported; contact Dr. S. Prinsenberg at BIO (902-426-6598).
19.	1983 Apr [83-0017]	Prince Regent Inlet	CCIW	Four meters, all at 10 m depth. Record lengths 5-47 days. Meters were nearshore, and possibly not representative of currents in the centre of the inlet. Data analyzed but not reported; contact Dr. S. Prinsenberg at BIO (902-426-6598).
20.	1984-1985	M'Clure Strait & Ballantyne Strait	Frozen Sea Research Group	Data not fully processed. Direction channel should be inspected for proper response since no rigid connection to surface was used (Perkin, pers. comm.).
21.	1985 Spring	Arnot Strait	CCIW	Contact D. St. Jacques at CCIW (416-637-4384).

APPENDIX 2

SUMMARY STATISTICS OF CURRENT RECORDS USED TO SUPPLEMENT
THE DATA OBTAINED BY THE INSTITUTE OF OCEAN SCIENCES DURING 1982-85

Area	Stn#	Latitude		Longitude		CM Depth (m)	Start (yr/mo/dy)	Stop (yr/mo/dy)	Record Length (days)	Vector- Averaged Current (cm/s) °True		Comments	Source
		Deg	Min	Deg	Min								
Robeson	1	81	58.8	62	6.5	5	72/04/24	72/06/04	41	11	195		Sadler (1976)
Channel	1	81	58.8	62	6.5	20	72/04/24	72/06/04	41	30	200*		
	1	81	58.8	62	6.5	100	72/04/24	72/06/04	41	45	230		
	2	81	55.9	61	49.3	5	72/04/24	72/06/02	39	9	220		
	2	81	55.9	61	49.3	10	72/04/24	72/06/04	39	10	215		
	2	81	55.9	61	49.3	20	72/04/24	72/06/04	39	12	210*		
	2	81	55.9	61	49.3	50	72/04/24	72/06/04	39	19	205		
	3	81	53.2	61	16.4	10	72/04/24	72/05/31	37	11	345		
	3	81	53.2	61	16.4	20	72/04/24	72/05/04	37	5	345*		
	3	81	53.2	61	16.4	100	72/04/24	72/05/04	37	4	360		
Fury & Hecla Strait	1	69	52.2	84	15.6	11	76/04/26	76/05/27	21	3	105		Sadler, Serson & Chow (1979)
	1	69	52.2	84	15.6	40	76/04/23	76/05/27	21	9	135		
	2	69	54.0	84	15.6	11	76/04/24	76/05/27	29	1	225		
	2	69	54.0	84	15.6	40	76/04/25	76/05/27	32	8	295		
	3	69	55.7	84	15.6	11	76/04/25	76/05/26	30	3	130		
	3	69	55.7	84	15.6	40	76/04/25	76/05/26	30	4	320		
	4	69	57.5	84	15.6	11	76/04/27	76/05/26	19	7	60		
	4	69	57.5	84	15.6	40	76/04/27	76/05/26	18	1	240		
Lancaster Sound, NW Baffin Bay (EAMES)	77-1	74	5.5	81	11.0	39	77/07/28	77/09/26	60	16.2	177		Fissel & Wilton (1978); Fissel, Lemon, & Birch (1981)
	77-3	74	7.4	82	13.0	35	77/07/29	77/09/29	63	19.0	233		
	79-2	75	41.8	77	51.8	35	79/07/25	79/09/24	61	6	256		
	79-3	75	26.3	76	20.6	35	79/07/26	79/09/26	62	4.8	220		
	79-5	74	59.6	79	8.9	24	79/07/25	79/09/18	56	18	210		

*Indicates that the data were interpolated to the 20 m level.

Area	Stn#	Latitude		Longitude		CM Depth (m)	Start (yr/mo/dy)	Stop (yr/mo/dy)	Record Length (days)	Vector- Averaged Current (cm/s) °True		Comments	Source
		Deg	Min	Deg	Min								
	79-6	74	58.5	78	29.1	29	79/07/24	79/09/25	63	17.5	205		
	79-7	74	58.9	78	51.6	57	79/07/24	79/09/25	63	2.2	327		
	78-1	74	35.9	79	28.6	34	78/08/04	78/09/18	45	20.3	230		
	78-4	74	29.8	80	38.0	46	78/08/04	78/08/24	20	57.6	251		
	78-6	73	47.1	80	5.1	29	78/08/06	78/09/20	46	45.3	110		
	78-8	73	42.3	78	11.3	83	78/07/31	78/09/28	45	20.6	96		
	79-10	74	26.3	81	55.1	42	79/07/23	79/09/22	61	6.8	208		
	79-12	74	7.0	82	11.0	41	79/08/01	79/09/22	52	26.7	154		
	79-13	73	49.9	82	7.4	35	79/08/01	79/09/22	52	6.6	134		
	79-14	74	9.0	82	53.5	37	79/08/02	79/09/20	50	9.0	25		
	79-16	73	51.9	80	11.3	50	79/07/29	79/09/23	56	34.3	105		
	78-7	74	6.8	78	29.4	35	78/08/01	78/09/16	46	4.8	257		
	78-9	74	7.4	77	25.4	35	78/08/01	78/09/28	58	0.5	3		
	78-11	72	22.8	74	3.9	38	78/08/10	78/10/03	53	15.1	130		
	78-13	72	30.7	72	45.7	31	78/08/11	78/10/03	54	7.6	175		
	78-14	71	39.8	71	8.6	38	78/08/14	78/10/05	46	17.1	131		
	78-15	71	45.1	70	49.3	19	78/08/14	78/10/04	51	20.9	132		
	79-24	71	46.0	70	44.5	35	79/08/09	79/10/02	54	7.1	156		
Prince Regent Inlet	A	72	53.5	91	44.0	10	83/03/17	83/05/01	45	1.3	338		Prinsenber (pers. comm.)
	B	73	14.0	89	5.0	10	83/03/20	83/04/30	41	0.8	19		
	C	73	49.0	90	17.5	10	83/03/20	83/04/30	41	0.4	354		
Peel Sound	81	73	41.6	96	49.0	10	81/03/29	83/04/27	29	1.2	142		Prinsenber (pers. comm.)
	82	73	41.6	96	37.0	10	81/03/28	83/04/26	29	0.9	19		
	83	73	41.6	96	18.5	10	81/03/29	81/04/27	29	2.7	32		
	84	73	41.6	96	0.0	10	81/03/23	81/04/24	32	5.5	6		
	85	73	41.6	95	48.2	10	81/03/29	81/04/27	29	7.0	4		
Byam Channel	B1	75	32.7	105	25.2	0.5	76/04/20	76/06/25	96	0.8	245		Greisman & Lake (1978)
	B2	75	30.2	105	8.7	0.5	76/04/22	76/07/15	83	2.6	195		
	B4	75	26.9	104	46.5	0.5	76/04/28	76/06/28	61	2.0	200		
	B5	75	25.5	104	37.8	0.5	76/05/12	76/07/25	73	1.1	115		

Area	Stn#	Latitude		Longitude		CM Depth (m)	Start (yr/mo/dy)	Stop (yr/mo/dy)	Record Length (days)	Vector- Averaged Current (cm/s) °True		Comments	Source
		Deg	Min	Deg	Min								
Austin Channel	A1	75	25.2	103	50.1	0.5	76/05/10	76/07/21	72	1.7	110	Greisman & Lake (1978)	
	A2	75	26.4	103	38.7	0.5	76/05/09	76/07/02	53	2.1	135		
	A3	75	28.2	103	21.6	0.5	76/05/08	76/06/18	40	5.6	135		
	A4	75	30.2	103	01.0	0.5	76/05/13	76/07/22	79	5.2	125		
	A5	75	31.5	102	49.2	0.5	76/05/02	76/06/15	41	4.2	110		
Crozier Strait	C1	75	31.6	97	22.2	0.5	77/03/27	77/06/11	76	6.0	170		
	C2	75	31.5	97	19.8	0.5	77/03/30	77/06/11	73	1.0	55		
	C3	75	30.5	97	10.4	0.5	77/04/13	77/06/12	0?	9.5	180		
	C4	75	30.3	97	8.0	0.5	77/04/10	77/06/14	65	9.5	180		
	C5	75	30.0	97	5.1	0.5	77/04/06	77/06/12	66	9.0	175		
	C6	75	28.8	97	2.9	0.5	77/04/04	77/06/12	69	8.0	165		
Pullen Strait	P3	75	26.5	96	5.9	0.5	77/04/21	77/06/15	55	2.5	255		
Danish Strait	32	77	50.0	100	46.0	5	79/04/08	79/04/30	22	5.1	138	Peck (1980b,c)	
Maclean Strait	35	77	37.0	102	55.0	50	79/04/08	79/04/25	17	2.1	290		
	37	77	30.0	103	58.0	50	79/04/08	79/05/07	12	0.5	354		
Desbarats Strait	12	76	55.0	103	49.0	50	79/04/03	79/05/01	28	1.1	127		
	14	76	47.0	103	52.0	5	79/04/03	79/04/27	10	0.8	85		
Hazen Strait	24	76	52.0	107	52.0	5	79/04/03	79/05/02	29	2.5	145		
Austin Channel	82	75	27.3	103	5.4	50	78/03/15	78/04/26	42	1.9	242	not plotted	Peck (1980a)
	95	75	7.4	102	59.6	5	78/03/15	78/04/01	17	1.7	169		
Western Barrow Strait	28	74	40.3	96	43.8	4	78/03/10	78/04/12	33	4.6	110	Peck (1980a)	
	28	74	40.3	96	43.8	50	78/03/10	78/04/02	23	5.6	92		
	35	74	52.8	98	17.0	4	78/03/11	78/04/22	42	5.3	92		
	35	74	52.8	98	17.0	50	78/03/11	78/04/22	42	5.1	21		
	38	74	38.3	97	58.2	4	78/03/13	78/04/29	47	3.6	202		
	38	74	38.3	97	58.2	50	78/03/13	78/04/22	40	6.3	186		
	42	74	26.7	98	6.4	4	78/03/11	78/04/23	43	6.8	127.5		

Area	Stn#	Latitude		Longitude		CM Depth (m)	Start (yr/mo/dy)	Stop (yr/mo/dy)	Record Length (days)	Vector- Averaged Current (cm/s) °True		Comments	Source
		Deg	Min	Deg	Min								
	42	74	26.7	98	6.4	50	78/03/11	78/04/12	32	3.6	338		
	45	74	10.0	98	34.0	4	78/03/11	78/04/23	43	4.7	79		
	45	74	10.0	98	34.0	50	78/03/11	78/04/23	43	1.1	70		
Barrow Strait	41	74	36.2	94	2.8	10	82/03/19	82/04/23	35	5.0	88		Prinsenber (pers. comm.)
	42	74	34.0	94	1.1	10	82/03/24	82/04/22	29	7.7	80		
	42	74	34.0	94	1.1	50	82/03/24	82/04/22	29	7.9	116		
	42	74	34.0	94	1.1	10	83/03/29	83/04/27	29	6.5	103		
	42	74	34.0	94	1.1	40	83/03/28	83/04/25	28	3.3	83		
	44	74	24.1	93	54.7	10	82/03/22	82/04/30	39	7.7	86		
	44	74	24.1	93	54.7	50	82/03/22	82/04/30	39	6.3	101		
	44	74	24.1	93	54.7	10	83/03/29	83/04/27	29	8.3	119		
	46	74	13.4	93	41.2	10	82/03/20	82/04/19	30	11.7	80		
	46	74	13.4	93	41.2	50	82/03/20	82/04/19	30	14.1	76		
	46	74	13.1	93	45.5	10	83/03/29	83/04/27	29	10.6	76		
	46	74	13.1	93	45.5	40	83/03/25	83/03/31	6	6.4	81	short record	
	47	74	11.3	93	33.9	10	82/03/20	82/04/19	30	5.1	73		
47	74	11.3	93	43.0	10	83/03/29	83/04/27	29	9.8	85			
M'Clure Strait	1	73	24.5	114	25.6	3	79/02/26	79/04/19	52	0.7	328		Polar Gas (1979)
	2	73	38.6	114	12.9	3	79/03/04	79/04/18	45	2.5	249		
	3	73	54.1	113	55.1	3	79/03/06	79/04/18	43	1.3	153		
	4	74	09.1	113	36.6	3	79/03/12	79/04/19	38	3.2	86		
	5	74	24.9	113	15.3	3	79/03/13	79/04/18	36	0.9	130		
	5	74	24.9	113	15.3	18	79/03/23	79/04/16	25	4.4	218		
M'Clure Strait Prince of Wales Strait	31	74	20.26	113	21.84	6	77/04/03	77/05/07	31	1.1	79		Peck (1978)
	34	73	42.96	114	46.05	6	77/04/03	77/05/12	32	0.3	75		
	42	73	20.98	115	36.06	6	77/04/01	77/05/11	40	1.9	251		
	42	73	20.98	115	36.06	34	77/04/01	77/05/11	40	2.4	233		

Area	Stn#	Latitude		Longitude		CM Depth (m)	Start (yr/mo/dy)	Stop (yr/mo/dy)	Record Length (days)	Vector- Averaged Current (cm/s) °True		Comments	Source
		Deg	Min	Deg	Min								
Wellington Channel	1	75	15.5	93	17.5	12	78/04/25	78/07/09	75	6.8	169	Lake (pers. comm.)	
	2	75	15.9	93	00.5	12	78/04/19	78/07/09	81	2.0	140		
	2	75	15.9	93	00.5	100	78/04/19	78/07/06	78	0.6	109		
	3	75	15.8	92	51.0	20	78/04/04	78/07/08	94	4.6	133		
	3	75	15.8	92	51.0	100	78/04/03	78/07/08	96	2.5	138		
	4	75	16.3	92	37.2	12	78/04/06	78/07/08	92	1.7	16		
M'Clure Strait	B07	74	24.8	123	53.1	36	84/04/11	85/05/02	?	?	?	Prelim. analysis suggests strong residual flow towards east	Perkin (pers. comm.)
Ballantyne Strait	P01	77	43.2	116	00.1	35	84/??/??	85/??/??	?	?	?	Prelim. analysis suggests weak residual flow	Perkin (pers. comm.)
Nares Strait	4	81	12.0	65	27.8	6	85/03/10	85/04/28	49	4.0	242	Directions may be incorrect	Griesman et al. (1986)

APPENDIX 3
SUMMARY OF COMPUTATIONAL TECHNIQUES FOR AUTO-
AND CROSS-SPECTRAL ANALYSIS

The time-series current records were subjected to several stages of processing and analysis prior to the computation of the auto- and cross-spectral estimates. Initially the major and minor components were computed from each residual current meter data set. The component orientations were determined through computation of the principal axis from the time series data, by means of the following algorithm:

$$\text{TAN}(2 \times \text{PHI}) = \frac{-2 \times \text{COV}(U \times V)}{\text{VAR}(U) - \text{VAR}(V)}$$

where:

- PHI is the angle of the major axis in degrees counterclockwise from the easterly direction;
- U, V are the easterly and northerly current components
- TAN() is the tangent function
- VAR(), COV() are the variance and covariance functions.

The remaining analysis stages are summarized below:

- (1) tidal and other fluctuations having periods less than 1.25 days were removed from the data with a low-pass digital filter (see Section 2.2.2 for details).
- (2) the mean over each time series was computed and removed from the record.
- (3) the time series data were pre-whitened to guard against very long-term variations being misinterpreted as periodic fluctuations at higher frequencies (Bath, 1974; p. 260). The algorithm applied to each time series data value $X(i)$ was:

$$X(i) = X(i) - \text{PW} \times X(i-1)$$

where $\text{PW} = 0.99$.

- (4) a cosine taper window was then applied to the time series to reduce the effects of sideband leakage, associated with computation of Fourier transforms of series of finite length (Bath, 1974; p. 161).
- (5) the Fourier coefficients were computed using the algorithm of Singleton (1969).
- (6) the Fourier coefficients were then corrected for frequency-dependent modifications resulting from the application of previous data-processing steps, specifically the low-pass filtering, the pre-whitening and the cosine taper, as described above.

The corrected spectral coefficients were then band- and block-averaged in order to improve statistical reliability, as discussed in Sections 3.2 and 3.3 of this report.

